



ΕΘΝΙΚΟ ΜΕΤΣΟΒΙΟ ΠΟΛΥΤΕΧΝΕΙΟ
ΣΧΟΛΗ ΜΗΧΑΝΟΛΟΓΩΝ ΜΗΧΑΝΙΚΩΝ
ΤΟΜΕΑΣ ΒΙΟΜΗΧΑΝΙΚΗΣ ΔΙΟΙΚΗΣΗΣ &
ΕΠΙΧΕΙΡΗΣΙΑΚΗΣ ΕΡΕΥΝΑΣ
ΜΟΝΑΔΑ ΕΡΓΟΝΟΜΙΑΣ

Development and Evaluation of a Wearable Motion Tracking System, to Support Hand-Tool Design

Ανάπτυξη και Αξιολόγηση Ενδυόμενου
Συστήματος Καταγραφής Κίνησης, για
Υποστήριξη Σχεδιασμού Εργαλείων Χειρός

Διπλωματική Εργασία

Καρακικές Μιχαήλ

Επιβλέπων: Δημήτριος Ναθαναήλ, Επίκουρος Καθηγητής Ε.Μ.Π.

Αθήνα, Φεβρουάριος 2017

Ευχαριστίες

Η ιστορία της ολοκλήρωσης των προπτυχιακών σπουδών μου είναι γεμάτη με θυσίες, αγρυπνία, κόπωση, αλλά ταυτόχρονα και επιμονή, επιβράβευση, δικαίωση. Τα πολύτιμα μαθήματα της θα με ακολουθούν για το υπόλοιπο της ζωής μου, και νιώθω ότι οφείλω ευγνωμοσύνη σε όλους όσους συνέβαλαν σε αυτήν την πορεία, που αποκορυφώνεται με την παρούσα Διπλωματική εργασία.

Πρωτίστως, θέλω να ευχαριστήσω ειλικρινά τον επιβλέποντα καθηγητή, κ. Δημήτρη Ναθαναήλ, για την ανελλιπή βοήθεια και τη στιβαρή καθοδήγηση του. Το γνήσιο ενδιαφέρον του, καθώς και το ιδιαίτερο γνωστικό εύρος του ήταν καθοριστικά για αυτήν την έρευνα, αλλά και την προσωπική μου επιμόρφωση σε νέους επιστημονικούς –και όχι μόνο– ορίζοντες.

Στη συνέχεια, θα ήθελα να ευχαριστήσω όλα τα μέλη της Μονάδας Εργονομίας, για τις ενδιαφέρουσες συζητήσεις, τη δημιουργία απρόσμενα ευχάριστου εργασιακού περιβάλλοντος, και τον απαραίτητο αθλητικό ανταγωνισμό. Ιδιαίτερα, ευχαριστώ τον κ. Κώστα Γκίκα, για τη κρίσιμη υποστήριξη του στη διεξαγωγή των πειραμάτων και σε όλες τις δυσκολίες που προέκυψαν. Οι γνώσεις του πάνω στο σχεδιασμό βοήθησαν σημαντικά στην εξέλιξη της αισθητικής, και της ικανότητας μου στη μετάδοση πληροφορίας.

Ακόμη, δεν μπορώ να παραλείψω να ευχαριστήσω θερμά όλους όσους συμμετείχαν με χαρά στο πείραμα που διεξήχθη, καθώς και τον φίλο μου Χ. Παγκαλίδη που ήταν πάντα πρόθυμος να συμμετέχει σε καταιγισμό ιδεών, όποτε ανέκυπτε πρόβλημα σχετικό με το επιστημονικό αντικείμενο του.

Κλείνοντας, το μεγαλύτερο ευχαριστώ το οφείλω στην οικογένεια μου, που έχει καταστήσει όλα αυτά εφικτά. Χάρη στη δική τους βαθιά και ουσιαστική υποστήριξη, είμαι αισιόδοξος για τον δρόμο που ανοίγεται μπροστά μου.



Abstract

Hand-operated tools are part of everyday life for various professions, such as industrial workers, craftsmen, surgeons and physicians. Studies have demonstrated that improper hand tool use can cause discomfort, along with risk for musculoskeletal disorders on the upper extremities. Suitable hand tool design can promote safe use of hand tools and reduce the occurrence of these issues.

Among other factors, extreme wrist and forearm posture of the hand tool user is associated with these problems. In this thesis, an inexpensive, wearable system to track wrist and forearm joint motion is developed, using Inertial Measurement Units (IMUs). Its purpose is to be used in hand tool evaluation studies, which examine wrist and forearm posture, and assist in identifying fitting design solutions for hand tools.

A methodology for comparing alternative design solutions, using this wearable system, is proposed, through a study on shaving razor handles. In this experimental research, we monitored wrist and forearm motion of subjects using three different razors, and used the results in conjunction with video analysis to (a) determine if a correlation exists between wrist motion and razor handle design, (b) recognize the effect of design features.

Results revealed that such correlation does exist. Namely, larger handle length, combined with higher shaving head mobility, led to increased wrist deviation, but decreased forearm deviation from neutral posture. The amplitude of wrist and forearm motion during shaving strokes was found to be independent from the razor used. However, wrist and forearm posture during shaving were not extreme, and the task would not likely cause adverse health outcomes.

In conclusion, in order to fully evaluate design solutions of razors, further metrics, both subjective and objective, are needed. Nevertheless, the results do demonstrate how this method can be used to obtain useful information for the design process in hand tools.



Περίληψη

Εργαλεία χειρός χρησιμοποιούνται καθημερινά από πολλούς επαγγελματίες, όπως εργαζόμενοι στη βιομηχανία, τεχνίτες, οδοντίατροι, χειρουργοί κλπ. Έρευνες έχουν καταδείξει ότι η ακατάλληλη χρήση των εργαλείων αυτών ενδέχεται να προκαλέσει καταπόνηση, ή και κίνδυνο για εμφάνιση κάποιας μυοσκελετικής διαταραχής στα άνω άκρα. Ο κατάλληλος σχεδιασμός εργαλείων χειρός μπορεί να προάγει την ασφαλή χρήση τους, και να ελαττώσει την πιθανότητα εμφάνισης των προβλημάτων αυτών.

Ακραίες γωνίες στις αρθρώσεις του καρπού και του αντιβραχίου, σε συνδυασμό με άλλους παράγοντες, προκαλούν τέτοιες αρνητικές επιπτώσεις στην άνεση και την υγεία. Σε αυτή την εργασία, αναπτύχθηκε ένα χαμηλού κόστους, ενδύομενο σύστημα καταγραφής της κίνησης των αρθρώσεων αυτών, χρησιμοποιώντας αδρανειακούς αισθητήρες (IMUs). Σκοπός του είναι να αξιοποιηθεί σε μελέτες αξιολόγησης εργαλείων χειρός, και να συνεισφέρει στην αναγνώριση κατάλληλων σχεδιαστικών λύσεων.

Πέραν της ανάπτυξης του, το ενδύομενο σύστημα χρησιμοποιείται για να προταθεί μια μεθοδολογία σύγκρισης εναλλακτικών σχεδιαστικών λύσεων, πάνω σε μια έρευνα που αφορά λαβές ξυριστικών συστημάτων. Στο πείραμα που διεξήχθη, μετρήθηκε η κίνηση του καρπού και του αντιβραχίου των συμμετεχόντων, ενώ χρησιμοποιούσαν τρία διαφορετικά ξυράφια χειρός. Τα αποτελέσματα χρησιμοποιήθηκαν σε συνδυασμό με παρατήρηση από μαγνητοσκόπηση, ώστε (α) να διερευνηθεί η ύπαρξη συσχέτισης μεταξύ σχεδιασμού λαβής και κινηματικής συμπεριφοράς καρπού, και (β) να προσδιοριστεί η επίδραση συγκεκριμένων σχεδιαστικών χαρακτηριστικών.



Contents

List of Tables	10
List of Figures	11
A. Human wrist and forearm anatomy	13
A.1 Bones & Joints	13
A.2 Muscles.....	14
A.3 Kinematics	15
A.4 Neutral Posture	16
A.5 Ranges of Motion.....	16
A.6 Negative Effects of Extreme Joint Angles.....	18
A.7 Wrist Motion Coupling.....	20
A.8 Kinematic Modeling	21
B. Ergonomics of hand tool use.....	23
B.1 Types of Grip	23
B.1.1 Precision Grip	24
B.1.1.1 Internal Precision Grip.....	24
B.1.1.2 External Precision Grip.....	24
B.1.1.3 Pinch Grip	24
B.1.2 Power Grip.....	25
B.1.2.1 Hook Grip	25
B.2 Hand Tools	26
B.2.1 Hand Tool Types.....	26
B.2.2 Hand Tool Design.....	26
B.2.3 Ergonomic Principles for Hand Tool Design.....	27
B.3 On Performance and Comfort Metrics.....	28
B.3.1 Subjective Measurements.....	29
B.3.2 Objective Measurements.....	31
B.3.2.1 Working posture	31
B.3.2.2 Muscle Activity.....	32
B.3.2.3 Performance	33
B.3.2.4 Pressure and Force Distribution.....	33
C. Wrist & Forearm Motion Tracking.....	35
C.1 Overview of Available Solutions	35
C.1.1 Inertial Sensors and Magnetometers.....	35

C.1.1.1	Inertial Measurement Units (IMU)	36
C.1.1.2	Datagloves	37
C.1.2	Goniometers	38
C.1.3	Optical Motion Capture (OMC)	40
C.1.4	Magnetic Systems	41
C.1.5	Optical Fiber Sensors	43
C.1.6	Summary	43
C.2	Development of Tracking System	44
C.2.1	Placement	45
C.2.2	Components and Specifications	47
C.2.2.1	MPU-6050	47
C.2.2.2	Arduino Nano	51
C.2.3	Wiring	52
C.2.4	Mounting	55
C.2.5	Setup Procedure	55
C.3	Mathematics of Rotation	56
C.3.1	Rotation Matrix	56
C.3.2	Quaternions to Rotation Matrix	57
C.3.3	Estimation of Anatomical Angles	58
C.3.3.1	Rotation Matrices between IMUs	58
C.3.3.2	Inverse Kinematics	58
C.3.4	Global Reference Frame	59
C.4	Algorithm	60
D.	Experiment – Product Design Evaluation	63
D.1	Experimental Design	63
D.1.1	Products	63
D.1.2	Task	65
D.1.2.1	Lower Leg Segmentation	65
D.1.2.2	Upper Leg Segmentation	66
D.1.2.3	Task Sequence	67
D.1.2.4	Subject Freedom vs Controlled Conditions	67
D.1.3	Measurements	67
D.1.4	Subjects	68
D.1.5	Procedure	68
D.2	Results	69

D.2.1	Wrist & Forearm Joint Angles.....	69
D.2.1.1	Comparison of Joint Angles	71
D.2.2	Intrasubject Analysis.....	77
D.2.3	Video Analysis	81
D.2.3.1	Grip Type.....	81
D.2.3.2	Shaving Stroke Style.....	82
D.2.4	Questionnaire.....	83
D.3	Discussion	84
D.3.1	Explanation of Joint Angle Differences	84
D.3.2	Comparison of Razors.....	86
D.3.3	Challenging the Results.....	86
D.4	Conclusions.....	87
D.5	Limitations.....	87
D.5.1	Motion Tracking System.....	87
D.5.2	Experiment.....	88
D.5.3	Analysis.....	88
D.6	Recommendations for Future Research.....	89
D.6.1	Fit in hand.....	89
D.6.2	Natural Behavior	89
D.6.3	Correlation between Discomfort and Risk of MSD.....	89
Appendix.....		90
A. Code		90
Bibliography.....		97

List of Tables

Table 1: RoM of wrist and forearm	17
Table 2: Neutral zone amplitude	20
Table 3: Advantages and disadvantages of IMUs.....	37
Table 4: Advantages and disadvantages of datagloves.....	38
Table 5: Advantages and disadvantages electrogoniometers	40
Table 6: Advantages and disadvantages of OMC systems	41
Table 7: Advantages and disadvantages of electromagnetic systems	43
Table 8: Motion tracking solutions for wrist and forearm.....	43
Table 9: Cost of individual components	45
Table 10: Specifications of the MPU-6050.....	49
Table 11: Specifications of the Arduino Nano v3.0	51
Table 12: Connections between a single MPU-6050 and Arduino Nano.....	53
Table 13: Connections between three MPU-6050s and Arduino Nano.....	54
Table 14: Design features of the tested razors.....	63
Table 15: Sign convention (used throughout this thesis)	69
Table 16: Joint angle limits (as in Table 2)	69
Table 17: Mean joint angles (in deg.), across all subjects,.....	70
Table 18: Mean joint angles as a fraction of joint angle limits	71
Table 19: Euclidean Norms of normalized joint angles.....	76
Table 20: Mean joint angles (in deg.), of a representative subject	77

List of Figures

Figure 1: Bones of hand, wrist and forearm	13
Figure 2: Wrist and forearm joints	14
Figure 3: Muscles and tendons	15
Figure 4: Three degrees of freedom	15
Figure 5: Radius rotates around the ulna during pronation	15
Figure 6: Neutral wrist, hand and forearm posture	16
Figure 7: Resting wrist and hand posture	16
Figure 8: RoM of wrist and forearm	17
Figure 9: Carpal Tunnel (cross section across wrist)	18
Figure 10: Carpal Tunnel Syndrome	19
Figure 11: Wrist motion coupling	21
Figure 12: Types of grip	24
Figure 13: Power grip with ulnar deviation	25
Figure 14: Basic variables of the working environment	27
Figure 15: Examples of body and hand maps	30
Figure 16: Comfort Questionnaire for Hand tools	31
Figure 17: Example of wrist posture measurement with an electrogoniometer	32
Figure 18: Example of EMG measurement	33
Figure 19: Example of pressure distribution measurement	34
Figure 20: Example of an IMU breakout board	36
Figure 21: Example of a dataglove	38
Figure 22: Potentiometric and Flexible electrogoniometers	39
Figure 23: Example of OMC system and reflective markers	40
Figure 24: Example of captured data representation	40
Figure 25: Example of Electromagnetic Tracking	42
Figure 26: Wrist and forearm motion tracking system	45
Figure 27: IMU placement & reference frames	46
Figure 28: MPU-6050 GY-521 breakout board	47
Figure 29: MPU-6050 block diagram	48
Figure 30: Arduino Nano board	51
Figure 31: Prototyping on a solderless breadboard	53
Figure 32: Permanent circuit	53
Figure 33: Wearable System	55
Figure 34: Local reference frame, rotated in relation to global reference frame	57
Figure 35: The three razors and their planes of motion	64
Figure 36: Leg regions	65
Figure 37: Three leg postures for three lower leg regions	66
Figure 38: Leg posture for the upper leg front region	66
Figure 39: Task sequence for right-handed subject	67
Figure 40: Sign convention (used throughout this thesis)	69
Figure 41: Bar graphs of normalized mean angles	75
Figure 42: Wrist and forearm motion graphs for a single subject	81
Figure 43: Grips for razors	82
Figure 44: Visualization of questionnaire results	83
Figure 45: Ulnar deviation with razor A is smaller than with razor C	85

Introduction

This thesis is organized in four major chapters:

Chapter A provides the background for this study. The anatomy of the human hand and forearm is presented, and principles of biomechanics are used to describe wrist and forearm joint motion. The adverse effects of extreme joint angles on comfort and health are illustrated.

Chapter B introduces research on the ergonomics of hand tool use. Principles for hand tool design and methods for hand tool evaluation are presented.

Chapter C introduces a review of modern wrist and forearm motion tracking techniques, and the development of a novel, wearable system, of much lower cost.

Chapter D illustrates the capabilities of the novel system, through an experimental research on razor handle design. A method is proposed for evaluating alternative design solutions, by capturing and analyzing motion data.

A. Human wrist and forearm anatomy

This chapter provides the background and justification for work, for this study.

A.1 Bones & Joints

The human hand is a complex organ containing 27 bones organized into the following skeletal components. Starting from the end of the forearm and moving toward the fingers, the hand comprises the wrist joint and the *carpal* bones (8 bones, arranged in two rows in the wrist area), the *metacarpal* bones (5 bones in the area of the palm), and the *phalanges* (14 bones of the digits—each finger has 3 phalanges and the thumb has 2).

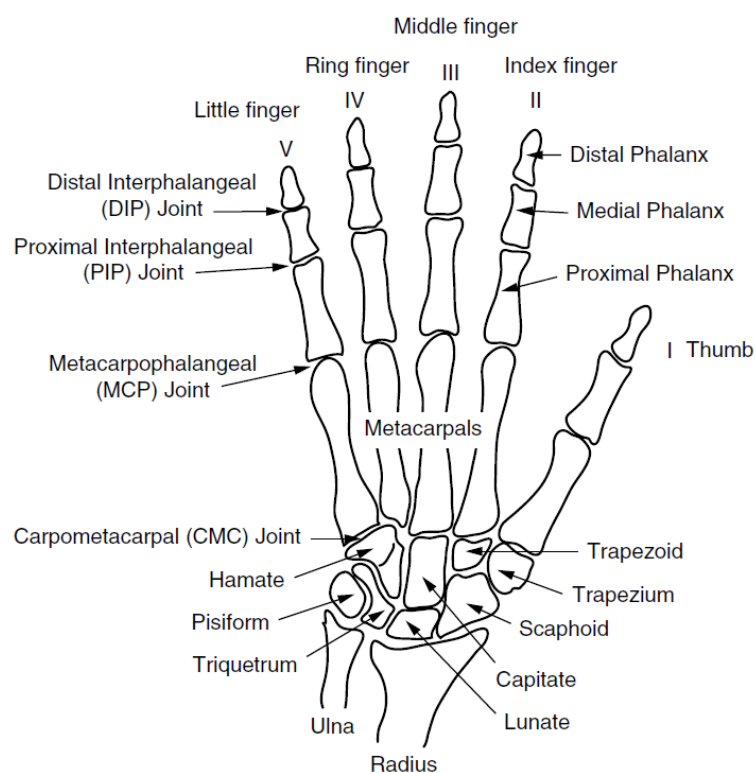


Figure 1: Bones of hand, wrist and forearm

The forearm consists of two bones, the *Radius* and *Ulna*, which articulate with the proximal row of the carpal bones, forming the *radiocarpal joint*. This joint –along with the *midcarpal joint* (between the proximal and distal rows of carpal bones), the *carpo-metacarpal joint* (between the distal row of carpal bones and the metacarpal bones), and the movement of individual carpal bones– permit the wrist to flex/extend and to abduct/adduct. The distal *radioulnar joint* (between the radius and ulna), which allows pronation/supination of the forearm, is proximal to the wrist joint and is generally not considered part of the wrist.

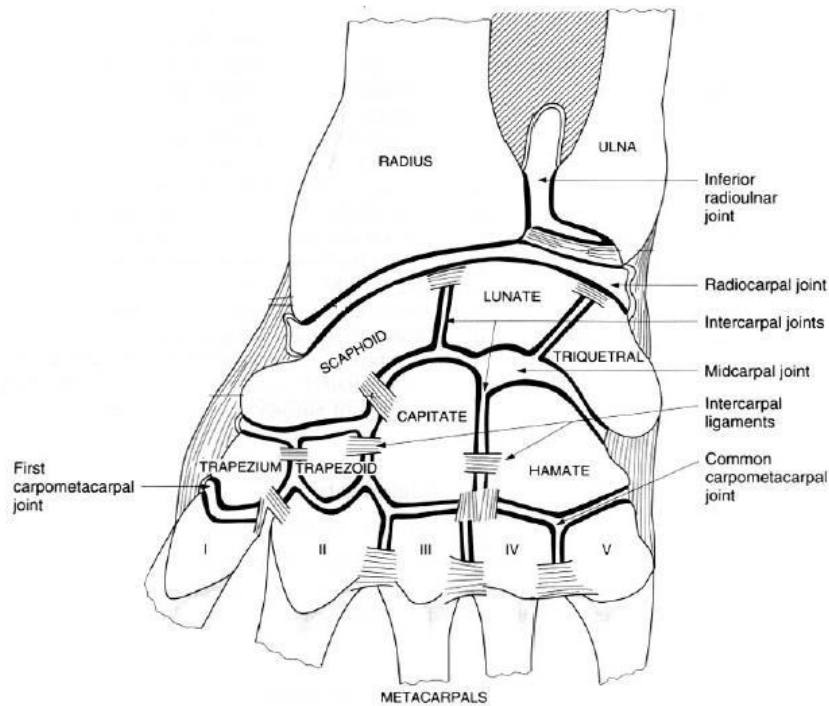


Figure 2: Wrist and forearm joints

While the motion of the bone structures mentioned above constitutes a complex phenomenon, one can view global wrist motion simply as the motion of the hand relative to the forearm. Global wrist motion, which is the focus of this research, can be reduced to a simple model with 3 degrees of freedom (see ch. “A.3 Kinematics”).

A.2 Muscles

There are 29 muscles that control movements of the hand, most of which are located in the forearm and are known as the *extrinsic* hand muscles. These muscles are responsible for wrist and major finger movements. Muscles that take their origin and insertion within the hand are known as the *intrinsic* hand muscles, and they are used for many finer finger and thumb movements, such as opposing the thumb, flexing/extending the fingers without moving the wrist, abducting/adducting the fingers, and so on.

Muscles at the back (*dorsal* side) of the forearm are responsible for extending the fingers and wrist, whereas muscles at the front (*ventral* side) of the forearm are responsible for flexing the fingers and wrist. These are called *extensor* and *flexor* muscles, respectively. Note that the flexor muscles of the forearm are much larger than the extensor muscles, which confirms that the hands are developed primarily to flex the fingers in order to grasp objects.

All major hand movements involve the use of *tendons*. Tendons connect muscle to bone, and when a muscle contracts, the force is transferred to the appropriate bone via the tendons, which causes the joint to move.

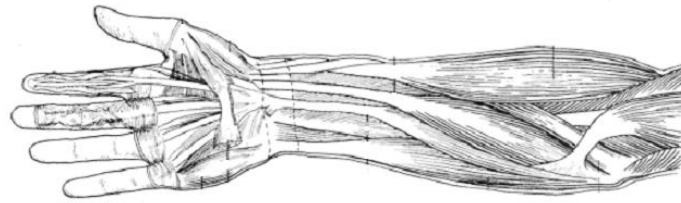


Figure 3: Muscles and tendons

A.3 Kinematics

According to the International Society of Biomechanics (Wu, et al., 2005) global wrist motion is typically considered as the motion of the second and/or third metacarpal with respect to the radius. The 3 degrees of freedom (DoFs) of the wrist and forearm, which involve multiple bones, are commonly described as the following:

- Pronation /Supination (P/S) of the forearm
- Flexion/Extension (F/E) of the wrist
- Radial/Ulnar deviation (R/UD) of the wrist

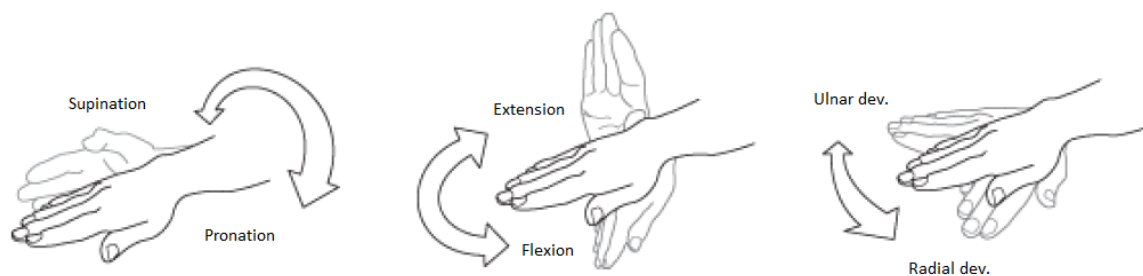


Figure 4: Three degrees of freedom

It is worth noting that pronation/supination occurs in the forearm, not in the wrist (as mentioned by convention in some cases). In supination the radius and ulna are parallel. During pronation the radius crosses over the ulna. Therefore, this motion is often considered as a rotation of the radius around the ulna (Charles, 2008). The fact that this rotation occurs near the wrist joint, while the bones are always almost parallel near the elbow, is useful for the placement of sensors on the arm (see ch. “C.2.1 Placement”).

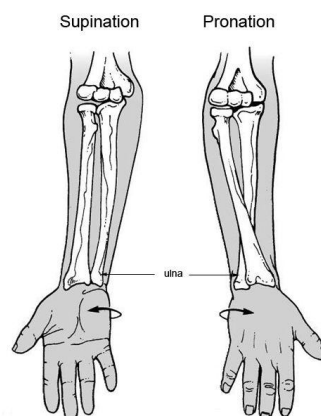


Figure 5: Radius rotates around the ulna during pronation

A.4 Neutral Posture

Neutral wrist and forearm positions (0° of P/S, F/E, R/UD) are clinically defined according to the recommendations of the *International Society of Biomechanics* (Wu, et al., 2005): For F/E and R/UD, the wrist is in neutral position when the *third metacarpal* long axis is parallel to the long axis in the *radius*. For P/S, the forearm is in neutral position when the elbow is flexed 90° and the (radially abducted) thumb is pointing to the shoulder. In other words, the neutral position for F/E and R/UD is when the longitudinal axes of the hand and forearm are in parallel (meaning the dorsal side of hand and forearm are one the same plane) and also P/S when the palmar side of the hand is facing the body.



Figure 6: Neutral wrist, hand and forearm posture

However, according to Lee and Jung (2014), to achieve the posture defined above requires intentional force exertion to flatten the hand and wrist. A *resting* hand posture is one where no exertion of force is required. In other words, it is where the musculoskeletal system is in equilibrium, without any conscious muscle activity. For the wrist, this is achieved in slight extension, while the fingers are curled. Therefore, resting and neutral wrist postures may be considered discrete, depending on the definition of the neutral position. Throughout this thesis, we consider the neutral position to be identical to the resting position.



Figure 7: Resting wrist and hand posture

A.5 Ranges of Motion

Wrist joint *ranges of motion* (RoM) have been investigated by various researchers, but no clear consensus has been reached. There are significant interpersonal differences regarding this characteristic, while the posture of other nearby joints affects the amplitude of motion of the wrist and forearm joints. Moreover, inconsistency in study

results could partly be attributed to the accuracy and repeatability of the measurements, depending on the technology used in the experiments.

Li, Kuxhaus, Fisk, and Christophel, (2005) cited multiple studies on wrist joint RoM and calculated mean values derived from those studies, leading to a more representative conclusion: 63° flexion, 66° extension, 38° ulnar deviation and 21° radial deviation. Standard deviations usually range from 10° to 20° for flexion and extension and from 7° to 12° for radial and ulnar deviation, in most studies (Schoenmarklin & Marras, 1993; Crisco, Heard, Rich, Paller, & Wolfe, 2011), which provides an indication of the level of interpersonal differences.

The RoM of forearm rotation, as cited by (Hale, Dorman, & Gonzalez, 2011; Paschoarelli, de Oliveira, & Coury, 2008) is approximately 90° for pronation and 90° for supination. Standard deviations range from 20° to 25°, in some studies (Schoenmarklin & Marras, 1993). The neutral position of the forearm (0° of P/S), as described above, lies approximately in the middle of the total RoM.

The RoMs which are considered representative of the population for this study are summarized (see Table 1):

Table 1: RoM of wrist and forearm

Joint Motion		Amplitude (\pm St.dev.)
Forearm	Pronation / Supination	90° (\pm 20°) / 90° (\pm 20°)
Wrist	Flexion / Extension	63° (\pm 15°) / 66° (\pm 15°)
	Radial dev / Ulnar dev	21° (\pm 10°) / 38° (\pm 10°)

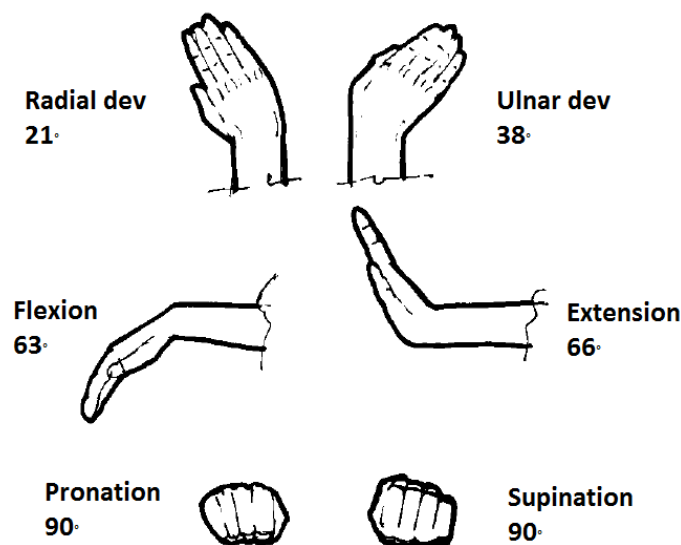


Figure 8: RoM of wrist and forearm

A.6 Negative Effects of Extreme Joint Angles

Working with the wrist and forearm in a neutral posture zone is a means of minimizing two issues: (a) *discomfort*, and (b) *risk of cumulative trauma* to the hand or wrist.

The *carpal tunnel* is the passageway between the carpal bones and a transverse flat ligament (*flexor retinaculum*) inside the wrist joint, through which the tendons that flex the fingers and the thumb pass, along with a nerve (the *median nerve*). A potential compression of this nerve can cause discomfort and pain – a condition referred to as *Carpal Tunnel Syndrome* (CTS).

Research shows that wrist deviation from the neutral position can increase interstitial fluid pressure within the carpal tunnel (Putz-Anderson, et al., 1997), and compress the median nerve and other structures, causing discomfort (Kuijt-Evers, 2007). *Carpal tunnel pressure* (CTP) increase is linked to an increase in wrist F/E, R/UD or/and forearm P/S (Werner, Armstrong, Bir, & Aylard, 1997). Extreme wrist positions, such as acute flexion combined with ulnar deviation, can prevent the free flow of blood into the palm of the hand, whereas it flows freely into the palm with the hand near the neutral posture.

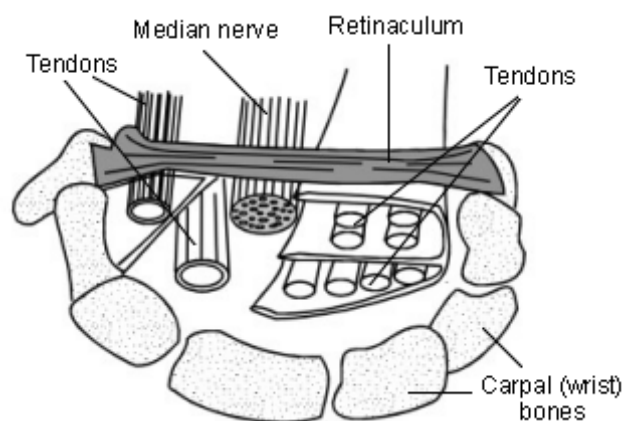


Figure 9: Carpal Tunnel (cross section across wrist)

Furthermore, when a non-neutral posture is assumed, some of the body's muscles are forced to provide supplementary support to compensate for the uneven weight distribution created by the non-neutral position. This compensatory muscle activity places the body's muscles, tendons, ligaments, and joints at risk for overloading and injury (Schall, 2014). The risk is further exacerbated when the non-neutral postures are held continuously (often referred to as "static postures"), are performed repeatedly, or are accompanied by forceful muscle exertions (Carey & Gallwey, 2002; Putz-Anderson, et al., 1997).

Discomfort is the precursor to more prolonged pain and perhaps a *musculoskeletal syndrome* (Carey & Gallwey, 2002; Mital & Kilbom, 1992). In case of repeated exertions and excessive movements of the hand, disorders of the soft tissues (most frequently the tendons and nerves) may occur. These are called *cumulative trauma disorders* (CTDs) and common occurrences include *carpal tunnel syndrome* (CTS), *tendinitis* (also tendonitis) and *tenosynovitis*. Industrial workers (Schoenmarklin & Marras, 1993; Marras & Schoenmarklin, 1993; Lee, Nelson, Davis, & Marras, 1997; Spielholz, Bao, &

Howard, 2001), but also surgeons (Shimomura, Minowa, Kawahira, & Katsuura, 2016), dentists (Nevala, Sormunen, Remes, & Suomalainen, 2013), laboratory workers (Lintula & Nevala, 2006; Paschoarelli, de Oliveira, & Coury, 2008) are subject to work-related *musculoskeletal disorders* (MSDs) of the hand and wrist. Sometimes characterized as adverse health outcomes of “non-traumatic manual actions repeated over an extended period of time”, MSDs may fluctuate in severity from mild periodic symptoms to severe chronic and debilitating conditions.

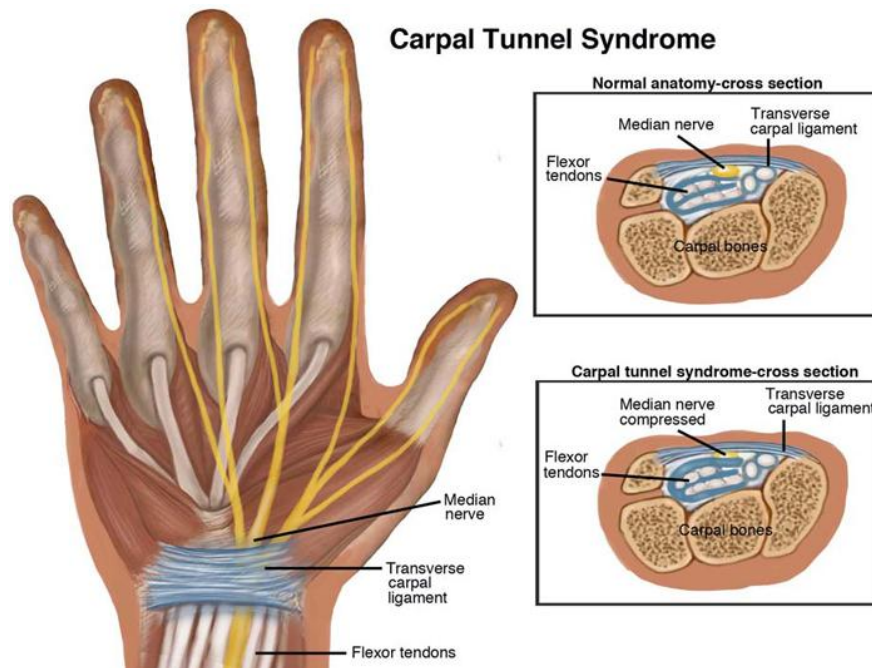


Figure 10: Carpal Tunnel Syndrome

Wrist deviation from neutral posture –in some form– is often used as a metric in ergonomic evaluation studies, for hand tools. Commonly, different prototypes are compared based on which requires less wrist deviation to operate (Nevala, Sormunen, Remes, & Suomalainen, 2013; Paschoarelli, de Oliveira, & Coury, 2008; Lee, Nelson, Davis, & Marras, 1997). Some researchers recommend that wrist motion amplitudes should be defined as percentages of maximum wrist mobility (RoM) in order to reduce the effect of individual differences (Carey & Gallwey, 2002; Kuijt-Evers, 2007; Lee, Nelson, Davis, & Marras, 1997).

A few studies (Hedge, 1998; Keir, Bach, Hudes, & Rempel, 2007; Werner, Armstrong, Bir, & Aylard, 1997; Carey & Gallwey, 2002) suggested that critical amplitudes of joint motion can be defined, above which wrist and forearm posture is considered non-neutral, because carpal tunnel pressure increases above a threshold. These limits are presented and averaged on the following table (see Table 2). However, it is questionable whether these limits are representative on their own, since it has been found that a combination of factors are responsible for discomfort and/or musculoskeletal disorders (Carey & Gallwey, 2002; Putz-Anderson, et al., 1997), while there is little consensus on the joint angle ranges (Keir, Bach, Hudes, & Rempel, 2007), because their definition is somewhat arbitrary. Nonetheless, they provide an approximate reference.

Table 2: Neutral zone amplitude

Study	Keir et al. (2005)	Hedge (1998)	Carey & Gallwey (2002)	Paschoarelli et al. (2008)	Average
Pronation	45°	-	-	45°	45°
Supination	45°	-	-	45°	45°
Flexion	38°	15°	25% ×RoM≈ 16°	15°	21°
Extension	27°	15°	25% ×RoM≈ 16°	15°	18°
Radial deviation	18°	15°	25% ×RoM≈ 5°	10°	12°
Ulnar deviation	12°	5°	25% ×RoM≈ 10°	15°	10°

A.7 Wrist Motion Coupling

Even though the anatomical axes of wrist and forearm motion are defined as presented above (P/S, F/E, R/UD), actual mechanical movement in those axes is not independent – there exists kinematic *coupling*. Several studies have examined this coupling, and how motion in one direction affects the motion capability in the others.

Importantly, wrist motion exhibits a form of coupling between flexion/extension and radial/ulnar deviation. In other words, F/E affects R/UD and vice versa. On the other hand, forearm rotation (P/S) has been found to have little effect on wrist F/E and R/UD (Li, Kuxhaus, Fisk, & Christophel, 2005).

Crisco et al. (Crisco, Heard, Rich, Paller, & Wolfe, 2011) stated that “the mechanical axes of the wrist are oriented obliquely to the anatomical axes” (see Fig. 11), meaning that natural wrist motion combines flexion with ulnar deviation and extension with radial deviation. Moreover, Li et al. (2005) and also Garg et al. (2014) attempted to quantify this coupling, which has been described as similar to a “dart thrower’s motion”.

In brief, studies have found that wrist F is accompanied by UD (and vice versa) and also wrist E is accompanied by RD (and vice versa). This fact is important for analyzing and explaining wrist motion data.

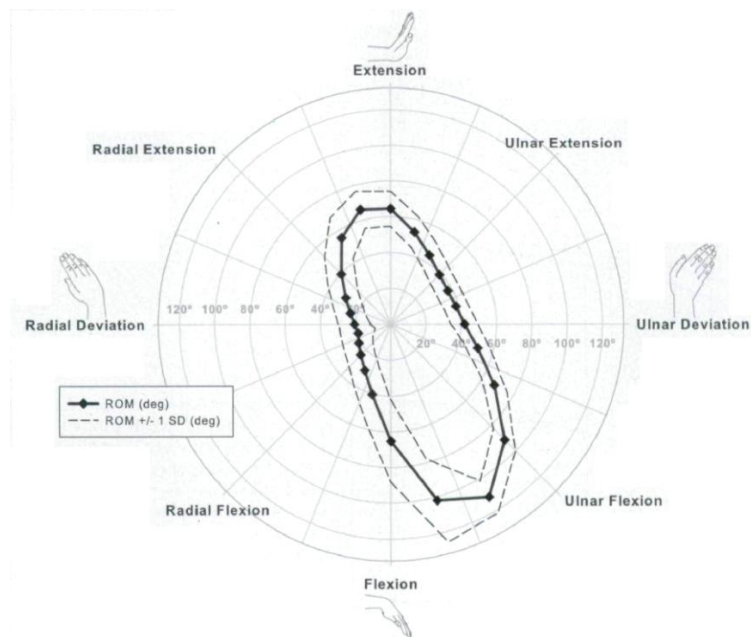


Figure 11: Wrist motion coupling (from Crisco et al. 2011)

A.8 Kinematic Modeling

Global wrist motion can be approximated by a simple model. The wrist has been variously modeled as a spherical, ellipsoidal (Chen X. , 2013), or universal joint (An, 1984; Tolani & Badler, 1996). In order to model wrist kinematics appropriately, one has to examine kinematic pairs, i.e. the constraints which a movement on one axis imposes on the other axes. Importantly, universal joints, unlike spherical and ellipsoidal joints, require by nature that one axis carry the other – there exists a kinematic hierarchy. In the following paragraphs we show that a universal joint is most consistent with studies of wrist biomechanics.

That the P/S axis should carry the F/E and R/UD axes is obvious: the wrist is clearly distal to the forearm. Pronation/supination of the forearm causes rotation of the wrist as a whole and therefore the axes of F/E and R/UD are rotated as well. However, the relation between the F/E and R/UD axes is less obvious.

Although the results of past studies have been conflicting, recent studies which investigate global wrist motion have found the R/UD axis to be distal to the F/E axis (Neu, Crisco, & Wolfe, 2001; Leonard, Sirkett, Mullineux, Giddins, & Miles, 2005). This implies that there exists a kinematic hierarchy in which the flexion/extension axis carries the radial/ulnar deviation axis.

In summary, studies of wrist biomechanics show a kinematic hierarchy in which the P/S axis carries the F/E and R/UD axes, and the F/E axis carries the R/UD axis. This kinematic description fits a universal joint with non-intersecting axes. Neither a spherical nor elliptical joint model could capture these characteristics of wrist kinematics. This choice will affect the representation of wrist orientation used in this thesis (see ch. “C.3.3.2 Inverse Kinematics”).



B. Ergonomics of hand tool use

According to the International Ergonomics Association, “Ergonomics/human factors is the scientific discipline concerned with the understanding of interactions among humans and other elements of a system, and the profession that applies theory, principles, data and methods to design in order to optimize human well-being and overall system performance.”

Generally, human factors include psychological/behavioral issues dealing with perception, cognition, decision making etc., in addition to questions related to the body. This thesis is mainly focused on physical interaction between humans and the artifacts they have created, from the scope of anatomy and biomechanics. The ergonomist applies the principles of anatomy, physiology and biomechanics to achieve a major mission: the control of musculoskeletal disease. Additional aims include the control of other diseases (e.g. cardiovascular disease) as well as providing a comfortable environment, leading to efficiency and decrease of human errors.

In this thesis, we examine the design of hand-operated devices or hand tools, by applying principles of biomechanics, in order to reduce discomfort, and the probability of musculoskeletal disease. The focus of this chapter is on the design principles that allow any hand-operated product to be used in a good posture that enables the user to sustain productive work in a safe manner.

Similar studies have examined other hand-operated tools, namely: pliers; industrial spray paint guns; orbital sanders; diagnostic ultrasound transducers; laparoscopic tools; instruments in dentistry; mechanical pipettes, and many more products (Dempsey, McGorry, Leamon, & O’Brien, 2002; Lee, Nelson, Davis, & Marras, 1997; Spielholz, Bao, & Howard, 2001; Paschoarelli, de Oliveira, & Coury, 2008; Yu, Lowndes, Morrow, Kaufman, Bingener, & Hallbeck, 2016; Nevala, Sormunen, Remes, & Suomalainen, 2013; Lintula & Nevala, 2006). Hand tools are part of everyday life for various professionals, such as industrial workers, craftsmen, laboratory workers, physicians, surgeons, etc.

B.1 Types of Grip

The use of hand-operated products requires humans to hold or grip the product in some way. It is important to note that the nature of the task is what primarily dictates the type of grip to be used, rather than the shape of the tool handle (Sperling, Dahlman, Wikström, Kilbom, & Kadefors, 1993). There are many variations, but the two most basic types of grip, as cited by Mital and Kilbom (1992), are the *precision grip* and the *power grip*. The most important variations of these types of grip are the following:

1. Precision grip:
 - a. Internal precision grip
 - b. External precision grip
 - c. Pinch grip
2. Power grip
 - a. Hook grip

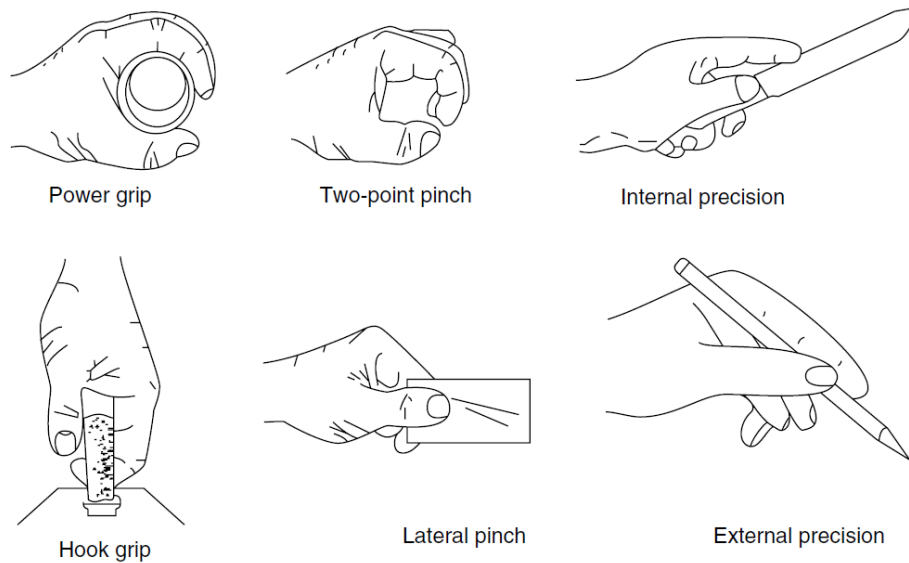


Figure 12: Types of grip (from Freivalds, 2011)

B.1.1 Precision Grip

The precision grip, in which the tool is pinched between the thumb and fingers, is primarily used for precision work, rather than exerting large forces. Whereas it offers a high degree of precision control, it provides only 20% strength of a power grip (Hedge, 1998; Mital & Kilbom, 1992). This is primarily due to the fact that a precision grip involves small (intrinsic) muscles of the hand, while a power grip involves larger muscle groups (extrinsic) (Sperling, Dahlman, Wikström, Kilbom, & Kadefors, 1993). The precision grip can be further classified into the following categories:

B.1.1.1 Internal Precision Grip

The internal precision grip is one where the tool handle lies internally to the hand, on the palmar side. The handle is held mainly by three fingers: the thumb, index and middle. Often, the 4th and 5th digits offer provide support on the handle, under the palm. In this grip, the tool handle is held almost parallel to the work surface. Examples of tools that are commonly held with this type of grip include cutters, surgical knives, wood carving tools, etc.

B.1.1.2 External Precision Grip

The external precision grip is one where the tool handle lies externally to the hand. Again, the 1st, 2nd and 3rd (and sometimes 4th) digits hold the handle. Support is provided by the skin and tissue between the thumb and index. Due to the positioning of the handle the 5th digit does not come into contact with the tool. In this grip, the hand tool is held at an angle relative to the work surface. Examples of tools that are held this way include pens/pencils, soldering irons, etc.

B.1.1.3 Pinch Grip

The pinch grip is used for smaller objects held by the edge, in which the “handle” is too short to reach the palm of the hand in order to form an internal or external precision grip. With this grip, objects are usually held between two fingers: the tip of the thumb and the tip (or the side) of the index (on occasion the middle finger is also used).

Sometimes, this grip is not listed separately from the previous two. Common examples include the use of a key in a keyhole, using tweezers, etc.

B.1.2 Power Grip

The power grip, in which the hand makes a fist around the tool handle, is used when the exertion of large forces is required. In this grip, contact is made mostly by the fingers and the thenar and hypothenar eminences –the areas of the palm under the thumb and little finger, correspondingly– while the centre of the palm is arched away from the surface of the handle. This is a natural posture for good reason: the center of the palm contains nerves and blood vessels close to the surface, rendering it a sensitive region of the hand; therefore pressure on that area should be avoided (Hedge, 1998).

A lot of research has been conducted to determine the optimum *grip span* for the power grip; namely the width that facilitates maximum grip force, since exerting force is the reason for using this specific grip. Consensus is not very clear on the subject, but a reference can be provided. Hedge (1998) suggests 4.5-5.9 cm, Radwin and Haney (1996) propose 4 cm or less, and Mital and Kilbom (1992) cite a grip span range of 5-6.5 cm, and a span of 5-10 cm for the case of double-handle tools like pliers, scissors etc.

It is the most powerful grip one can achieve because it uses the large (extrinsic) muscles in the forearm and in result, it is the most commonly used grip for larger hand tools. The direction of the exerted force varies according to the task, which could be carrying, pushing/pulling, rotating, and so forth. Typical examples of the power grip include hammering, using a power drill, using a wrench etc.

In the power grip, if the wrist is deviated from the neutral position, the force which can be generated by the hand decreases substantially. In extreme flexion/extension and/or radial/ulnar deviation, the hand can lose up to 40% of its maximum force exertion capacity (Hedge, 1998).



Figure 13: Power grip with ulnar deviation

B.1.2.1 Hook Grip

The hook grip can be viewed as a variation of the power grip. In the hook grip, one or more fingers hook onto a handle, holding the load, whereas the thumb is passive and used primarily to stabilize the load. This type of finger action is used where thumb counterforce is not needed, for instance in carrying scenarios (e.g. suitcase, bucket) and it does not cause stress on the skin over the metacarpophalangeal joints (MCP), which may develop calluses in some cases. The palm is almost flattened, due to pulling tension.

According to Mital and Kilbom (1992), this type of grip should be avoided if one intends to use the hand for precision tasks in the immediate future.

A list of all potential human grips would be endless, since there are several variations (e.g. finger positioning) to the ones described above, while there exist numerous special tasks that require other types or combination of grips. However, most ordinary industrial activities are completed with the types of grips discussed.

B.2 Hand Tools

B.2.1 Hand Tool Types

Non-powered tools include:

- Cutting, pinching, gripping tools (double-handle, e.g. knives, pliers, snips, cutters)
- Driving tools (e.g. screwdrivers, hand wrenches)
- Striking tools (e.g. hammers, axes)
- Struck or Hammered tools (e.g. punches, chisels, nail sets)
- Special purpose medical tools (e.g. scalpels, forceps)

Powered tools include:

- Cutting tools (saws, routers, shears and nibblers)
- Threaded fastener driving tools and hole preparation tools (nut-runners, wrenches, drills)
- Percussion tools (rammers, riveting tools)
- Abrasive tools (grinders, sanders, polishers)
- Special purpose medical tools (e.g. surgical staplers, endoscopes)

B.2.2 Hand Tool Design

From an ergonomic scope, the most important design features of a hand tool (Hedge, 1998; Mital & Kilbom, 1992) that have to be defined are:

- Product (as a whole)
 - Size/shape
 - Weight/balance
 - Human versus external power
 - Right/left/both hand use
 - Vibration characteristics
- Handle
 - Diameter/width
 - Length
 - Shape
 - Material/texture/friction
 - Design of trigger (for power tools)
 - Thermal/electrical insulation
 - Vibration isolation

However, when designing a hand tool, the designer has to consider the broader context of its use. This includes the user characteristics, task requirements, workplace environment and so on. This way, the user's manual capabilities and the task requirements in force, precision, duration, and repetition can be estimated. Sperling et al. (1993) proposed a suitable framework for defining the use context of a hand tool (see Fig. 14).

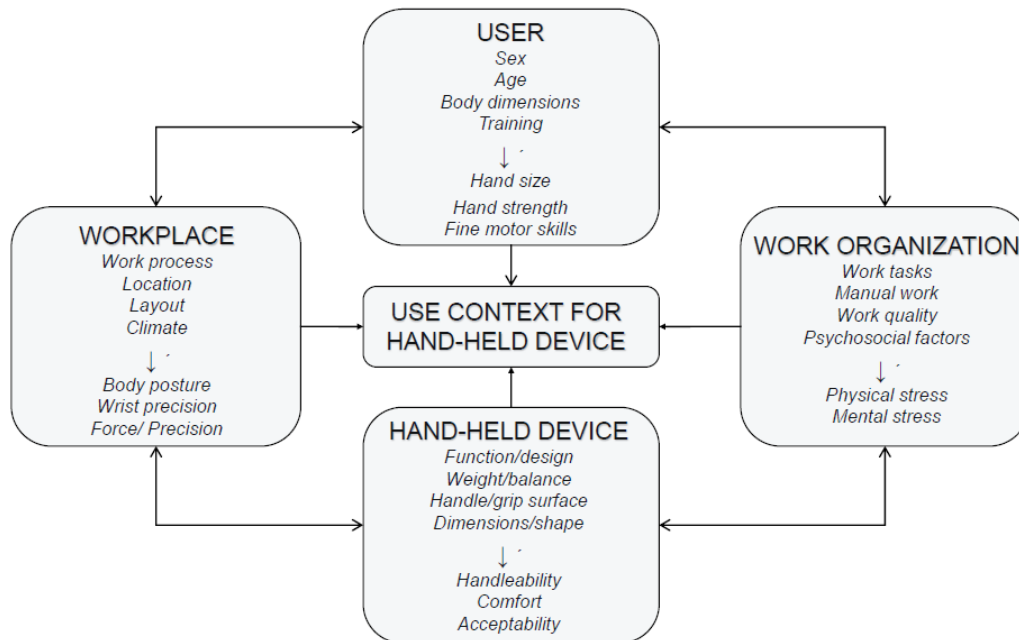


Figure 14: Basic variables of the working environment (adapted from Sperling et al., 1993)

B.2.3 Ergonomic Principles for Hand Tool Design

Principles for good ergonomic design of hand tools stem from fundamental requirements that apply to any hand-operated device. These basic requirements, for the design of the hand tool, adapted from Cacha (1999), are the following:

- Minimize wrist deviation from the neutral position
- Prevent tissue compression
- Minimize grip force & provide an optimal grip span
- Protect from heat/cold and vibration

We have already examined the reasons for *minimizing wrist deviation* (see ch. “A.6 Negative effects of extreme joint angles”) which are related to discomfort and CTDs, and we added the reduction of grip force capacity to those reasons. For example, this can be achieved by a bend in the tool shaft/handle or even a pistol shaped handle, rather than a straight design, if the task is appropriate.

Tissue compression can compress nerves and disrupt the flow of blood, also causing muscle soreness and discomfort (Aldien, Welcome, Rakheja, Dong, & Boileau, 2005; Björing, Johansson, & Hägg, 2002). A handle's shape and dimensions should serve to evenly distribute loads over as large an area of the palm as possible, in order to reduce

local compression (Kadefors, et al., 1993). If handles are too short, forces may be concentrated at the base of the palm, so for a power grip, the handle length should be greater than the hand width. Padding can also assist the even distribution of pressure. The padding should not be deeply contoured because this can create pressure points in the hands with forceful gripping, especially if the user's hand size does not match the contours.

Minimizing the force required to grip and operate the tool may mean minimizing its weight, improving its balance (position of the point of inertia not eccentric to the grip), increasing the mechanical advantage or making the tool powered. Moreover, providing an *optimal grip span* (see ch. "B.1.2 Power grip") facilitates the exertion of force by the user. Mechanical disadvantages in grip force occur if the fingers are excessively flexed around a small diameter handle or minimally flexed around a large diameter handle. These mechanical disadvantages lead to excessive grip force requirements which may result in fatigue tendinitis and the hazard of dropping the tool by accident. It's important to note that the handle size must suit the characteristics and capabilities of its target users and not necessarily those of the general population. Furthermore, the friction between hand and handle needs to be adequate, so that the user is not required to exert additional force to stabilize the handle (Hedge, 1998).

Symptoms associated with prolonged and repeated *vibration* exposure are collectively referred to as "Hand-Arm Vibration Syndrome" (HAVS) and may include episodic numbness, -tingling and blanching of the fingers, with pain in response to cold exposure- and reduction in grip strength and finger dexterity (Putz-Anderson, et al., 1997; Radwin & Haney, 1996). Furthermore, vibration of hand tools has been cited as a factor inducing Carpal Tunnel Syndrome, among other physical stress factors such as repeated exertions and extreme postures (Putz-Anderson, et al., 1997; Mital & Kilbom, 1992; Radwin & Haney, 1996). All hand tools and especially powered tools should be designed for adequate vibration absorption.

Cold and *heat* can also interfere with hand tool use. Cold hands can reduce strength, manual dexterity and tactile sensitivity (Radwin & Haney, 1996), while heat can cause discomfort and burns. Handles made of conductive materials can conduct heat to and from the hands, therefore the use of insulating materials is strongly recommended.

Finally, it is important to mention a few supplementary guidelines: The design should accommodate ambidextrous operation and tool use by different user groups. In addition, shoulder muscles should not be stressed for long periods of time, due to rapid fatigue. Tool design (depending on the task) should enable the user to hold it near the body during operation (Hedge, 1998).

B.3 On Performance and Comfort Metrics

From the ergonomics and usability perspective, evaluation of hand-operated products is about evaluating performance and comfort/discomfort for the user, as well as the risk of musculoskeletal disease. All of these factors are essential to the field of ergonomics, as we have mentioned in the beginning of this chapter.

Good functional performance of a hand tool equals an increase in productivity for a given task, which is of paramount importance, especially in an industrial environment. Depending on the task, the performance of a hand tool may be defined variously, from the level of quality of the output, to the time required for completing the task.

Comfort and discomfort are complex notions that lack a universal definition. Kuijt-Evers (2007) discusses previous research on the subject and concludes that, in using hand tools, comfort and discomfort can be viewed as two opposites on a continuous scale. However, researchers agree on an important issue—the nature of comfort/discomfort is purely subjective (Kuijt-Evers, 2007; Bisht & Khan, 2013). Therefore, the best way to measure comfort/discomfort is by questioning the users, although studies have tried to estimate perceived discomfort by directly measuring wrist posture, exerted force, pace etc. (Carey & Gallwey, 2002).

The issue of musculoskeletal disorders has already been discussed (see ch. “A.6 Negative effects of extreme joint angles”) and it is not irrelevant to comfort/discomfort; prolonged discomfort may imply a musculoskeletal disorder (Carey & Gallwey, 2002; Kuijt-Evers, 2007). Unnatural postures and repetitive forceful exertions are the major risk factors for hand/wrist trauma, thus these are the characteristics to be measured.

Several hand tool evaluation studies have been conducted in the past, with various objectives. Mainly, these studies aim to compare hand tools, recognize ergonomically well-designed tools, and also to contribute to the design community by offering new guidelines. In the following paragraphs, we discuss specific commonly measured characteristics in the evaluation and comparison of hand-operated products, which assist the examination of the factors mentioned above (comfort/discomfort, risk of musculoskeletal disease, performance).

B.3.1 Subjective Measurements

Subjective measurements are most common when hand tools are evaluated with respect to *comfort/discomfort*. Additionally, *perceived exertion* (RPE) and features of *usability* (Sperling, Dahlman, Wikström, Kilbom, & Kadefors, 1993; Bisht & Khan, 2013; Kuijt-Evers, 2007) can be subjectively evaluated, although all these issues are correlated. Usually, an overall preference or ranking of the evaluated tools is asked of the users participating in the study. The tools used to measure the above factors can be summed up to the following:

- Rating Scales
 - *Borg CR-10 scale*: respondents rate on a 6 to 20 scale, which is linked to heart rate and used for rating perceived exertion (RPE). Alternatively, a range of 0 to 10 is used for various ratings.
 - *Visual Analog Scale (VAS)*: respondents indicate a position along a continuous line (e.g. 0-100 mm line)
 - *Likert scale*: often 5 or 7 response levels are available, although one can use an even-point scale, where the middle “neutral” option is not available
- Body/Hand map, complemented by a discomfort rating scale for each region (see Fig. 15)

- Short answer questions
- Think-aloud responses during the test or interviews

A few issues, on which hand tools are commonly rated subjectively, are:

- *Comfort/discomfort or pain* (Paschoarelli, de Oliveira, & Coury, 2008; Lee, Nelson, Davis, & Marras, 1997; Spielholz, Bao, & Howard, 2001)
- *Perceived force exertion* (RPE) (Nevala, Sormunen, Remes, & Suomalainen, 2013; Shimomura, Minowa, Kawahira, & Katsuura, 2016; Lintula & Nevala, 2006; Spielholz, Bao, & Howard, 2001; Yu, Lowndes, Morrow, Kaufman, Bingener, & Hallbeck, 2016)
- *Usability* features, e.g. stability, fit in hand (Nevala, Sormunen, Remes, & Suomalainen, 2013; Shimomura, Minowa, Kawahira, & Katsuura, 2016; Yu, Lowndes, Morrow, Kaufman, Bingener, & Hallbeck, 2016)

Kuijt-Evers (2007) proposed a questionnaire, called “Comfort Questionnaire for Hand tools” (CQH), which focuses on rating several hand tool characteristics related to comfort/discomfort, on a rating scale (7-point Likert scale) (see Fig. 16). This questionnaire includes several descriptors of comfort/discomfort (e.g. pressure on the hand, handle feeling) and provides a more detailed assessment of a hand tool, than a single comfort/discomfort question. However, it is debatable whether this approach fits all hand product evaluation cases; for example, tools that are used for precision work rarely cause “blisters”. We recommend that it is mainly used as a source for inspiration for composing a tailored questionnaire for each study.

Subjective methods are simple to distribute, low in cost, are applicable to a wide range of situations, and may provide a useful estimate of work exposure in a short time. Self-report studies have validity issues, however, as participants may exaggerate or under-report information in an effort to make their working situation seem better or worse to an investigator. They also often lack precision and accuracy that may result in exposure misclassification, thus they are often used in conjunction with objective methods (Schall, 2014; Bisht & Khan, 2013).

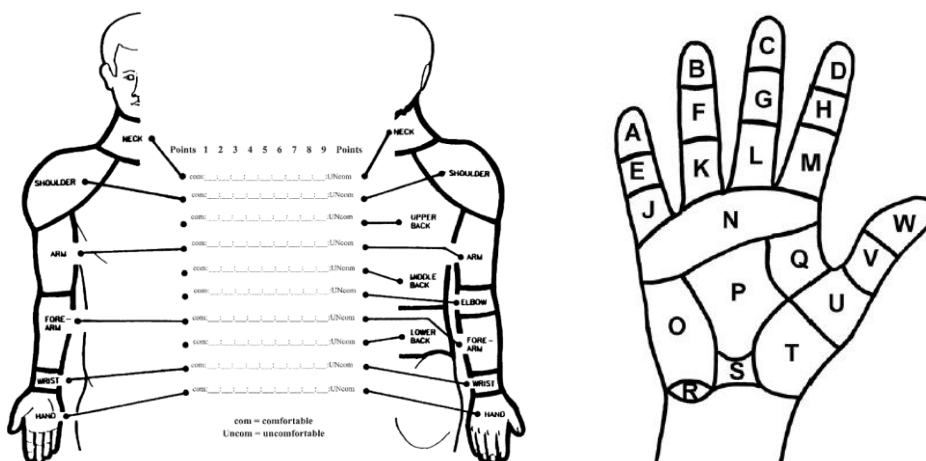


Figure 15: Examples of body and hand maps

Comfort Descriptors							
This hand tool	Totally disagree	•	Disagree somewhat	•	Agree somewhat	•	Totally agree
Fits the hand	1	2	3	4	5	6	7
Is functional	1	2	3	4	5	6	7
Is easy in use	1	2	3	4	5	6	7
Has a good force transmission	1	2	3	4	5	6	7
Is a high quality tool	1	2	3	4	5	6	7
Has a nice-feeling handle	1	2	3	4	5	6	7
Offers a high task performance	1	2	3	4	5	6	7
Provides a high product quality	1	2	3	4	5	6	7
Looks professional	1	2	3	4	5	6	7
Needs low hand grip force supply	1	2	3	4	5	6	7
Has a good friction between handle and hand	1	2	3	4	5	6	7
Causes an inflamed skin of hand	1	2	3	4	5	6	7
Causes pressure on the hand	1	2	3	4	5	6	7
Causes blisters	1	2	3	4	5	6	7
Feels clammy	1	2	3	4	5	6	7
Causes numbness and lack of tactile feeling in hand	1	2	3	4	5	6	7
Causes cramped muscles	1	2	3	4	5	6	7
Comfort after use							
This hand tool is	Very uncomfortable	•	A little uncomfortable	•	A little comfortable	•	Very comfortable
	1	2	3	4	5	6	7

Figure 16: Comfort Questionnaire for Hand tools (Kuijt-Evers, 2007)

B.3.2 Objective Measurements

Objective measurements are robust methods of evaluating hand tools. They provide a sound representation of reality, without subjective distortion and they can serve as means to explain subjective responses. They provide the most precise estimates and informational content for estimation of exposure to physical risk factors associated with MSDs. The challenge lies in selecting the appropriate parameters to be gathered. The most common objective measurements are addressed in this section.

- Working posture
- Muscle activity
- Performance
- Pressure and force distribution

However, these methods are often accompanied with high equipment costs and time demands for calibration and analysis. Field-based direct measures of physical exposure also have limitations in challenging work settings and generate a large amount of raw data that must be appropriately reduced and synthesized to produce relevant summary measures (Schall, 2014).

B.3.2.1 Working posture

The working posture of a hand tool user is dictated by the task to be completed, the workplace layout and the design of the tool. However, whole body monitoring is not a prime interest in hand tool evaluation. Specifically, wrist and forearm motion is of essence in hand tool evaluation studies, especially in combination with force exertion (Kadefors, et al., 1993), due to the reasons examined in a previous chapter (see ch. “A.6 Negative effects of extreme joint positions”).

Many studies examine postures of wrist and forearm in industrial tasks (Lee, Nelson, Davis, & Marras, 1997; Spielholz, Bao, & Howard, 2001; Dempsey, McGorry, Leamon, & O'Brien, 2002) or medical tasks (Paschoarelli, de Oliveira, & Coury, 2008; Nevala, Sormunen, Remes, & Suomalainen, 2013; Lintula & Nevala, 2006; Yu, Lowndes, Morrow, Kaufman, Bingener, & Hallbeck, 2016). As we have repeatedly stated in this thesis, extreme wrist and forearm joint postures (high percentage of range of motion) are accompanied by high discomfort levels and could lead to musculoskeletal disorders, when accompanied by other factors such as high exertion of force (Carey & Gallwey, 2002; Kuijt-Evers, 2007).

Suitable sensors and measurement technologies for wrist motion tracking include:

- Electronic goniometers
- Inertial Measurement Units
- Optical Motion Capturing systems

Wrist and forearm motion tracking techniques are discussed extensively in the following chapter (see ch. "C.1 Overview of available solutions")

When designing other tools or workspaces, the posture of other body parts may also be important; for instance the elbow, shoulder, back and neck (Björing & Hägg, 2000). However, these are not the focus of this Diploma thesis.



Figure 17: Example of wrist posture measurement with an electrogoniometer

B.3.2.2 Muscle Activity

It is desirable to create tools that generate lower levels of muscle activity of the user, for a given task, which implies lower levels of force requirements. High levels of force exertion are highly linked to discomfort (Carey & Gallwey, 2002) and constitute a cause for CTDs (Radwin & Haney, 1996).

Surface electromyography (EMG) is often used to obtain muscle activity, which is indicative of force requirements and muscle fatigue (Nevala, Sormunen, Remes, & Suomalainen, 2013; Shimomura, Minowa, Kawahira, & Katsuura, 2016; Lee, Nelson,

Davis, & Marras, 1997; Lintula & Nevala, 2006; Spielholz, Bao, & Howard, 2001). Adhesive electrodes are placed on the skin, above the desired muscle groups and muscular activity is measured and calculated as a percentage of the activity during maximal voluntary isometric contraction (MVC).

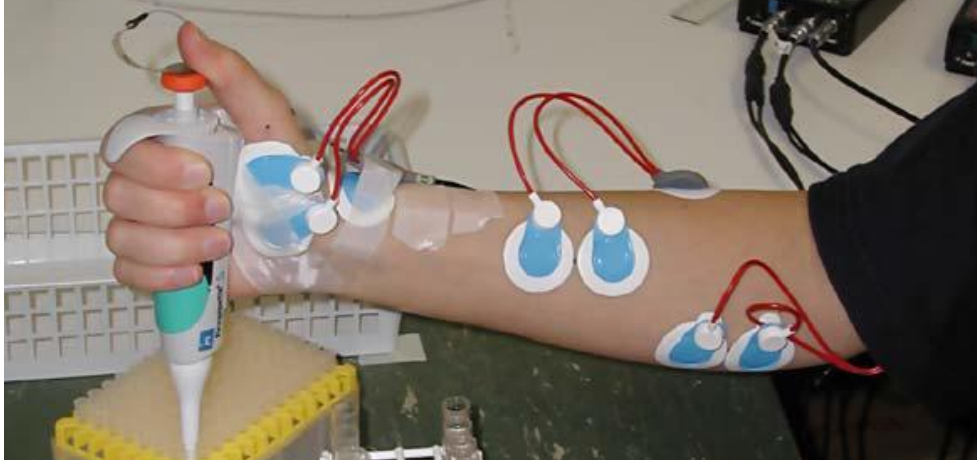


Figure 18: Example of EMG measurement

B.3.2.3 Performance

The performance of a hand tool can be assessed by measuring various parameters (Yu, Lowndes, Morrow, Kaufman, Bingener, & Hallbeck, 2016):

- Time required for completing a task / productivity
- Quality of the output, depending on the task
- Number/frequency of errors

B.3.2.4 Pressure and Force Distribution

Several studies assess force distribution and pressure on the hand of the user (Aldien, Welcome, Rakheja, Dong, & Boileau, 2005; Björing, Johansson, & Hägg, 2002). Contact stress is related to the force and the area of contact between the handle and the palm and described by the pressure exerted against the skin.

Research suggests that it is best to avoid force concentration on small areas of the palm, as forces are transmitted through the skin and compress underlying blood vessels, tendons and nerves (Kadefors, et al., 1993; Hedge, 1998; Radwin & Haney, 1996) (see ch. “B.2.3 Ergonomic principles for Hand tool design”). Specifically, the centre of the palm is more sensitive, since the underlying nerves and blood vessels are close to the surface (Hedge, 1998).

Moreover, pressure on the fingers may be a causative factor for *vibration-induced-white fingers* (VWF), where blood flow to the fingers is obstructed, since the amount of transmitted and absorbed vibrations increase with higher pressure on the fingers (Björing, Johansson, & Hägg, 2002). Discomfort and pain are also linked to local pressure peaks (Kuijt-Evers, 2007; Aldien, Welcome, Rakheja, Dong, & Boileau, 2005).

Pressure sensors generally measure the strain of a material (of known properties) due to applied force over an area (pressure), in order to indirectly determine applied pressure. Common pressure sensors technologies include:

- Capacitive type
- Resistive type
- Piezoelectric type

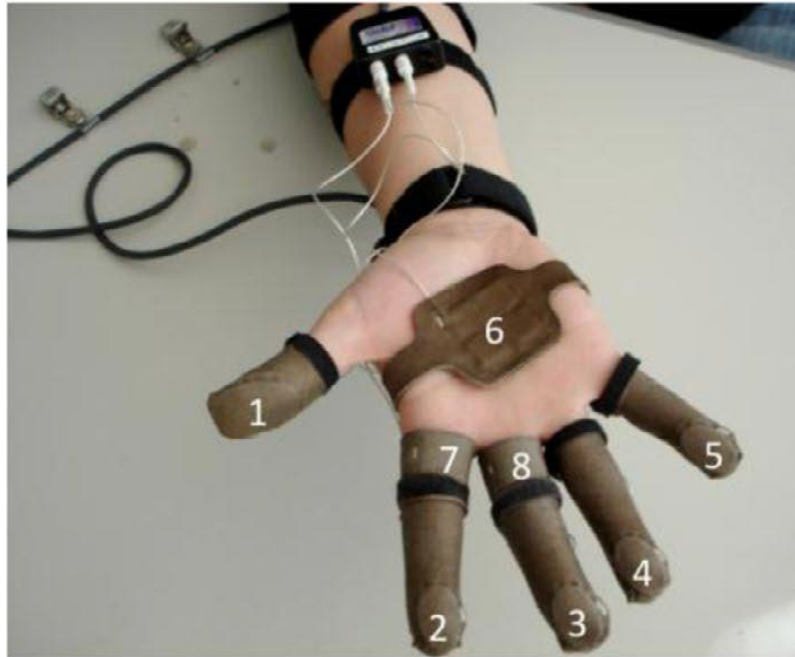


Figure 19: Example of pressure distribution measurement system

C. Wrist & Forearm Motion Tracking

In this thesis, we develop an inexpensive system for measuring wrist joint and forearm motion. This chapter includes an overview of available solutions for wrist & forearm motion tracking, for various scientific needs, although our main focus is hand-tool evaluation. We discuss our choice of technology –*Inertial Measurement Units* (IMUs), and its characteristics. A description of our tracking system and its development are included.

C.1 Overview of Available Solutions

There are various technological solutions that enable tracking of wrist joint and forearm motion, as well as other joints. Each of them has different advantages and disadvantages, which also depend on the context of the measurements (e.g. laboratory versus workplace, moving around versus sitting). Determining joint angles is important not only to ergonomics specialists, but also to rehabilitation and biomedical engineers as well as physiotherapists. We discuss available solutions, in multiple levels (from basic sensor technology, to commercially available systems) in the following paragraphs.

C.1.1 Inertial Sensors and Magnetometers

Electromechanical sensors, which can be mounted on body parts (e.g. clothing, gloves, adhered directly on the skin) are: *accelerometers*, *gyroscopes*, *magnetometers*.

Traditionally, they are used in aircrafts, ships, and land vehicles to provide a reference for attitude and heading information, but they have proved to be a convenient method for capturing human posture and movement information. Inertial sensors are *self-contained* (no need for external elements) since they directly measure physical quantities, meaning that they are not constrained neither in motion nor to any specific environment or location (Sabatini, 2011).

Micro-machined *accelerometers* are small, relatively cheap and have low energy consumption (Luinge, Veltink, & Baten, 2007). They measure linear acceleration and gravity and can be used as an inclinometer for movements in which the acceleration can be neglected with respect to gravity. Their limitations include sensitivity to noise, and the fact that rotations about the line of gravity cannot be assessed by an accelerometer (Schall, 2014).

Gyroscopes measure angular velocity, which can be used to estimate a change in orientation, by integration (Luinge, Veltink, & Baten, 2007). Fundamentally, a mechanical gyroscope is a gimbaled wheel or disk whose axle is free to take any orientation and can be set to rotate in any plane. The drawback of gyroscopes is that the estimation of orientation change is prone to integration error, which increases over time –a phenomenon called *drift* (Schall, 2014). Because of this, gyroscopes are rarely used alone for human motion tracking.

Magnetometers are used to measure the local magnetic field vector (direction and magnitude), which usually originates primarily from the Earth. However, the fixed

magnetic field, and thus the derived orientation, is disturbed in the vicinity of ferromagnetic metals and by electronic equipment generating magnetic fields (Luinge, Veltink, & Baten, 2007). The data provided by magnetometers alone is of little use for ergonomic assessment of human posture; rather, they are used to provide additional information about orientation (Schall, 2014).

Several combinations of the sensors described above have been proposed in order to overcome the drawbacks of the separate sensors. For instance, a gyroscope is less sensitive to linear mechanical movements, the type of noise that accelerometer suffers from, but it is susceptible to drift problems. Properly averaging the data that comes from accelerometers and gyroscopes can produce a better estimate of orientation than obtained using one type of sensor alone. When a triaxial accelerometer, a triaxial gyroscope, and potentially a triaxial magnetometer are combined, the sensor system is called an *Inertial Measurement Unit (IMU)*. The combination of sensors requires sensor data fusion algorithms.

C.1.1.1 Inertial Measurement Units (IMU)

With the progress of Micro-electromechanical Systems (MEMS) technology nowadays, inertial sensors are becoming smaller, low-cost and can obtain accurate inertial measurements, with limited power consumption (Chen X. , 2013). IMUs, containing inertial and sometimes magnetic sensors, have proven to be accurate in estimating body segment orientations without the need for external actuators or cameras (Kortier, Sluiter, Roetenberg, & Veltink, 2014). These devices can be implemented in textile clothing easily without impairing the freedom of movement. In other words, they are cheap, easy to set up, small in size and non-intrusive to the subject, while they also provide the option of wireless communication.



Figure 20: Example of an IMU breakout board (MPU-9250)

However, the use of IMUs for human motion tracking comes with a few disadvantages. *Drift* issues, which are inherent in gyroscope components of an IMU, still occur, even though accelerometers and magnetometers help correct for the drift (Chen X. , 2013; Schall, 2014). Moreover, human *soft tissue artifacts* (or skin artifacts) are a main source of errors (Chen X. , 2013; El-Gohary & McNamers, 2012), no matter the wearable sensors are mounted on a garment or directly attached to skin. This is caused by the fact that the skin surface is not rigidly connected to the underlying bone; therefore the skin can be deformed and displaced with respect to the bone, moving the placement of sensors. This movement represents an artifact, which affects body posture estimation (Leardini, Chiari, Croce, & Cappozzo, 2005). Due to the two issues explained above (drift, sensor displacements), a *re-calibration* procedure during utilization is often necessary to

mitigate estimation errors (Kortier, Sluiter, Roetenberg, & Veltink, 2014), which costs time and may disrupt the experiment.

Another issue to be taken into consideration when using IMUs is the *placement* of the sensors on the body. Determining the exact location of the sensors is an important task of the experiment design, because this affects the level of skin artifact occurrence, while also taking into account the complex anatomical structure of joints and body segments (Chen X. , 2013).

Data fusion algorithms are required to combine the information originating from multiple sensors into a single useful output, which compensates for the limitations of each individual sensor, while canceling noise. Such algorithms include *Kalman filters* (linear models) and their extended versions (non-linear models), the *complementary weighting algorithm*, the *Madgwick* filter and others (Madgwick, Harrison, & Vaidyanathan, 2011; Schall, 2014; Sabatini, 2011; El-Gohary & McNames, 2012). Developing and implementing proper data fusion algorithms, that produce accurate orientation estimation on the field and not only within controlled laboratory environment, is of utmost importance for human motion capture, together with evolving MEMs technology.

The price of a single IMU ranges from €3 to €1000 depending on its specifications and purpose. Most IMUs however cost under €50, with adequate accuracy and precision. In order to create a wrist and forearm tracking system, one would need at least 2 IMUs and a microcontroller, meaning that the actual price can start from as little as ~€20 or it could be quite high if one uses expensive sensors.

In summary, the advantages and disadvantages of IMUs are:

Table 3: Advantages and disadvantages of IMUs

+	-
Low-cost	Drift
Free movement in space (if wireless)	Frequent re-calibration
Portable	Skin artifact

C.1.1.2 Datagloves

The term “dataglove” describes wearable gloves, which combine various mounted sensors (e.g. IMUs, magnetic sensors, flex sensors) in order to allow accurate hand tracking. Plenty of commercially available datagloves exist, and they are used as input devices for human-computer interaction (e.g. Virtual Reality, gaming applications) or less commonly as a hand tracking method for other purposes.



Figure 21: Example of a dataglove

Generally, these systems are used for tracking motions of the fingers and wrist, although they can be modified to capture forearm motion. This thesis is not focused on finger posture, thus datagloves provide more features than necessary for our purposes. For the same reason, these systems are not commonly used in hand tool evaluation and work exposure studies.

A general disadvantage of datagloves is the lack of user customization for individual subjects' hands and obstruction of tactile sensing from the palmar surface of the hand, which is important in testing hand tools. Often this inherently goes with mounting space required for embedding the sensors in clothing (Kortier, Sluiter, Roetenberg, & Veltink, 2014). Moreover, commercially available datagloves are costly (€500 - €13.000).

To summarize, the advantages and disadvantages of datagloves are:

Table 4: Advantages and disadvantages of datagloves

+	-
Free movement in space (if wireless)	Fit on each subject
Portable	Obstruction of tactile sensation
	Focused on fingers, not wrist and forearm

C.1.2 Goniometers

Goniometers measure the angle between two joints but not the inclination with respect to gravity (as accelerometers do). Two types exist: mechanical and electronic goniometers. The former are primarily used in clinical settings, by physicians and are not applicable to continuous, dynamic motion tracking, thus they present no interest for this thesis. The latter, named *electrogoniometers*, are a popular method for wrist motion tracking –arguably the most popular in hand tool evaluation studies– and these are the point of focus of this section.

There exist two types: *potentiometric* and *flexible* electrogoniometers. Flexible electrogoniometry is advantageous compared to potentiometric goniometry, with better adjustment to body parts and less sensitivity to misalignment problems (Wang, King,

Do, & Nenadic, 2011). These devices consist of two plastic end blocks that are separated by a flexible spring, protecting a wire (see Fig. 22b). Flexible electrogoniometers incorporate sets of strain gauge elements that measure bending strain of the wire along or around a particular axis, by changing their electrical resistance. A goniometer should also accommodate length changes that are required during angular movements.

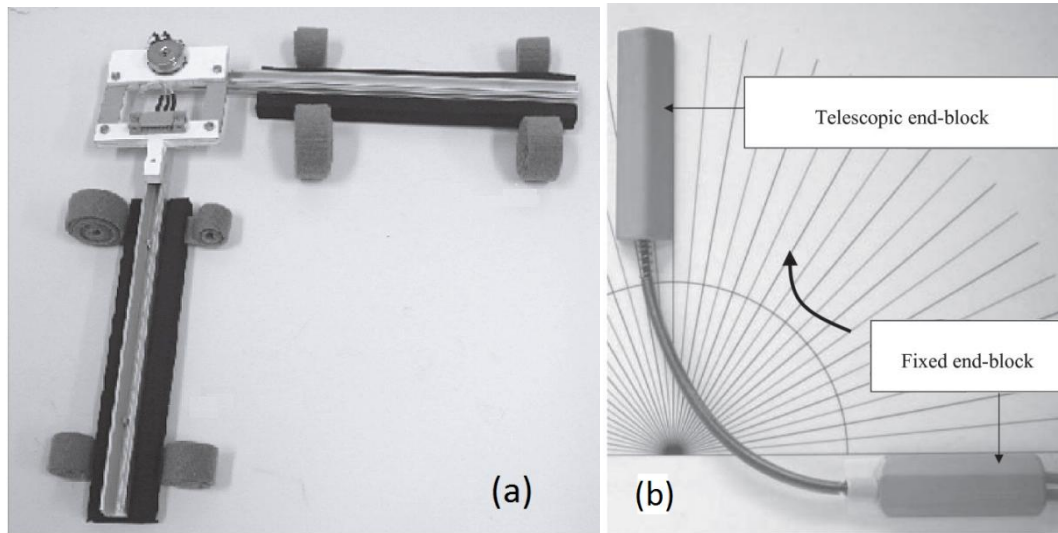


Figure 22: (a) Potentiometric and (b) Flexible electrogoniometers

Biaxial (or twin-axis) electrogoniometers measure orthogonal rotational axes simultaneously (e.g. wrist flexion/extension and radial/ulnar deviations), while *torsiometers* are used to measure angular twisting (e.g., forearm pronation/supination) as opposed to bending (Freivalds, 2011).

A common problem arises in the application of the goniometer across the wrist joint during measurement of wrist flexion/extension and radial/ulnar deviation. The distal end block is mounted on the dorsal surface of the hand over the third metacarpal, and the proximal end block is mounted on the dorsal surface of the forearm. When the forearm rotates, however, the distal and proximal end blocks do not rotate together, causing twist in the goniometer wire. This twist is primarily the result of the kinesiology of forearm rotation. The radius rotates around the ulna, causing the surface of the forearm at the wrist to rotate with the hand while the surface of the forearm at the elbow has little rotation (Buchholz & Wellman, 1997). The proximal end block is attached toward the middle of the forearm and in result it rotates less than does the distal end block. The resulting twist leads to *cross talk* and *zero drift* errors because the strain gauges that define the measurement axes are rotated with respect to the movement planes of the wrist. Such common measurement errors occur as a result of the complexity of human joints and should be continually corrected (Freivalds, 2011). A way to achieve this directly is by reducing the distance between the two end blocks (shorter wire), which reduces the wire twist (Buchholz & Wellman, 1997). Furthermore, because goniometers cross a joint, they need to be exactly aligned with the joint rotation center (Luinge, Veltink, & Baten, 2007).

While simple in their construction and use, electrogoniometers may restrict natural movement, causing participants to modify their natural motion patterns (Schall, 2014).

Although commercial electrogoniometers are available (~€700), one can build a custom electrogoniometer, using low-cost *flex sensors* (~€60 for the whole system) (Wang, King, Do, & Nenadic, 2011).

To recapitulate, the advantages and disadvantages of electrogoniometers are:

Table 5: Advantages and disadvantages electrogoniometers

+	-
Simple operation	Intrusive / restricts natural movement Cross talk

C.1.3 Optical Motion Capture (OMC)

Optical motion capture (OMC) systems make use of one or usually more video cameras to quantify joint angles. OMC typically employs an array of high-speed cameras arranged around the perimeter of a measurement volume. These systems are regarded as the gold-standard of human motion analysis (Chen X., 2013; Schall, 2014). There exist two types of OMC systems: *marker-based* and *marker-less*.

Marker-based systems include bright markers placed at various locations on the patient's body, depending on the body segment of interest. These markers are either active (e.g. Infrared – IR, Light Emitting Diodes – LEDs) or passive (retroreflective elements). The system keeps track of the coordinates of each marker, and computer software processes this information to determine the angle on the body segments of interest. Marker-less systems make use of the contours of body segments instead of markers, to estimate body posture. Both methods can be used for various body parts, not only the upper limbs.

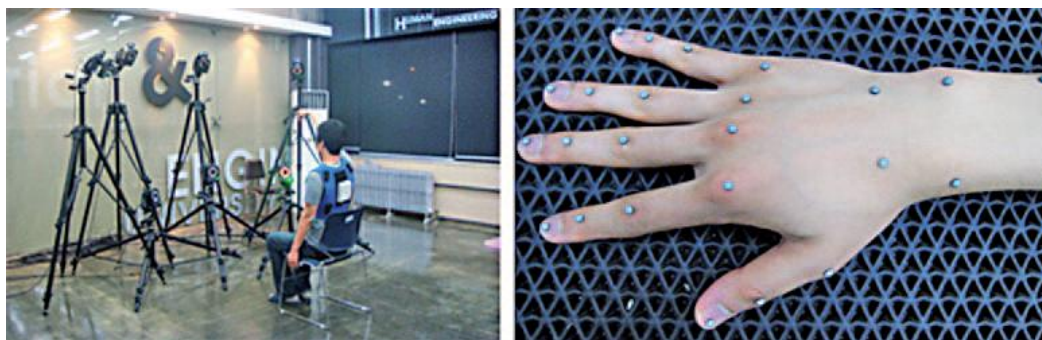


Figure 23: Example of OMC system (left) and reflective markers on hand and forearm (right)

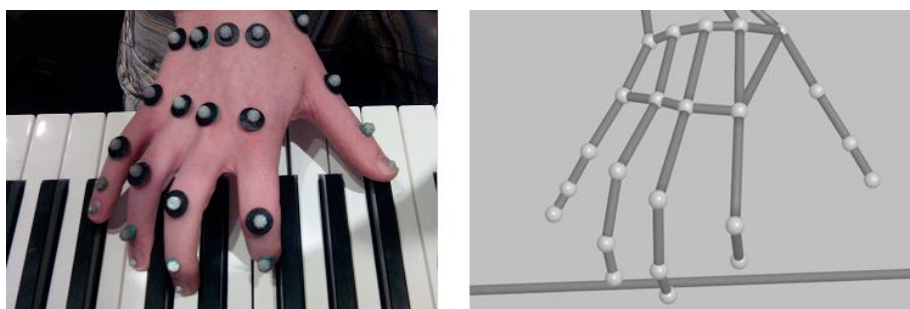


Figure 24: Example of captured data representation

OMC systems are very accurate, and are commonly used as a benchmark for the performance of motion tracking systems (Chen X. , 2013; Lopez-Nava, Marquez-Aquino, Munoz-Melendez, Carrillo-Lopez, & Vargas-Martinez, 2015; Smeragliuolo, Hill, Disla, & Putrino, 2016). They are also non-intrusive, due to small size of markers and lack of wires, and allow mobility of the subject, in a controlled space. Marker-based systems are more robust and accurate, therefore they more popular than marker-less systems, for demanding applications, because in marker-less systems the motion of body segments can be ambiguous in certain degrees of freedom. (Chen X. , 2013; Smeragliuolo, Hill, Disla, & Putrino, 2016; Moeslund, Hilton, & Krüger, 2006).

However, OMC systems have a few disadvantages: they are very expensive (€15.000 and upwards, for marker-based commercial systems), due to camera infrastructures, numbers of markers and massive computing for data analysis (Chen X. , 2013), hence it is unadvisable to purchase one solely for hand tool evaluation studies; they are usually used for whole body motion capturing. Setup times are lengthy (especially for marker-based systems) and specific technical knowledge is required to operate the system (Smeragliuolo, Hill, Disla, & Putrino, 2016). Line-of-sight *occlusions* of the hand-segments or markers (markers/hands not visible by camera, due to blockages by the subject's body or other objects in the scene) result in a non-observable situation, inducing a poor estimate (through interpolation) of the hand pose (Schall, 2014; Kortier, Sluiter, Roetenberg, & Veltink, 2014). Soft tissue artifacts occur with this technology, as with IMUs. Furthermore, the measurements to be performed are restricted to the volume in which the cameras are placed, usually in a controlled laboratory setting (Schall, 2014; Kortier, Sluiter, Roetenberg, & Veltink, 2014). In other words, this system is not portable and cannot be applied to the workplace or home. Finally, other light sources cause interference (false readings), for both types of systems, while marker-less systems face noise issues when body motions are fast (Chen X. , 2013).

In brief, the advantages and disadvantages of OMC systems are:

Table 6: Advantages and disadvantages of OMC systems

+	-
Most accurate	Expensive
Non-intrusive	Lengthy setup time
Whole body posture tracking (if needed)	Occlusions
	Skin artifact
	Limited to a small volume
	Not portable
	Light interference

C.1.4 Magnetic Systems

Magnetic tracking systems make use of magnetic field sensing. Fundamentally, magnetic transmitters (magnetic sources), which produce magnetic field, and receivers (also called magnetic sensors, magnetometers), which measure that field, are used to track their relative distance and, in some cases, orientation in space (6 DoF). For instance, Hall Effect sensors, which detect magnetic fields, can be configured as proximity sensors to

provide a linear output proportional to distance from a magnetic source (Simone & Kamper, 2005). There are two basic variations of this technology:

- External transmitter and body-mounted receivers (Leonard, Sirkett, Mullineux, Giddins, & Miles, 2005; Mitobe, et al., 2006; Ascension)
- Body-mounted transmitters and external receivers (Chen, Patel, & Keller, 2016; Rowe, Friedman, Bachman, & Reinkensmeyer, 2013)



Figure 25: Example of Electromagnetic Tracking. External transmitter & finger-mounted receivers

Transmitters (magnetic sources) can be electromagnets (Leonard, Sirkett, Mullineux, Giddins, & Miles, 2005; Mitobe, et al., 2006; Chen, Patel, & Keller, 2016; Ascension) or permanent magnets (Chen, Patel, & Keller, 2016; Rowe, Friedman, Bachman, & Reinkensmeyer, 2013), however electromagnets are more popular, because they can be customized. Namely, alternating current (AC) can be used, so that each electromagnet operates at a distinct frequency, which allows its identification, among multiple electromagnets (Chen, Patel, & Keller, 2016).

It is important to note that multiple magnetic sensors (receivers), placed strategically, are often required, in order to determine the 3D position of electromagnets (Chen, Patel, & Keller, 2016). For this reason, the cost and the computational power required for such a system rapidly increases as the degrees of freedom required increase (Kortier, Sluiter, Roetenberg, & Veltink, 2014).

Another issue is the placement of the external elements: the transmitter or the group of receivers, depending on the type of the system. When either of these is located in a fixed point in space, the sensing range of the system is limited in a relatively small volume proximal to that point, reducing mobility in space for the subject (Chen, Patel, & Keller, 2016; Leonard, Sirkett, Mullineux, Giddins, & Miles, 2005). On the other hand, the external element could be mounted on the body as well (Rowe, Friedman, Bachman, & Reinkensmeyer, 2013), to provide a larger range of movement, but this would be intrusive to the subject, because such elements are usually bulky, in order to be powerful enough to provide accurate estimates.

Furthermore, magnetic systems are susceptible to noise issues. The Earth's magnetic field and electromagnetic waves emitted from nearby electronic devices and ferromagnetic objects are common sources of noise, which could interfere with the signals of the system, decreasing tracking accuracy (Kortier, Sluiter, Roetenberg, & Veltink, 2014; Chen, Patel, & Keller, 2016). Hence, proper functioning of these trackers is mostly achieved within controlled experimental setups (laboratory).

These systems are expensive (€2.000 - €8.000) and are rarely applied to hand tool evaluation studies.

In brief, the advantages and disadvantages of magnetic tracking systems are:

Table 7: Advantages and disadvantages of electromagnetic systems

+	-
Very accurate	Limited sensor range Bulky, when all components are body-mounted Magnetic interference (controlled environment)

C.1.5 Optical Fiber Sensors

Optical fiber sensors have been used to measure bend. To the best of our knowledge, this technology has only been integrated into datagloves for finger motion tracking (Wise, et al., 1990; Kortier, Sluiter, Roetenberg, & Veltink, 2014), which is not the primary focus of this thesis.

Measuring bend with fiber optics requires a light source (e.g. LED) and a photodetector. The amount of bend is proportional to the attenuation of detected light in specially treated sections of fiber that pass over the finger joints (Simone & Kamper, 2005). Disadvantages of this method include the complexity of glove construction and price.

C.1.6 Summary

The characteristics of the most wide-spread, commercially-available solutions for wrist and forearm motion tracking are summarized (see Table 8). It is important to note that this table is merely indicative, and aims to provide a general understanding of the differences between these systems. The figures are based on rough estimates, formed by combining several sources: manufacturers' websites/brochures (Vicon; Polhemus; Ascension; Biometrics Ltd) and scientific studies (Leonard, Sirkett, Mullineux, Giddins, & Miles, 2005; Buchholz & Wellman, 1997; Cook, Baker, Cham, Hale, & Redfern, 2007; Wang, King, Do, & Nenadic, 2011), hence they should not be taken literally for specific commercial products.

Table 8: Motion tracking solutions for wrist and forearm

Feature	OMC	Magnetic	Electrogoniom.	IMU
Cost	>€ 15.000	€ 2.000 – € 8.000	€ 700 – € 1200	€ 20 – € 500
Accuracy	<1 mm (<1°)	1.5 mm (<1°)	2°	3°
Precision	<0.3 mm (<1°)	0.6 mm (<1°)	1°	2°
Non-intrusive	***	**	*	**
Simple	*	**	***	**
Portable	*	**	***	***
Distance range	*	*	**	***

It is also important to clarify that the feature of *precision* (repeatability) mentioned in the table mostly refers to the sensors alone. However, precision of the actual human posture measurement depends heavily on the manner of mounting the sensors on the body (e.g. glove, clothing, adhered on the skin). For instance, if a glove is large and fits loosely around the subject's hand, it may slip locally from the underlying skin when movement is performed, introducing random error. This means that one should not expect this level of repeatability from any method, unless he/she addresses the issue of mounting the sensors on the body of each subject with consideration.

C.2 Development of Tracking System

Taking into account the information presented in the previous chapter, we decided to implement *IMU* technology for wrist and forearm motion tracking.

We built our own original tracking system, because, to the best of our knowledge, no IMU-based system exists which solely tracks wrist and forearm motion. This enabled us to design a very low-cost system, with acceptable accuracy and repeatability, for human motion tracking purposes. The main characteristics which favored the selection of IMU technology are:

- Inexpensiveness
- Small size, non-intrusiveness
- Sufficiency of accuracy and precision, for wrist and forearm tracking ($\sim 3^\circ$)
- Availability of prototyping platforms

The validity of the characteristics mentioned above has been acknowledged by other researchers as well (Chen X. , 2013; McGinnis, et al., 2015; Vanegas & Stirling, 2015).

The system we developed consists of the following components:

- 3 IMUs (MPU-6050)
- 1 microcontroller (Arduino Nano)
- Wires (24AWG, Stranded core for flexibility)
- Glove and elbow patch, for mounting sensors with Velcro straps

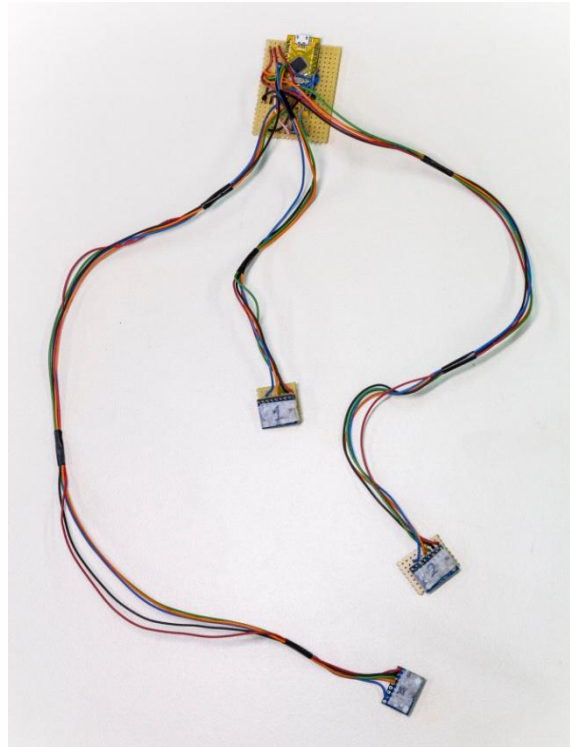


Figure 26: Wrist and forearm motion tracking system

The total cost of the system, excluding the cost of equipment required (soldering iron, solder, breadboard) is presented in the following table:

Table 9: Cost of individual components (estimation June 2016, prices are rounded)

Component	Cost
3 x MPU-6050 (GY-521)	€12
1 x Arduino Nano	€6
7m Wire (24AWG)	€2
1 x Glove & 1 x Elbow patch	€3
0.3m Velcro straps	€2
Total	€25

C.2.1 Placement

The placement of the IMUs on the body was determined by both empirical observation of upper limb joint and skin movement, and previous research (Chen X. , 2013; Buchholz & Wellman, 1997; Leonard, Sirkett, Mullineux, Giddins, & Miles, 2005; Smeragliuolo, Hill, Disla, & Putrino, 2016; Oberländer, 2015).

An IMU has a local x-y-z Cartesian reference frame, which is used to describe its orientation relative to a global reference frame. Therefore, the placement of the IMUs denotes both position and orientation:

- IMU#1 was placed proximally on the dorsal surface of the forearm, close to the elbow joint. The x-axis was aligned with the longitudinal axis of the forearm, while the z-axis was normal to the local surface of the forearm. The orientation of the y-axis is produced from the previous two axes (right-hand system).
- IMU#2 was placed distally on the dorsal surface of the forearm, near the wrist joint (between radius and ulna). Similarly to IMU#1, the x-axis was aligned with the longitudinal axis of the forearm, while the z-axis was normal to the local surface of the forearm.
- IMU#3 was placed approximately over the center of the third metacarpal bone of the hand, on the dorsal side. The x-axis was aligned to the axis of the third metacarpal, and the z-axis was normal to the dorsal surface of the hand, locally.

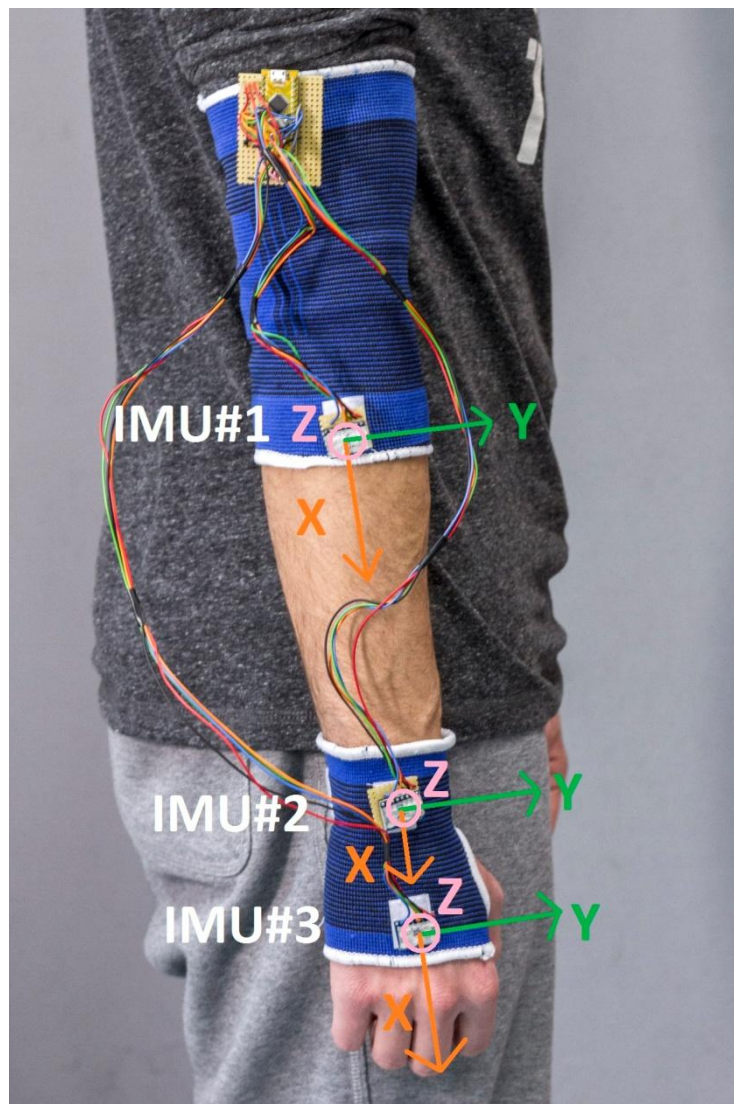


Figure 27: IMU placement & reference frames

With this placement, we hoped to achieve the following:

- IMU#1 is always aligned with the forearm in elbow flexion/extension, since it is positioned distally to the elbow joint; however it does not rotate with the forearm in pronation/supination (P/S), because the radius' movement around

the ulna during P/S occurs more near the wrist joint, than near the elbow joint (see ch. “A.3 Wrist and forearm kinematics”). Therefore, the skin in the surface of the forearm at the elbow has little rotation during P/S (Buchholz & Wellman, 1997).

- IMU#2 is also aligned with the forearm at all times, but it does rotate with the forearm in P/S. Because the forearm itself has no other DoF than P/S, the relative angle formed between IMU#1 and IMU#2 can be attributed only to P/S (and little skin deformation). Consequently the tracking of forearm motion (P/S) can be achieved through estimating the relative angle between IMU#1 and IMU#2, around the axis of the forearm.
- IMU#3 always lies on the plane defined (roughly, because skin surface is not flat) by the dorsal surface of the hand, following hand movements. Between IMU#2 and IMU#3 the wrist joint allows 2 DoF: wrist flexion/extension (F/E) and radial/ulnar deviation (R/UD). Consequently, tracking these two motions can be achieved by examining the relative angles between IMU#2 and IMU#3.

It is worth noting that the original design included 2 IMUs instead of 3, placed in the positions of IMU#1 and IMU#3. However, through informal testing, it was found that 2 IMUs were not enough to extract accurate information about all 3 DoFs (P/S, F/E and R/UD).

C.2.2 Components and Specifications

C.2.2.1 MPU-6050

This is an IMU (see ch. “C.1.1.1 IMU”) by the company *InvenSense* that combines a MEMS 3-axis gyroscope and a 3-axis accelerometer (no magnetometer) on the same silicon die. It also incorporates an onboard *Digital Motion Processor (DMP)*, which processes “6-axis” (3 axes from the gyro, 3 axes from the accelerometer) data fusion algorithms and returns orientation information.

Specifically, *breakout board GY-521* (see Fig. 28) of the MPU-6050 was selected, which “breaks out” the IMU pins onto a printed circuit board, in order to facilitate prototyping. The overall dimensions of the board are $21 \times 15 \times 3 \text{ mm}$. The reference frame x-y-z of the MPU is noticeable, as it is denoted with white symbols for the x and y axes on the board; the z-axis can be inferred from the x, y axes and the right hand rule.

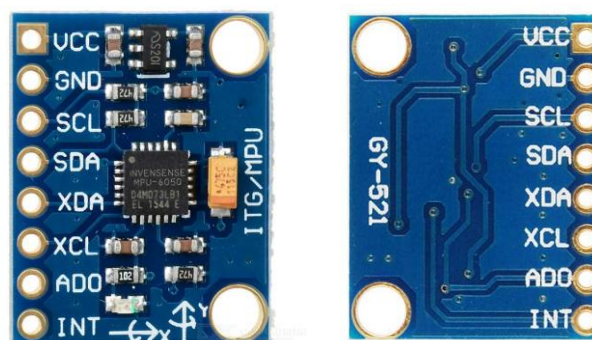


Figure 28: MPU-6050 GY-521 breakout board front (left) and back (right)

Generally, there exist two classes: simple IMU combo boards, which just mount an accelerometer and gyro onto a single printed circuit board, and more complex units that interface a microcontroller with the sensors. The first class outputs raw data from the sensors, whereas the second class can process that raw data, coming from the sensors, to produce a serial output. The MPU-6050 belongs to the second class, because it includes the DMP unit which can execute data fusion algorithms on the IMU chip, and send the processed data to the host microcontroller. This is a valuable feature, considering that data fusion algorithms such as the Kalman filter are computationally demanding (Schall, 2014; Madgwick, Harrison, & Vaidyanathan, 2011), and this frees computational load and memory on the microcontroller, which is usually limited in small size boards. The DMP can also handle the issue of sensor timing synchronization.

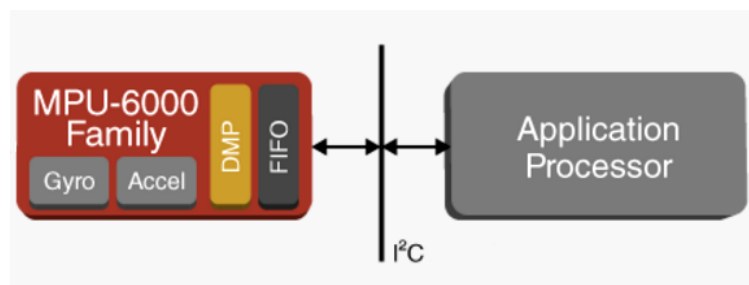


Figure 29: MPU-6050 block diagram

The MPU-6050 can access external magnetometers or other sensors, if needed. However, it is worth noting that InvenSense also produce a chip that combines the MPU-6050 (accelerometer and gyroscope) with a tri-axial magnetometer (compass) on the same board. This 9-DoF IMU is called MPU-9150, while a later, smaller version is the MPU-9250. However, to the best of our knowledge, no open source code exists which makes use of the DMP for 9-axis motion fusion, meaning that data fusion would need to be carried out on the host processor, increasing the computational load.

C.2.2.1.1 Specifications

Accelerometers generally measure linear acceleration along 1 to 3 axes, including gravity, represented in units of meters per second squared (m/s^2), or G-force (g) which is about $9.8m/s^2$. The *range* of an accelerometer refers to the maximum and minimum acceleration that can be measured by that sensor. Generally, a smaller range means a more sensitive output, meaning higher accuracy measurement; nevertheless it is only valid for measuring accelerations in that range. It is important to select a fitting sensing range for each individual project.


Gyroscopes (often called *gyros*) measure angular velocity about 1 to 3 axes, represented in units of rotations per minute (RPM), or degrees per second ($^{\circ}/s$ or dps). The range of a gyroscope refers to the maximum and minimum angular velocity which can be measured by that sensor. Similarly to accelerometers, increased sensitivity is achieved when the range of the sensor is not much larger than the actual velocity to be measured.

For tracking both slow and fast motions, the full-scale ranges of the gyro and accelerometer of the MPU-6050 are user-programmable. The available options are ± 250 , ± 500 , ± 1000 , and ± 2000 $^{\circ}/sec$ (dps) for the gyroscope, and $\pm 2g$, $\pm 4g$, $\pm 8g$, and $\pm 16g$ for the accelerometer.

Sensitivity of an accelerometer is usually expressed in mV/g or inversely in g/mV for analog-output sensors and LSB/g or g/LSB for digital-output sensors (LSB – Least Significant Bit) like those on the MPU-6050. Similarly for gyroscopes, sensitivity is expressed in mV/dps or dps/mV for analog-output sensors and LSB/dps or dps/LSB for digital-output sensors. For a digital-output sensor, higher LSB/unit (an output change for a given change in input parameter) means higher sensitivity, whereas higher unit/LSB (the input parameter change required to produce a standardized output change) means lower sensitivity.

Specifications on range and corresponding sensitivity, for accelerometers and gyroscopes in the MPU-6050, along with other information, are summed up in the following table (see Table 10):

Table 10: Specifications of the MPU-6050

Part #	Gyro Full Scale Range	Gyro Sensitivity	Accel Full Scale Range	Accel Sensitivity	Digital Output	Operating Voltage Supply
UNITS:	($^{\circ}/\text{sec}$)	(LSB/ $^{\circ}/\text{sec}$)	(g)	LSB/g		(V +/-5%)
 MPU-6050	± 250	131	± 2	16384	I ² C	2.375V–3.46V
	± 500	65.5	± 4	8192		
	± 1000	32.8	± 8	4096		
	± 2000	16.4	± 16	2048		

C.2.2.1.2 ADC Conversion

The MPU-6050 features three 16-bit analog-to-digital converters (ADCs) for digitizing the gyroscope outputs and three 16-bit ADCs for digitizing the accelerometer output, which enable simultaneous sampling of all axes. Therefore the output of the sensor is digital, and analog-to-digital conversion does not need to be conducted on the microcontroller.

C.2.2.1.3 Temperature Sensor

The chip also includes an embedded temperature sensor with a digital output, which can be used to compensate for the effect of changing temperature on the accelerometer and gyroscope measurements.

C.2.2.1.4 FIFO Buffer

Another element of the MPU-6050 is the 1024-byte FIFO (First In – First Out) register that is accessible via the Serial Interface. Sensor data or data coming from the DMP can be stored in the FIFO buffer, waiting to be read by the host processor (Arduino). A FIFO counter keeps track of how many bytes of valid data are contained in the FIFO. The interrupt function (INT pin) may be used to determine when new data is available, allowing the system processor to read the sensor data in bursts and then enter a low-power mode as the MPU collects more data.

C.2.2.1.5 Communication

Communication between the MPU-6050 and the Arduino (or other) microcontroller is achieved through an I²C-bus, where the IMU acts as *slave* to the Arduino (*master*). The I²C-bus allows communication between the Arduino and multiple sensors, using only two bus lines (SCL–clock signal and SDA–data signal) to exchange information bi-

directionally, rather than a different line –and an extra pin– for each connected sensor; otherwise, the integration of multiple sensors would require many pins on the microcontroller and many wires, making the system more cumbersome. An example is the *SPI* serial communication protocol, which is not available for the MPU-6050.

The speed of the original I²C communication protocol was *100kHz* (kbit per second), and was increased in a later version to *400kHz* (fast-mode) which was used for this project. Serial communication, such as SPI, is usually faster.

Every slave on an I²C-bus needs to have an address which is used to identify corresponding data. The three MPUs used in this system act as slaves to the master Arduino; hence they are required to have three different I²C addresses. This posed a challenge because the MPU-6050 can only obtain one of two addresses: *0x68* or *0x69*, depending on the logic level on pin AD0. This allows no more than two MPU-6050s to be connected to the same I²C bus, simultaneously. There are two ways to overcome this issue:

1. Use hardware multiplexers
2. Software workaround which changes I²C addresses periodically

The second method is cheaper and quicker to implement, which is why it was preferred in this project. It is based on the concept of changing the I²C addresses of the MPUs, by providing “high” voltage for one AD0 pin and “low” voltage for all other AD0 pins (or vice versa). This forces one of the MPUs acquire a different address than the others, making it easy to read data from. In a very short time (relatively to the speed of the motion we are measuring), the addresses change again, and the next MPU is made available for “reading”. This way, the MPUs are read one at a time, but with a very short time interval, adequate for the purpose of measuring wrist and forearm motion.

C.2.2.1.6 Open-Source Code

The MPU-6050 was chosen due to the availability of extensive open-source code, which has been developed by various programmers around the world. The most commonly used algorithms (credit to Jeff Rowberg) offer useful features:

- Ready sensor data synchronization and fusion algorithms, executed on the DMP, that directly return estimated orientation (required reverse engineering, because DMP information have not been disclosed by InvenSense)
- Automatic calibration procedure, every time the IMU is initialized (the sensor needs to be static for approximately 15 sec)

In other words, this IMU board offers a well-tested commercial solution, with useful embedded features off-the-shelf. If desired, raw values can also be extracted from each sensor, so that custom data fusion algorithms can be executed, on an external microcontroller. However, in this thesis, the IMU was mostly treated as a “black box”, by deploying open-source code, since there is agreement in online sources that using the DMP firmware of the MPU-6050 works very well, sometimes better than using custom algorithms on the microcontroller. Moreover, the focus of this thesis is not to investigate the specifics of IMU technology, neither to optimize data fusion algorithms, but rather to implement inertial sensor technology for motion tracking in hand tool evaluation.

C.2.2.1.7 Calibration

Calibration is the process of using a known reference input and extracting the sensor output for that input. This can be used to calculate the corrected output from a sensor reading.

In the case of the MPU-6050, gravitational force is used as a reference, while keeping the sensor static. Calibration is conducted for all 3 gyroscope axes and 3 accelerometer axes. In most open-source algorithms, a calibration scheme is executed every time the MPU is initialized, which requires the sensor to be still and lie on a flat horizontal surface for approximately 15 seconds, in order for it to converge. This process corrects the output of the sensor.

Through testing and online forums, it has been found that this recurrent calibration process can be assisted by providing suitable axes offsets, determined by a separate calibration scheme which needs to be conducted only once for each sensor. This “double” calibration may seem exaggerated, yet testing has shown that it significantly increases the stability of sensor measurements and decreases the time required for calibration.

C.2.2.2 Arduino Nano

For this project, a version of the *Arduino Nano v3.0* (see Fig. 30) board was used as a host device, to capture IMU measurements and process them, in order to estimate wrist and forearm joint angles. The specifications of the board are presented (see Table 11).

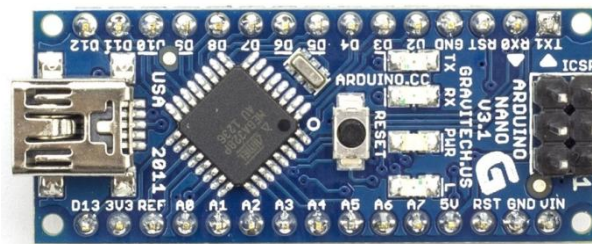


Figure 30: Arduino Nano board

Table 11: Specifications of the Arduino Nano v3.0

Microcontroller	ATmega328 – Atmel
USB port	Mini-B (or Micro-B in some boards)
Operating Voltage (logic level)	5 V
Input Voltage (recommended)	7-12 V
Input Voltage (limits)	6-20 V
Digital I/O Pins	14 (D2-D13, TX, RX), of which 6 provide PWM output
PWM ports	6 (D3, D5, D6, D9, D10, D11)
Analog Input Pins	8 (A0-A7)
DC Current per I/O Pin	40 mA
Flash Memory	32 KB, of which 2 KB used by bootloader
SRAM	2 KB
EEPROM	1 KB
Clock Speed	16 MHz
Length	45 mm
Width	18 mm
Weight	5 g

C.2.2.2.1 *Pins with specialized functionality*

Interrupt pins: D2 and D3. These pins can be configured to trigger an interrupt, for instance to read data from the FIFO when they are ready.

I²C pins: A4 (SDA) and A5 (SCL). I²C communication is supported by the appropriate libraries

C.2.2.2.2 *Power*

The Arduino Nano can be powered via the Mini-B (or Micro-B) USB connection, or an external power supply, such as a 9V battery. The board used in this project had a USB Micro-B port, and power was supplied from a computer through a USB cable.

C.2.2.2.3 *Memory*

The ATmega328 has 32 KB of flash memory for storing code, (of which 2 KB is used for the bootloader, which allows installing new firmware without the need of an external programmer). It also has 2 KB of SRAM (where variables are created and manipulated – lost when power is turned off) and 1 KB of EEPROM (to store long-term information – kept when the power is turned off).

C.2.2.2.4 *Communication*

The Arduino Nano allows communication with a computer, another Arduino, or other microcontrollers. In this project, the Arduino communicated with a computer through the USB connection and data were displayed in the computer via the *serial monitor* included in the Arduino software, which allows simple textual data to be sent to and from the board.

Serial communication (like UART), can be achieved through digital pins RX and TX, which allows exchange of information between two Arduinos, for example.

C.2.2.2.5 *Programming*

The Arduino Integrated Development Environment – or Arduino Software (IDE) – is open-source and makes it easy to write code and upload it to the board. It contains a text editor for writing code, a message area, a text console, a toolbar with buttons for common functions and a series of menus. It connects to the Arduino hardware to upload programs and communicate with them.

C.2.3 *Wiring*

In this section, the physical connection between the MPU-6050 and the Arduino is addressed. At first, the connection of a single MPU to the Arduino is presented and then the work is extended to three MPUs, which are required for this system.

The process of developing the system involved building a prototype on a solder-less breadboard (see Fig. 31) – a common practice for electronics projects. For this reason, headers were soldered on the pins of the MPU-6050 breakout boards and the Arduino and connections were tested. The spacing of headers is standardized, so that they fit nicely in breadboard holes, without needing permanent soldering. During this phase, the algorithms were tested and developed further to suit the needs of the project.

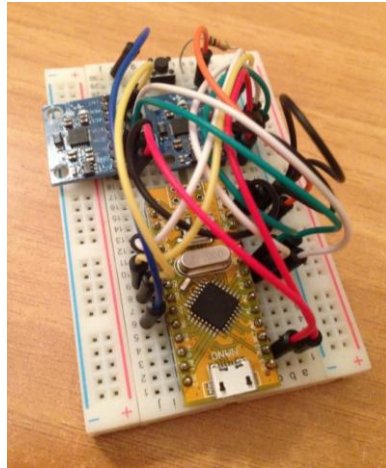


Figure 31: Prototyping on a solderless breadboard

Finally, after ensuring the system is functional with the current configuration, the circuit was soldered permanently. Stranded core wires were used, so that they are flexible and allow mobility of the subject wearing the system. Small solderable breadboards were used under each sensor and the Arduino (see Fig. 32) to connect the wires and headers, while header length was clipped, to reduce size. The system was then ready to be tested in measuring joint angles.

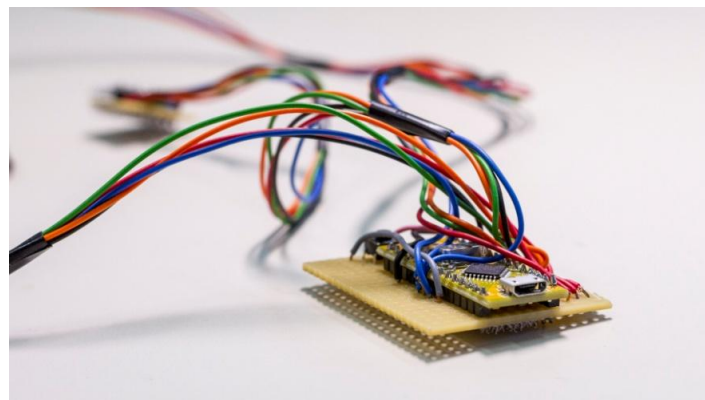


Figure 32: Permanent circuit

A list of the wirings required for a *single* MPU-6050 is presented in the following table (see Table 12).

Table 12: Connections between a single MPU-6050 and Arduino Nano

MPU-6050	Arduino Nano
VCC	5V (or if VDD -> 3V3)
GND	GND
SCL	A5
SDA	A4
XDA	(only used if connecting other sensors)
XCL	(only used if connecting other sensors)
AD0	- no connection or GND (for I ² C address 0x68) - 3V3 (for I ² C address 0x69)
INT	D2 or D3 (if interrupts are used in the code)

A few notes:

- Many breakout boards have a VDD pin for power supply, which requires a supply voltage range of 2.375V–3.46V. Therefore, if a using an MPU with a VDD pin, it is necessary to connect it the 3V3 pin of the Arduino. However, other boards (e.g. GY-521), have a voltage regulator which allows them to be supplied by the 5V pin of the Arduino. These boards have a VCC pin, instead of a VDD.
- The XDA and XCL pins can be used for the auxiliary I²C bus (see ch. “C.2.2.1.5 Communication”), which is available for communicating with additional sensors, for example an external magnetometer. If this functionality is not necessary, these pins can be left unconnected.
- The AD0 pin is used for selecting the I²C address of the MPU. If the pin is pulled “low” (GND or no connection) then the address is 0x68. On the other hand, if the pin is pulled “high” (3V3), the address is 0x69.
- The INT pin may be used or left unused depending on the algorithm implemented. This pin is responsible for producing interrupt signals.

Extending the system to include three MPU-6050s is relatively simple, from the perspective of the physical connectivity. The I²C protocol allows all IMUs to use the same two lines for transmitting data (A4, A5). Power supply and grounding is made through the same lines as well (5V, GND). Two issues arise when deciding about the AD0 pins (only two I²C addresses are available) and the INT pins (only two pins in the Arduino can handle interrupt signals). These issues were both resolved through software:

- a. The AD0 pins of the MPU-6050s were connected to digital I/O pins of the Arduino, so that the I²C addresses can be set at will, through the algorithm (see ch. “C.2.2.1.5 Communication”).
- b. The INT pins remained unconnected, because the algorithm was designed to not use interrupt signals, for determining when to read IMU data. Instead, we use polling combined with timekeeping (see ch. “C.4 Algorithm”).

For the algorithm developed for this project (see ch. “C.4 Algorithm”) the following wirings were used between the 3 MPU-6050s and the Arduino Nano (see Table 13):

Table 13: Connections between three MPU-6050s and Arduino Nano

3 MPU-6050s	Arduino Nano
All VCCs	5V
All GNDs	GND
All SCLs	A5
All SDAs	A4
All XDAs	(unused)
All XCLs	(unused)
AD0 of IMU#1	D4
AD0 of IMU#2	D5
AD0 of IMU#3	D6
All INTs	(unused)

C.2.4 Mounting

Mounting the IMUs on the upper limb was a challenge affecting repeatability of the measurements, as well as the setup time required. Solutions considered included:

1. Using adhesive tape to mount the components directly on the arm's skin (simple but time consuming and unpleasant for the subject to doff)
2. Stitching the sensors permanently on a wearable sleeve (convenient and time-saving, but lacks sensor position customization for individual subjects' hands. Moreover, calibration and re-calibration of the sensors would be difficult)
3. Using Velcro to attach the sensors on a wearable sleeve (easy to attach and detach sensors, without taking of the sleeve, making calibration simpler)

The third solution was implemented in our system (see Fig. 33) because it was found that frequent sensor re-calibration was necessary to correct for accumulation of errors. Using Velcro allows for the sensors to be detached without taking off the sleeve from the subject. A short re-calibration procedure can be executed and the sensors can be re-attached on roughly the same positions as before. A repeatability challenge arises though, since it is difficult to place the sensors at the exact same positions as they were, visually. In a future improvement of the system, a standard procedure for attaching the sensors could be developed, so that higher placement repeatability is achieved.

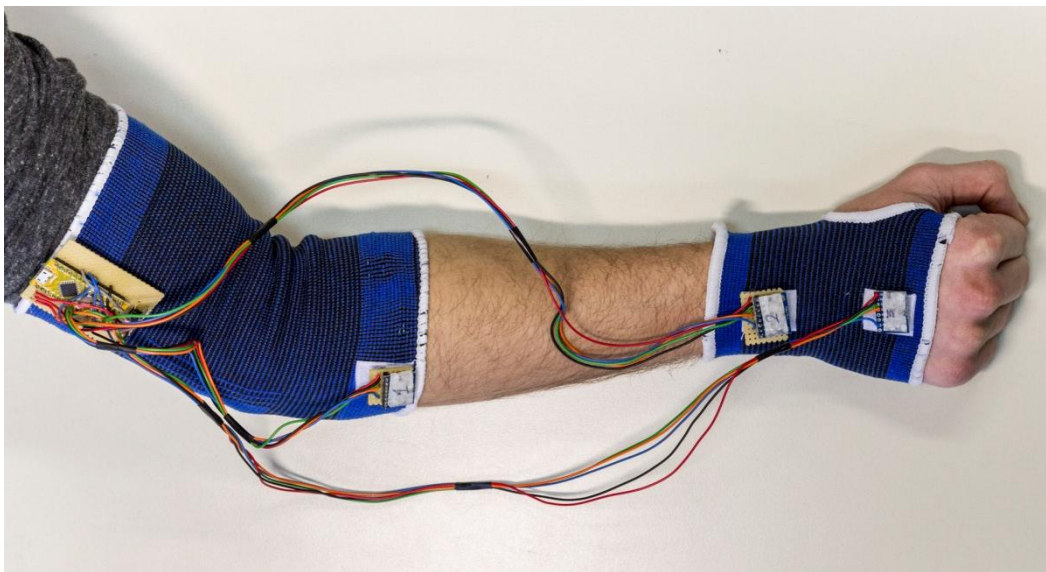


Figure 33: Wearable System. Velcro strips are used to attach sensors and processor on the fingerless glove and elbow pad

C.2.5 Setup Procedure

The full setup procedure consists of the following stages:

1. *Sensor calibration*: Placing all the sensors on a flat, horizontal surface, with the MPU z-axis parallel to gravity, and allowing approximately 15 seconds of stillness. The orientation angles read on the serial monitor should converge within this time period. This process is required every time the IMUs are initialized. This algorithm is part of the open-source code.

2. *Global reference system setting*: Aligning all 3 MPUs so that their respective axes are parallel and using this setup as a reference. This procedure is required because the MPU-6050s have no compass and therefore no global reference, hence their global reference system is random (around the gravity axis) each time they are initialized. This process needs to be executed every time the IMUs are initialized, and also when measurement errors have been accumulated (e.g. drift). This algorithm was developed specifically for this multi-sensor system (see ch. “C.3.4 Global Reference frame”).
3. *Mounting*: attaching the sensors on the subject’s upper limbs with Velcro
4. *Neutral posture*: letting the subject’s arm hang at a neutral posture and using the offsets for determining joint angles.

To facilitate sensor calibration and global reference system setting, a flat, rigid platform was used, with a Velcro strip for easily attaching the IMUs and aligning their axes.

The same platform was used to conduct a short informal test after each calibration, which empirically demonstrated the precision of the calibrated system; sometimes re-calibration was necessary due to poor initial alignment of the sensors or other unidentified factors: By attaching sensors on the rigid platform with Velcro, their relative position is always constant. Thus, ideally, rotating the whole platform would not produce a change in the estimated relative angles between the IMUs. In practice however, by rotating this platform with the sensors rigidly attached, it was found that estimated relative angles usually presented fluctuation of approximately 3°. The cause is that multiple sensors are rarely identical; each one “behaves” in a different way for a given input. As a consequence, each IMU’s output was slightly different than the others’, causing an artifact in relative angles. In cases where calibration had been executed poorly due to sensor misalignment or other factors, this artifact was magnified, rendering the system inaccurate and re-calibration was required.

C.3 Mathematics of Rotation

In this section, the mathematical approach of the problem is described. Understanding this analysis requires a background on mathematical representation of orientation, although a short explanation will be provided.

The goal is to create an algorithm that transforms the orientation data (quaternion representation) coming from three sensors to relative angles between the sensors, which correspond to the three anatomical angles (P/S, F/E, R/UD) of forearm and wrist joint motion.

C.3.1 Rotation Matrix

A rotation matrix 0R_i is a 3x3 matrix used to describe the orientation of a local reference frame (i) in relation to a global reference frame (0). Each of the three columns of this matrix represents the *projection* of a unit vector of the local reference frame ($\hat{x}_i, \hat{y}_i, \hat{z}_i$) on the unit vectors of the global reference frame ($\hat{x}_0, \hat{y}_0, \hat{z}_0$).

$${}^0R_i = \begin{bmatrix} x_{i,x} & y_{i,x} & z_{i,x} \\ x_{i,y} & y_{i,y} & z_{i,y} \\ x_{i,z} & y_{i,z} & z_{i,z} \end{bmatrix}$$

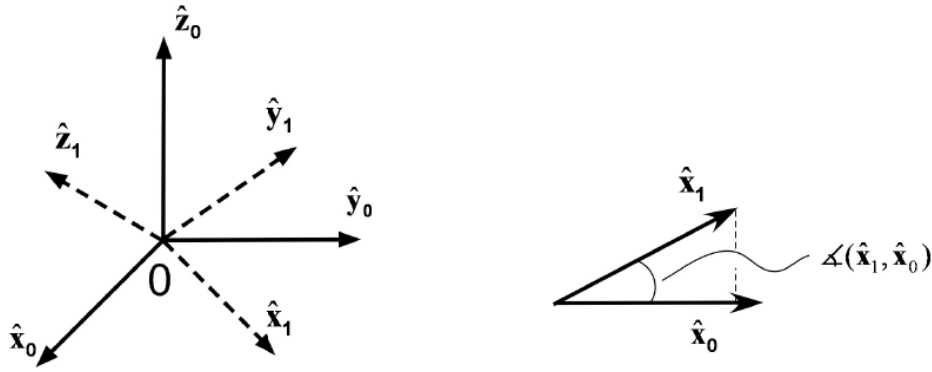


Figure 34: Reference frame $i=1$, rotated in relation to reference frame 0

A rotation matrix has a few useful properties, which reduce computational load when handling such matrices while some can be used to test for the validity of an algorithm:

- $({}^0R_i)^{-1} = {}^iR_0$
- $R^T = R^{-1}$ (orthogonal matrix)
- $\det({}^0R_i) = +1$
- The norm of each column is equal to 1

A major advantage of using a rotation matrix to represent orientation as opposed to other methods of representation such as *Euler angles* is that *singularities* (i.e. *Gimbal lock*) are avoided. For this reason, rotation matrices were selected as an appropriate method of representation for handling orientation data, until the anatomical angles are estimated.

C.3.2 Quaternions to Rotation Matrix

Another method for representing orientation is by using *quaternions* (also called Euler Parameters). Similarly to rotation matrices, quaternions do not present singularities, meaning that every possible orientation can be described without a problem. A quaternion \mathbf{q} is comprised of 4 elements (3 of which make a vector) and can be represented as such:

$$\mathbf{q} = qw + \mathbf{i}qx + \mathbf{j}qy + \mathbf{k}qz$$

One form of representation can be converted to another, if desired. The equivalent rotation matrix, to represent the same rotation as a quaternion, is:

$$R = \begin{bmatrix} 1 - 2qy^2 - 2qz^2 & 2qxqy - 2qzqw & 2qxqz + 2qyqw \\ 2qxqy + 2qzqw & 1 - 2qx^2 - 2qz^2 & 2qyqz - 2qxqw \\ 2qxqz - 2qyqw & 2qyqz + 2qxqw & 1 - 2qx^2 - 2qy^2 \end{bmatrix}$$

The open-source algorithm used in this project returns IMU orientation in the form of quaternions. The above conversion is necessary in order to make calculations using rotation matrices, which is the selected representation form for this thesis.

C.3.3 Estimation of Anatomical Angles

C.3.3.1 Rotation Matrices between IMUs

The IMUs return orientation in the form of quaternions. The quaternion-derived rotation matrices are calculated as presented above (see ch. “C.3.2 Quaternions to Rotation Matrix”). These matrices are denoted as such:

- 0R_1 for IMU#1 orientation, relative to a global reference system 0
- 0R_2 for IMU#2 orientation, relative to a global reference system 0
- 0R_3 for IMU#3 orientation, relative to a global reference system 0

C.3.3.1.1 Forearm

Rotation matrix between IMU#1 ref. fr. and IMU#2 ref. fr.

To determine forearm rotation (P/S), the rotation of IMU#2 in relation to IMU#1 is used. To calculate the rotation matrix 1R_2 of IMU#2 relative to IMU#1, the following computation is required:

$${}^1R_2 = {}^1R_0 {}^0R_2 = ({}^0R_1)^{-1} {}^0R_2 = ({}^0R_1)^T {}^0R_2$$

Notice that a property of rotation matrices is used; namely that the *inverse* of a rotation matrix is equal to the *transpose* of the same matrix. This feature is useful, because it decreases computational load on the processor; calculating the inverse of a matrix is computationally demanding.

C.3.3.1.2 Wrist

Rotation matrix between IMU#2 ref. fr. and IMU#3 ref. fr.

Wrist joint motion (F/E, R/UD) is determined by the two IMUs proximal to the wrist joint – IMU#2 and IMU#3. Similarly to 1R_2 , the relative matrix between IMU#2 and IMU#3 is determined by:

$${}^2R_3 = {}^2R_0 {}^0R_3 = ({}^0R_2)^{-1} {}^0R_3 = ({}^0R_2)^T {}^0R_3$$

C.3.3.2 Inverse Kinematics

Having determined the relative rotation matrices between IMUs, an estimation of three angles that correspond to forearm and wrist motion (P/S, F/E, R/UD) can be extracted. This process is similar to converting the rotation matrix representation to Euler angle (or Tait-Bryan angles) representation and it is sometimes loosely called “inverse kinematics” because an analogous process is used in robotics.

C.3.3.2.1 Forearm

Between IMU#1 (forearm, proximal to elbow joint) and IMU#2 (forearm, proximal to wrist joint) the only DoF allowed is pronation/supination (P/S). By placing the IMUs appropriately (see ch. “C.2.1 Placement”), this motion occurs together with the rotation of IMU#2 around its x-axis. In other words, the relative rotation between IMU#1 and IMU#2 is restricted to the x-axis, and the angle θ_1 of that rotation represents P/S of the forearm.

$${}^1R_2 = R_x(\theta_1) = \begin{bmatrix} 1 & 0 & 0 \\ 0 & \cos \theta_1 & -\sin \theta_1 \\ 0 & \sin \theta_1 & \cos \theta_1 \end{bmatrix}$$

Having the rotation matrix 1R_2 , one can easily determine the angle θ_1 which corresponds to P/S, through inverse trigonometric functions. The function $atan2(y,x)$ is used, because it is more computationally stable (uses two inputs, returns a solution in the appropriate quadrant, avoids division by zero):

$$P/S : \theta_1 = atan2(\sin \theta_1, \cos \theta_1) = atan2({}^1R_2(3,2), {}^1R_2(3,3))$$

C.3.3.2.2 Wrist

Between IMU#2 (forearm, proximal to wrist joint) and IMU#3 (dorsal surface of palm) lies the wrist joint, which allows for 2 DoF – flexion/extension (F/E) and radial/ulnar deviation (R/UD). The kinematic hierarchy between F/E and R/UD is important because the sequence of rotations affects the resulting rotation matrix (matrix multiplication is non-commutative). As discussed in a previous chapter (see ch. "A.8 Kinematic Modeling"), studies have shown that the F/E axis carries the R/UD axis, therefore rotation around the F/E axis is considered as the first rotation and rotation around the R/UD axis is considered as the second rotation.

If the convention regarding IMU placement (see ch. "C.2.1 Placement") is held, then F/E (θ_2 angle) occurs around the y-axis, and R/UD (θ_3 angle) occurs around z-axis of IMU#3:

$$\begin{aligned} {}^2R_3 = R_y(\theta_2) R_z(\theta_3) &= \begin{bmatrix} \cos \theta_2 & 0 & \sin \theta_2 \\ 0 & 1 & 0 \\ -\sin \theta_2 & 0 & \cos \theta_2 \end{bmatrix} \begin{bmatrix} \cos \theta_3 & -\sin \theta_3 & 0 \\ \sin \theta_3 & \cos \theta_3 & 0 \\ 0 & 0 & 1 \end{bmatrix} \\ &= \begin{bmatrix} c_2 c_3 & -c_2 s_3 & s_2 \\ s_3 & c_3 & 0 \\ -s_2 c_3 & s_2 s_3 & c_2 \end{bmatrix} \end{aligned}$$

The notation c_2 implies $\cos \theta_2$ and so on.

Similarly to P/S, we can use inverse trigonometric functions to determine θ_2 and θ_3 when the rotation matrix 2R_3 is given:

$$F/E : \theta_2 = atan2(s_2, c_2) = atan2({}^2R_3(1,3), {}^2R_3(3,3))$$

$$R/UD : \theta_3 = atan2(s_3, c_3) = atan2({}^2R_3(2,1), {}^2R_3(2,2))$$

It should be noted that there are more than one ways to calculate $\theta_1, \theta_2, \theta_3$, by using different elements of the rotation matrixes as arguments for the $atan2$ function.

C.3.4 Global Reference Frame

When determining the relative rotation matrices between two IMUs (see ch. "C.3.3.1 Rotation matrices between IMUs"), it was implied that IMUs need to have the same global reference system (0), for this approach to be valid. However, this is not the case with IMUs without a compass (such as the MPU-6050) because these can have no reference around the axis of gravity. Consequently, when multiple MPU-6050s are initialized, their original global reference frames do not coincide. To accomplish a common global reference system, the following scheme was developed:

-
- a. Physically align all 3 IMUs. In other words, make the x-axes of all IMUs parallel, and similarly for the y and z-axes, visually.
 - b. Save this orientation as the global reference frame –common for all 3 IMUs. From that point, every rotation of the IMUs will be expressed in relation to this global reference system.

The output of the sensor itself will always be relative to its original reference frame; for this reason the algorithm on the host processor needs to transform this data to orientation relative to the reset reference frame of our choice. This is accomplished through the following computation:

$${}^0R_l = {}^0R_r \cdot {}^rR_l = ({}^rR_0)^T \cdot {}^rR_l$$

Where:

- 0 is the global reference frame of our choice
- r is the random global reference frame of the IMU when initialized
- l is the local reference frame of the IMU

In brief, when all IMUs are aligned and that orientation is “stored” as the desired global reference frame (0), in essence it is the rotation matrix rR_0 which is being stored, and it is unique for every IMU. The matrix rR_l is the output of the IMU and, by combining it with the transpose of the rR_0 matrix, the orientation of the IMU in relation to the desired global reference frame 0 is determined.

It is important that IMUs are aligned properly, in the beginning of the scheme; otherwise the global reference frame 0 of each IMU will be different, leading to unexpected output.

C.4 Algorithm

The algorithm developed for this project includes several open-source libraries of functions but the main program loop has been specifically built to fit the needs of the system. A summary of the steps executed by the main algorithm is presented:

1. Setup
 - a. Initialize and test connection with IMUs
 - b. Initialize DMPs by a keyboard input
 - c. Set axes offsets of the IMU (initial calibration, offset values are determined by a separate calibration scheme)
2. Loop
 - a. For the 3 IMUs:
 - i. Select one IMU to read from (by altering its I2C address)
 - ii. If enough time has passed, check if data are available for reading
 - iii. Acquire DMP orientation data from the FIFO buffer, in the form of quaternions
 - iv. Convert quaternions to rotation matrix representation and store for processing
 - v. (Select different IMU and repeat)

- b. (If desired, store the current orientations as the global reference frames, by keyboard input or button press)
- c. Calculate IMU rotation matrices relative to the global reference frame
- d. Calculate rotation matrices between IMUs #1, #2 and IMUs #2, #3
- e. Extract angles that correspond to P/S, F/E, R/UD
- f. (If desired, store current angles as the neutral wrist and forearm posture, by keyboard input)
- g. Display angles (adjusted to the neutral posture) on the serial monitor

The full code is included in this thesis, in the Appendix (see Appendix “A. Code”).



D. Experiment – Product Design Evaluation

D.1 Experimental Design

In this section, we discuss the experiment conducted, in which human wrist and forearm motion was measured during use of 3 different design solutions of an everyday product – the shaving razor.

D.1.1 Products

We tested three different razors, which are available on the market. These razors had an increasing level of mobility:

- A. No mobility
- B. 1 DoF (pivoting shaving head)
- C. 2 DoFs (pivoting shaving head, and rotation around handle axis)

Moreover, the razor handles differed from each other, in the following features:

- Handle length
- Handle thickness, varying along the length
- Handle shape
- Shaving head contact area

Table 14: Design features of the tested razors

Code	Razor Name	Mobility	Length (cm)	Width (cm)	Shape
A	Blue	0 DoF	10.5	1	Straight
B	Soleil	1 DoF: pivoting head (30°)	12.6	1.1 – 1.6	Curved; flattened tail
C	Venus	2 DoF: pivoting head (48°); rotation around long axis (30°)	13.5	1.3 – 1.8	Curved

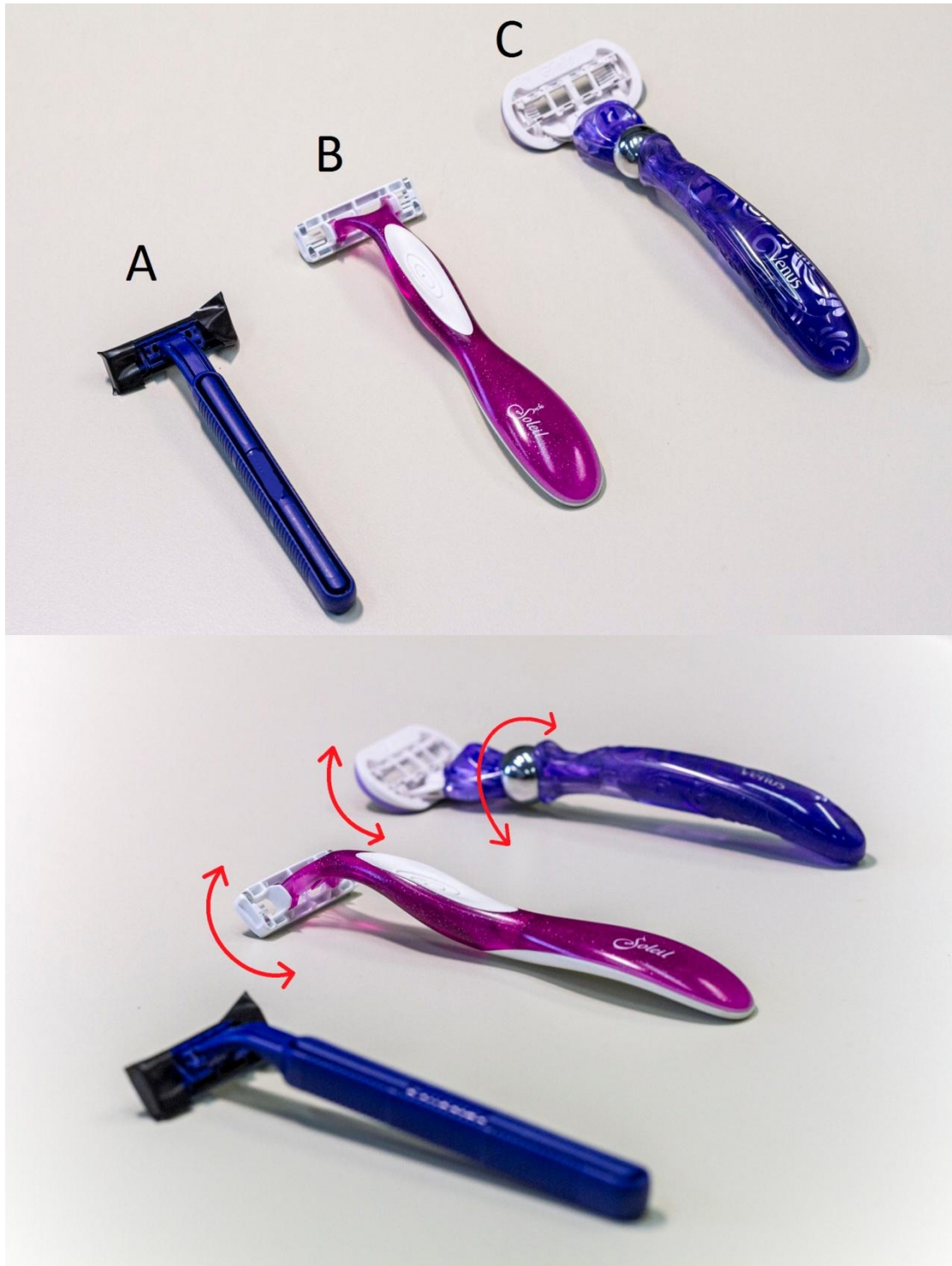


Figure 35: The three razors (A,B,C from left to right) and their planes of motion

D.1.2 Task

Leg shaving is a very common practice, especially among women. It can be completed in various body stances: seated, upright with an elevated leg, standing but bending the waist, etc.

In this thesis we opted to consider the case of leg shaving in a *seated* stance, using the dominant hand, in order to reduce factors of variability (e.g. whole body posture, changing hands) across subjects and achieve a more controlled setting.

Leg shaving while seated was examined in preliminary tests, which yielded the following classification:

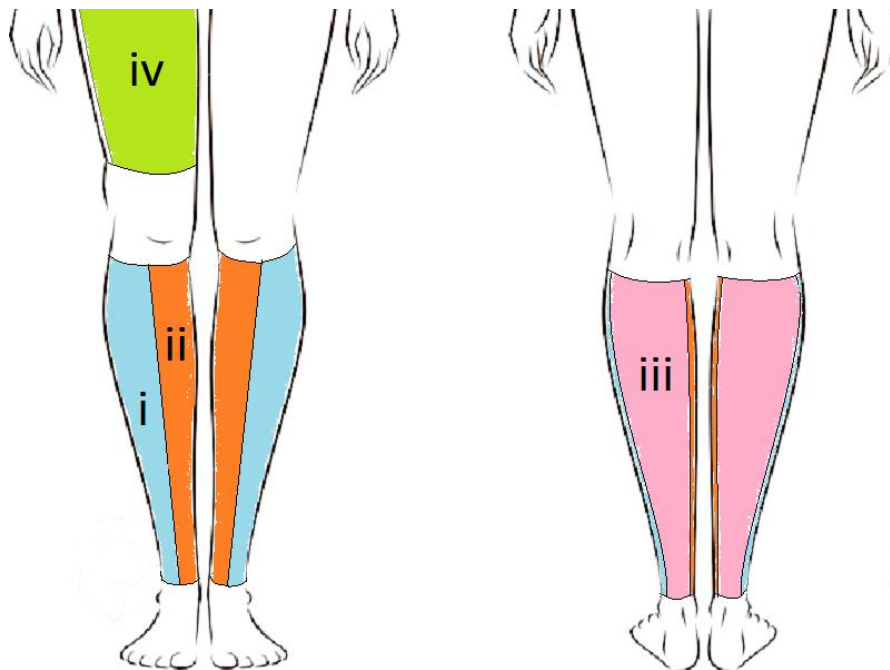


Figure 36: Leg regions

It is worth noting that in preliminary tests, subjects would change the hand holding the razor, if necessary. In other words they would use the non-dominant hand to shave the rear and outer sides of the corresponding non-dominant leg, whereas they used their dominant hand for all other regions, which are easier to reach. This action was not replicated in our experiment, in order to avoid doffing and donning of the wearable system.

D.1.2.1 Lower Leg Segmentation

The assumption was that women have three discrete leg postures during lower leg shaving while seated, which proved to be an adequate simplification through observation. Hence, the lower leg (shin and calf) was segmented into three areas, depending on the whole leg posture during shaving of each region:

- Region i. The outer (O) side of the lower leg, which is shaved with the leg in a normal resting posture
- Region ii. The rear (R) side of the lower leg (calf), which is rotated toward the front
- Region iii. The inner (I) side of the lower leg, which is rotated toward the front

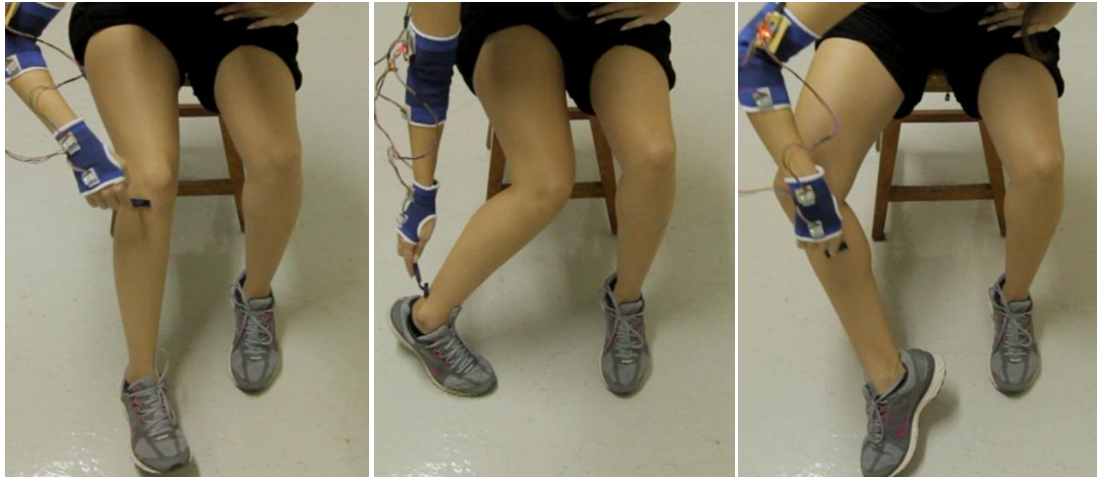


Figure 37: Three leg postures for three leg regions: Outer (left), Rear (middle), Inner (right)

In other words, it is a good approximation to assume that women only use three different leg postures to shave one lower leg while seated, moving from one posture to the other or alternating between postures, if necessary.

The reasons behind changing leg posture during leg shaving can be summed up to the following:

- Easier to reach certain areas
- Visual contact with the skin being shaved, for effectiveness and avoidance of cuts

D.1.2.2 Upper Leg Segmentation

Preliminary tests showed that a percentage of women rarely or never shave their upper legs (thigh), depending on their body hair. Moreover, it was found that the rear side of the upper legs is always shaved in an upright stance, not in a seated stance, which is the focal point of this thesis. Therefore, in this thesis we only considered shaving of the front side of the thigh. The resulting segmentation of the upper leg is:

- Region iv. The front (F) side of the thigh
- Region v. The rear side of the thigh (which was not included in this task)



Figure 38: Leg posture for the upper leg front region

D.1.2.3 Task Sequence

The sequence with which subjects were asked to shave regions was the following:

1. Right lower leg, Outer side – RO
2. Right lower leg, Rear side – RR
3. Right lower leg, Inner side – RI
4. Right upper leg, Front side – RF
5. Left lower leg, Inner side – LI
6. Left lower leg, Rear side – LR
7. Left lower leg, Outer side – LO

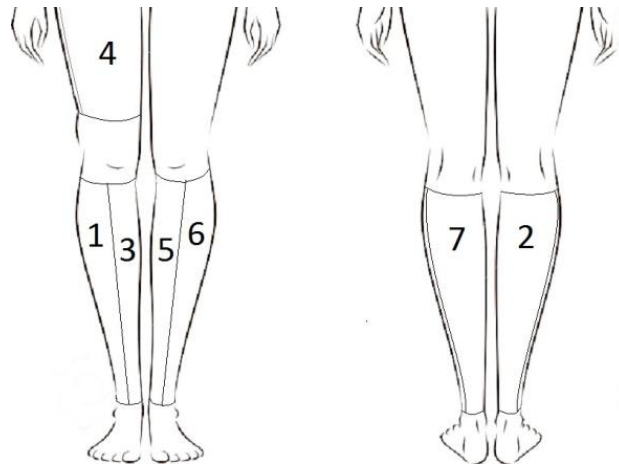


Figure 39: Task sequence for right-handed subject

The above sequence was intended for a right-handed subject. If the subject used the left hand as dominant, then he/she would be instructed to follow an analogous sequence, where “right leg” is replaced by “left leg” and vice versa.

Although, in preliminary tests, the sequence was not always consistent, the above succession of skin regions was favored by subjects because it requires smaller motions to move from one region to the next.

In the tests, subjects would occasionally return to a region they had already shaved, without following a specific pattern. However, it was deemed unnecessary to reproduce this randomness in the formal experiment.

D.1.2.4 Subject Freedom vs Controlled Conditions

The subjects were instructed to simulate shaving of each region separately, in order to reduce uncertainty factors and facilitate comparison across subjects. Within a specific region, subjects were given total freedom on the manner of shaving (e.g. long/short strokes, fast/slow, direction) and total time of completion. In this way we hoped to allow natural behavior of the subjects, and not restrict their thinking process and movements by over-defining the task to be completed.

D.1.3 Measurements

The wearable system which was developed for this thesis was used, to capture measurements of the 3 DoF of the wrist and forearm; namely pronation/supination (P/S), flexion/extension (F/E) and radial/ulnar deviation (R/UD). The system uses 3

inertial sensors (IMUs) and is described in chapter “C.2 Development of a Tracking System”.

A video-camera recorded task completion, from the abdomen and below, after obtaining oral consent of the subjects. This allowed video-analysis to be used in a later stage of processing the results.

Furthermore, a short questionnaire (2 min.) was used, in order to acquire information about factors that could affect the shaving behavior of subjects. Namely, subjects were asked about (a) their usual body stance during shaving, (b) their perceived level of hairiness in comparison to other women, and (c) their choice of lubrication fluid (e.g. shaving foam, bath foam, and soap).

D.1.4 Subjects

10 individuals participated in the evaluation of razors. All 10 were female and their average age was 23.2 (± 1.8) years, with no prior history of musculoskeletal conditions. 9 of them were right-handed, while 1 was left-handed, for whom the procedure was adjusted accordingly. Apart from one, all subjects were experienced in the task of shaving, since they reported they had regularly used it as a method of hair removal. Additionally to average sized subjects, the sample included both small and large hand and body sizes.

D.1.5 Procedure

Each subject completed the experiment individually, without having watched any previous subjects. The total duration of the procedure was approximately 30 minutes, while the duration of the actual measurements was approximately 10 minutes.

The purpose of this study was orally explained to the subjects, prior to the experiment. The 7 tasks were presented to the subjects and their permission for video-recording of the experimental setting was obtained. The glove and elbow patch was worn on their dominant arm and the tracking system was mounted, after having been calibrated (see ch. “C.2.2.1.7 Calibration”).

The subjects were given a razor and they were asked to complete all 7 tasks, before repeating the process with a different razor, until all 3 razors had been used. At the beginning, the subjects were asked to hang their arm at the neutral posture (see ch. “A.5 Ranges of motion”) which was used as a reference. Between different razors, the neutral posture was reset, to account for any displacement of the clothing over the skin. Occasionally, re-calibration of the sensors was deemed necessary.

To eliminate any effect of the sequence with which subjects used razors, their order was altered between the 10 subjects. All 6 different permutations of the 3 razors were used, while some combinations were used twice.

Finally, subjects completed a short questionnaire, with questions regarding factors which could affect their shaving behavior.

D.2 Results

D.2.1 Wrist & Forearm Joint Angles

The ultimate goal of these measurements is to compare the effect of razor handle design on wrist and forearm posture, if there is any. A representation of this is provided by Table 16, where the mean wrist and forearm joint angles (of all subjects) are displayed for each task, along with standard deviation, in degrees. Mean posture is an appropriate indicator of risk according to various studies (Keir, Bach, Hudes, & Rempel, 2007; Yu, Lowndes, Morrow, Kaufman, Bingener, & Hallbeck, 2016; Lintula & Nevala, 2006; Nevala, Sormunen, Remes, & Suomalainen, 2013).

The sign convention used, for the joint angles, throughout this thesis is presented in the following table (see Table 15) and figure (see Fig. 40):

Table 15: Sign convention (used throughout this thesis)

Pronation	-	Supination	+
Flexion	+	Extension	-
Radial dev.	+	Ulnar dev.	-

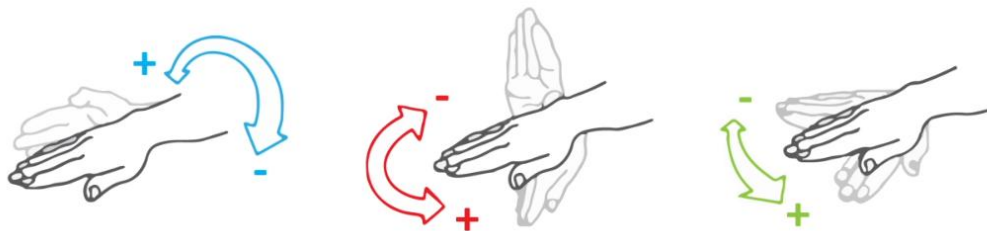


Figure 40: Sign convention

As discussed previously (see Table 2), the limits of wrist and forearm joint angles which are appropriate for tasks can be considered to be:

Table 16: Joint angle limits (as in Table 2)

DoF	Limit (suggested)
P/S	-45° / +45°
F/E	+21° / -18°
R/UD	+12° / -10°

Table 17: Mean joint angles (in deg.) and standard deviation, across all subjects, for the seven tasks

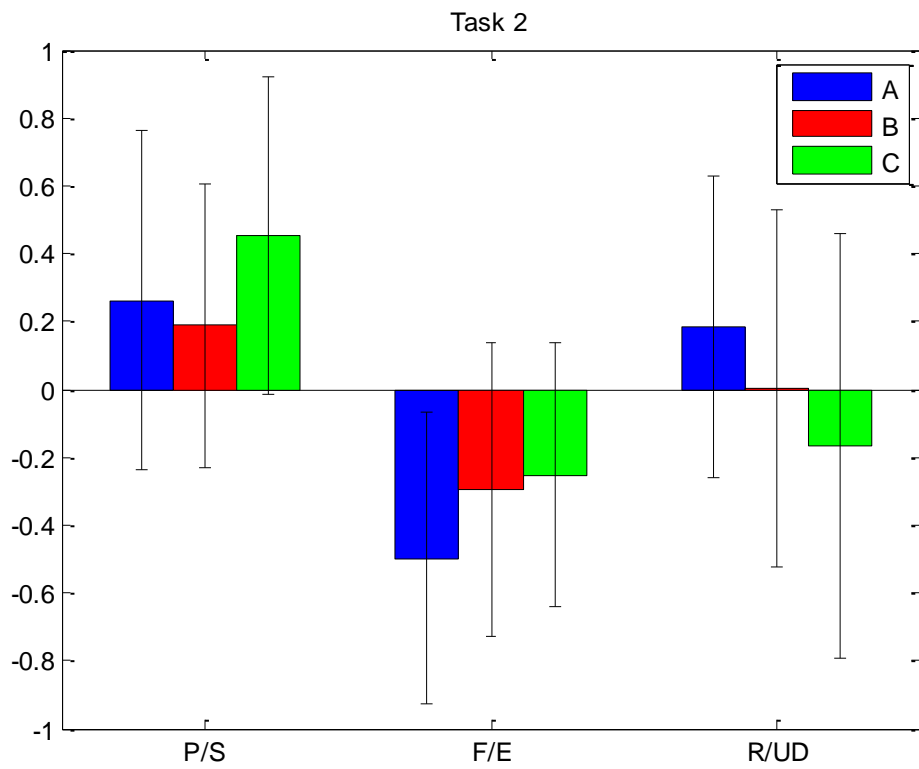
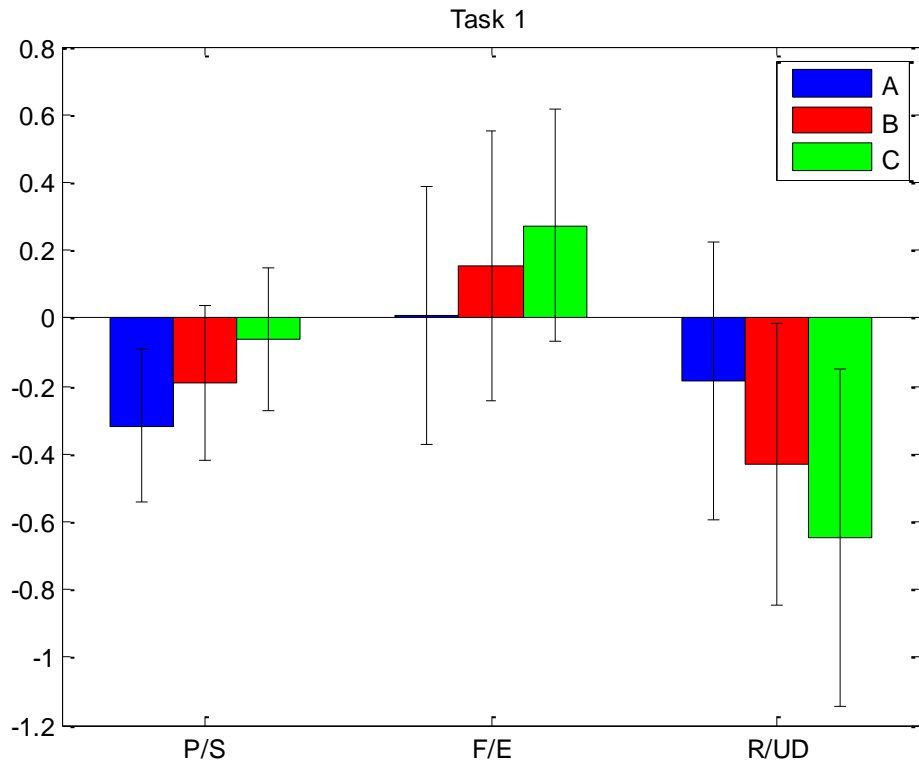
Razor	P/S (s.d.)	F/E (s.d.)	R/U (s.d.)	task1
A	-14.36(10.12)	0.21(7.98)	-1.87(4.09)	
B	-8.58(10.20)	3.25(8.34)	-4.31(4.16)	
C	-2.81(9.60)	5.73(7.14)	-6.49(4.98)	
	P/S	F/E	R/U	task2
A	11.78(22.47)	-8.97(7.73)	2.19(5.33)	
B	8.49(18.82)	-5.31(7.79)	0.04(6.32)	
C	20.44(21.06)	-4.54(7.02)	-1.66(6.26)	
	P/S	F/E	R/U	task3
A	-23.62(13.31)	7.39(8.42)	-6.62(4.89)	
B	-17.81(14.05)	13.60(8.68)	-6.54(5.53)	
C	-17.04(12.95)	9.79(9.08)	-8.31(5.84)	
	P/S	F/E	R/U	task4
A	-22.10(17.44)	4.92(7.87)	-3.35(6.06)	
B	-16.21(16.63)	6.82(9.26)	-3.64(6.23)	
C	-12.63(16.05)	7.63(9.12)	-4.36(8.01)	
	P/S	F/E	R/U	task5
A	-9.45(10.59)	1.99(7.94)	-3.27(4.05)	
B	-5.75(11.05)	5.62(9.65)	-5.06(4.48)	
C	-1.98(9.47)	6.00(9.28)	-7.05(6.66)	
	P/S	F/E	R/U	task6
A	1.64(18.14)	-2.68(9.32)	0.41(5.59)	
B	6.76(17.91)	0.42(9.04)	1.39(6.10)	
C	12.03(17.06)	-2.38(9.77)	-1.84(6.54)	
	P/S	F/E	R/U	task7
A	-18.73(14.51)	9.72(8.60)	-6.02(4.89)	
B	-18.44(14.67)	14.59(9.25)	-5.13(5.66)	
C	-14.95(15.25)	15.63(9.57)	-5.83(6.43)	

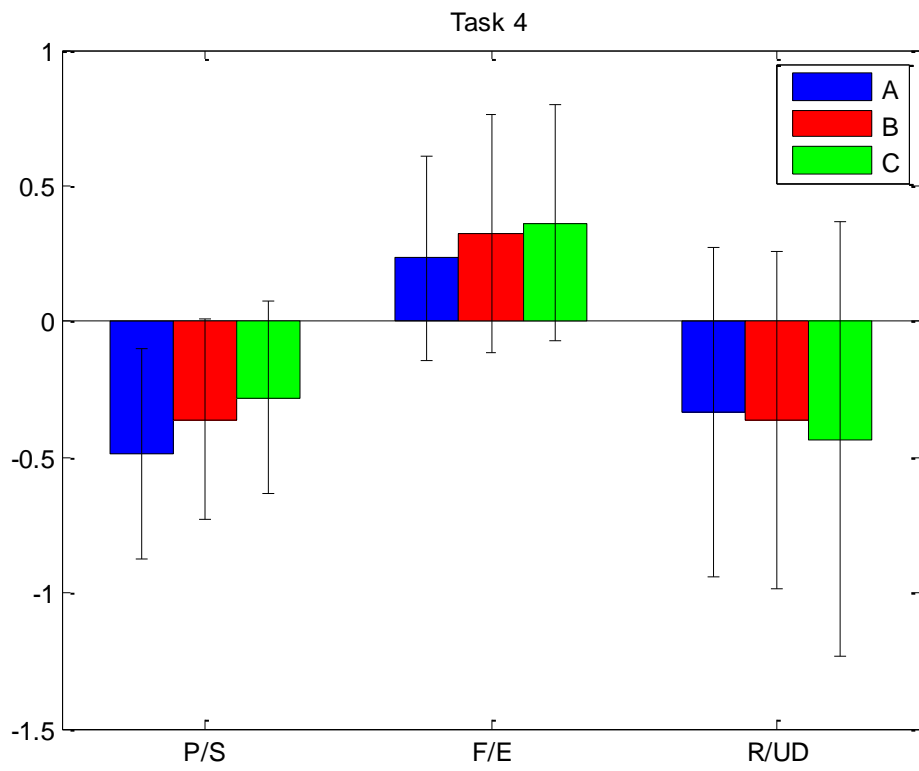
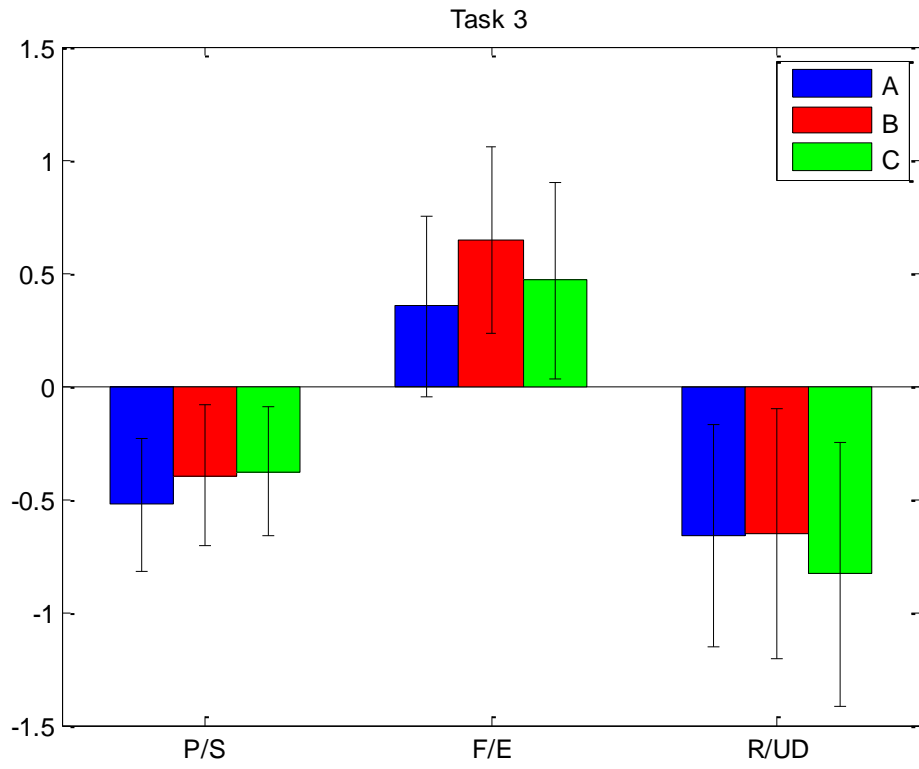
D.2.1.1 Comparison of Joint Angles

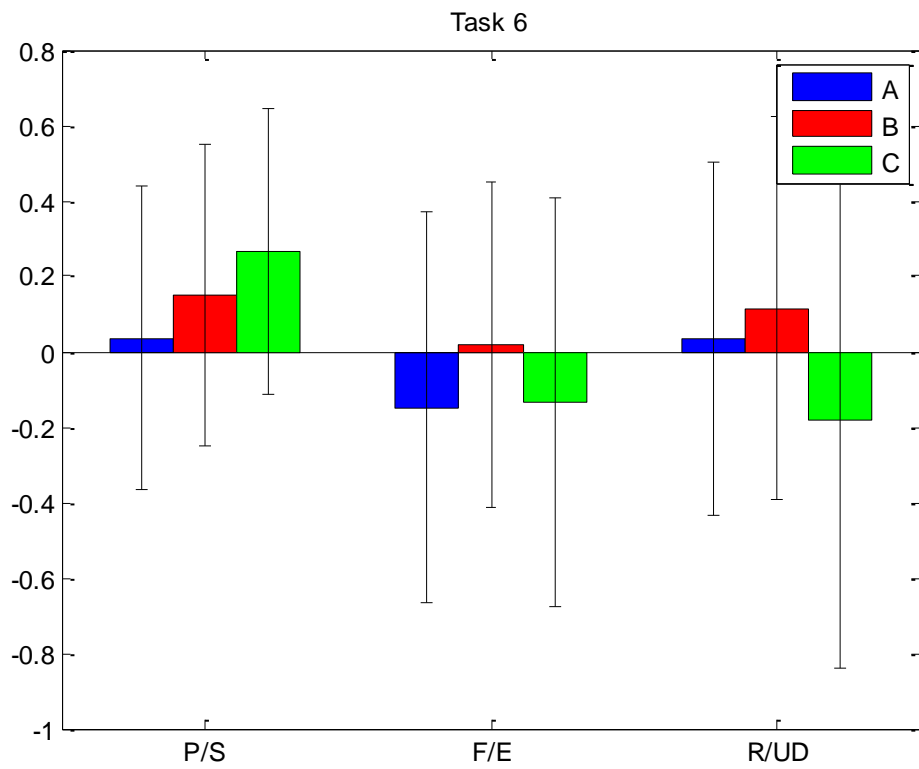
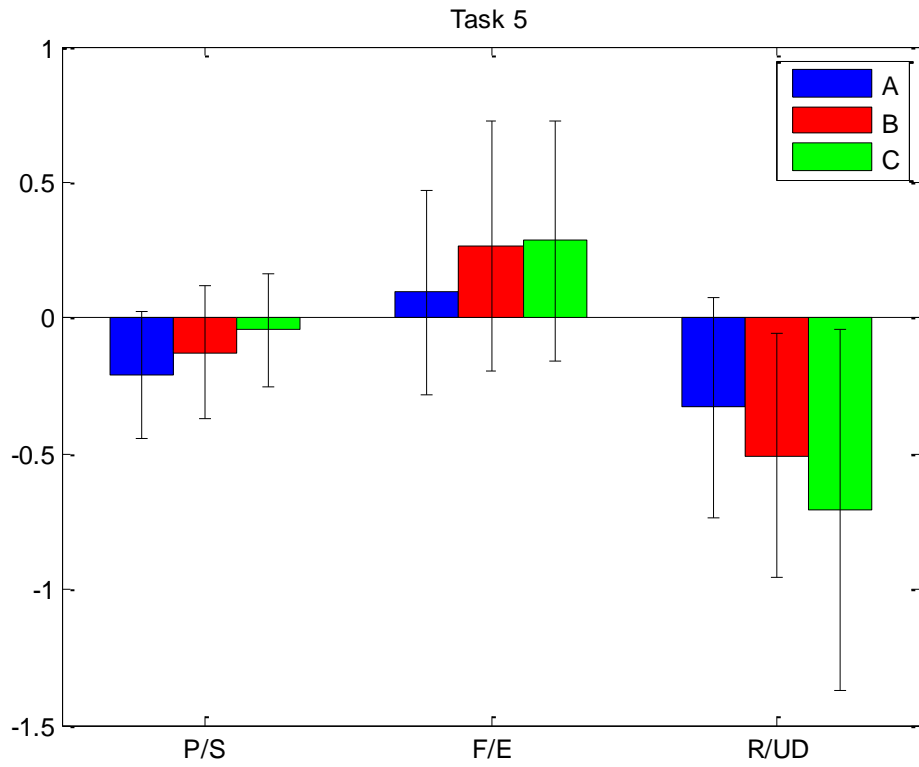
The joint angles displayed on Table 16 can be normalized, based on the corresponding suggested limits. Joint angles relatively to joint angle limits are presented in the following table (see Table 18) and the bar graphs (see Fig. 41. This is the result of simple division between mean joint angles of Table 16 and angle limits (see Table 17).

Table 18: Mean joint angles as a fraction of joint angle limits

Razor	P/S (s.d.)	F/E (s.d.)	R/U (s.d.)	task1
A	-0.319(0.225)	0.010(0.380)	-0.187(0.409)	
B	-0.191(0.227)	0.155(0.397)	-0.431(0.416)	
C	-0.062(0.213)	0.273(0.340)	-0.649(0.498)	
	P/S	F/E	R/U	task2
A	0.262(0.499)	-0.498(0.429)	0.182(0.444)	
B	0.189(0.418)	-0.295(0.433)	0.003(0.527)	
C	0.454(0.468)	-0.252(0.390)	-0.166(0.626)	
	P/S	F/E	R/U	task3
A	-0.525(0.296)	0.352(0.401)	-0.662(0.489)	
B	-0.396(0.312)	0.648(0.413)	-0.654(0.553)	
C	-0.379(0.288)	0.466(0.432)	-0.831(0.584)	
	P/S	F/E	R/U	task4
A	-0.491(0.387)	0.234(0.375)	-0.335(0.606)	
B	-0.360(0.369)	0.325(0.441)	-0.364(0.623)	
C	-0.281(0.357)	0.363(0.434)	-0.436(0.801)	
	P/S	F/E	R/U	task5
A	-0.210(0.235)	0.095(0.378)	-0.327(0.405)	
B	-0.128(0.245)	0.267(0.459)	-0.506(0.448)	
C	-0.044(0.210)	0.286(0.442)	-0.705(0.666)	
	P/S	F/E	R/U	task6
A	0.037(0.403)	-0.149(0.518)	0.034(0.466)	
B	0.150(0.398)	0.020(0.430)	0.116(0.508)	
C	0.267(0.379)	-0.132(0.543)	-0.184(0.654)	
	P/S	F/E	R/U	task7
A	-0.416(0.323)	0.463(0.410)	-0.602(0.489)	
B	-0.410(0.326)	0.695(0.441)	-0.513(0.566)	
C	-0.332(0.339)	0.744(0.456)	-0.583(0.643)	







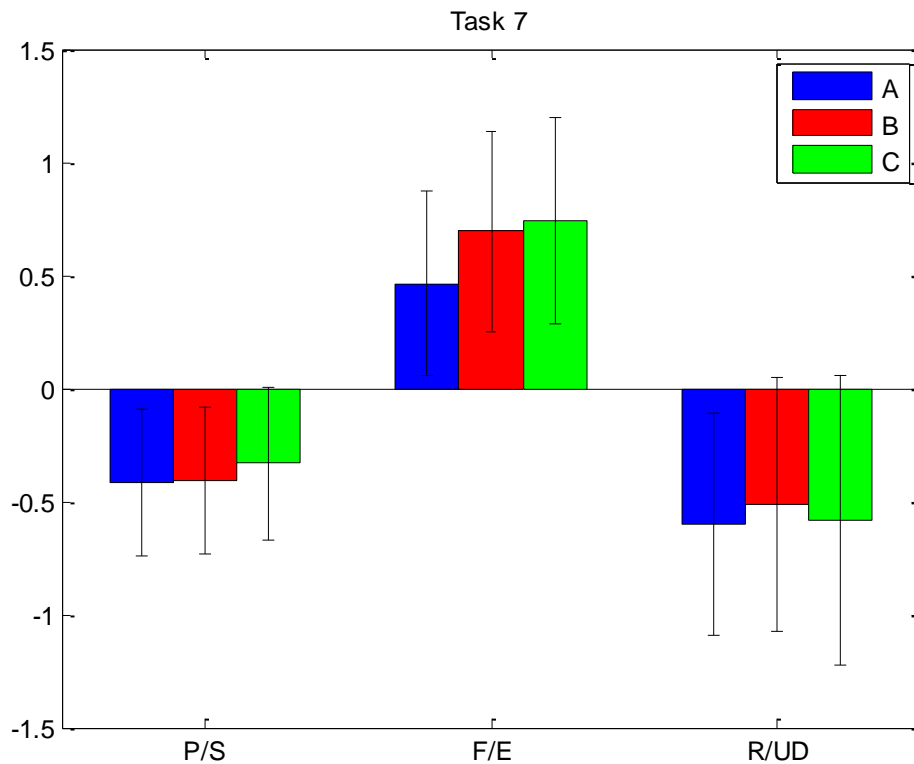


Figure 41: Bar graphs of normalized mean angles (based on suggested angle limits), with standard deviation as error bars.

Observations:

- On average, forearm is in pronation (-) in all tasks, except tasks 2-RR and 6-LR (rear side of lower legs), where it is generally supinated (+).
- On average, wrist is in flexion (+) in all tasks, except tasks 2-RR and 6-LR, where it is generally extended (-).
- On average, wrist is in ulnar deviation (-) in all tasks, except tasks 2-RR and 6-LR, where it is generally in radial deviation (+).
- P/S tends to increase (moving towards positive angles) from razor A to B to C, in most tasks. This means that the forearm is generally less pronated (or more supinated) when using razor C than razor B, and similarly when using razor B than A.
- R/U tends to decrease (moving towards negative angles) from razor A to B to C, in most tasks. This means that the wrist is generally more ulnarly deviated (or less radially deviated) when using razor C than razor B, and similarly when using razor B than A. The difference may seem slighter than in P/S, but the RoM of this DoF is also smaller.
- F/E tends to increase (moving towards positive angles) from razor A to B, in most tasks. However, the difference between razors B and C is minute. This means that the wrist is generally more flexed (or less extended) when using razors B and C, than razor A.
- Mean joint angles can generally be considered to lie inside the neutral posture zone defined by most studies, except ulnar deviation (UD) in some cases.
- Standard deviations of joint angles for the 3 razors have minute differences, in each task.

The above observations imply that there is indeed a correlation between handle design and wrist and forearm motion.

Although the above table (see Table 18) and graphs (see Fig. 41) contain extensive information, it is difficult to ultimately compare the 3 alternative design solutions. In order to facilitate comparison, the extraction of a single metric, indicative of the total wrist and forearm deviation for each razor, is needed. It is also useful to calculate an indicative metric for each DoF separately. This can be achieved, by calculating the *Euclidean norm* of a matrix (or vector for separate DoFs) for each razor, containing the joint angles relative to angle limits. The norm is a measure of the total magnitude of the elements of the matrix (or vector). The calculation of the norm for each razor returns the following results:

Table 19: Euclidean Norms of normalized joint angles

Razor	P/S norm	F/E norm	R/UD norm	Overall Eucl. Norm
A	0.9517	0.8199	1.0437	1.5704
B	0.7519	1.0913	1.1308	1.6890
C	0.7849	1.0681	1.4832	1.8297
Comparison	B<C<A	A<C<B	A<B<C	A<B<C

The actual figure of the norm does not have a physical meaning; it is merely a representation of magnitude. However, it can be used for relative comparison. The results clearly indicate that the least wrist and forearm deviation from neutral posture is achieved when using razor A. Razor B is second and razor C is last.

D.2.2 Intrasubject Analysis

Analysis within a subject is useful to validate the observations made. A single subject, which is representative of most subjects, is used to demonstrate the method of study.

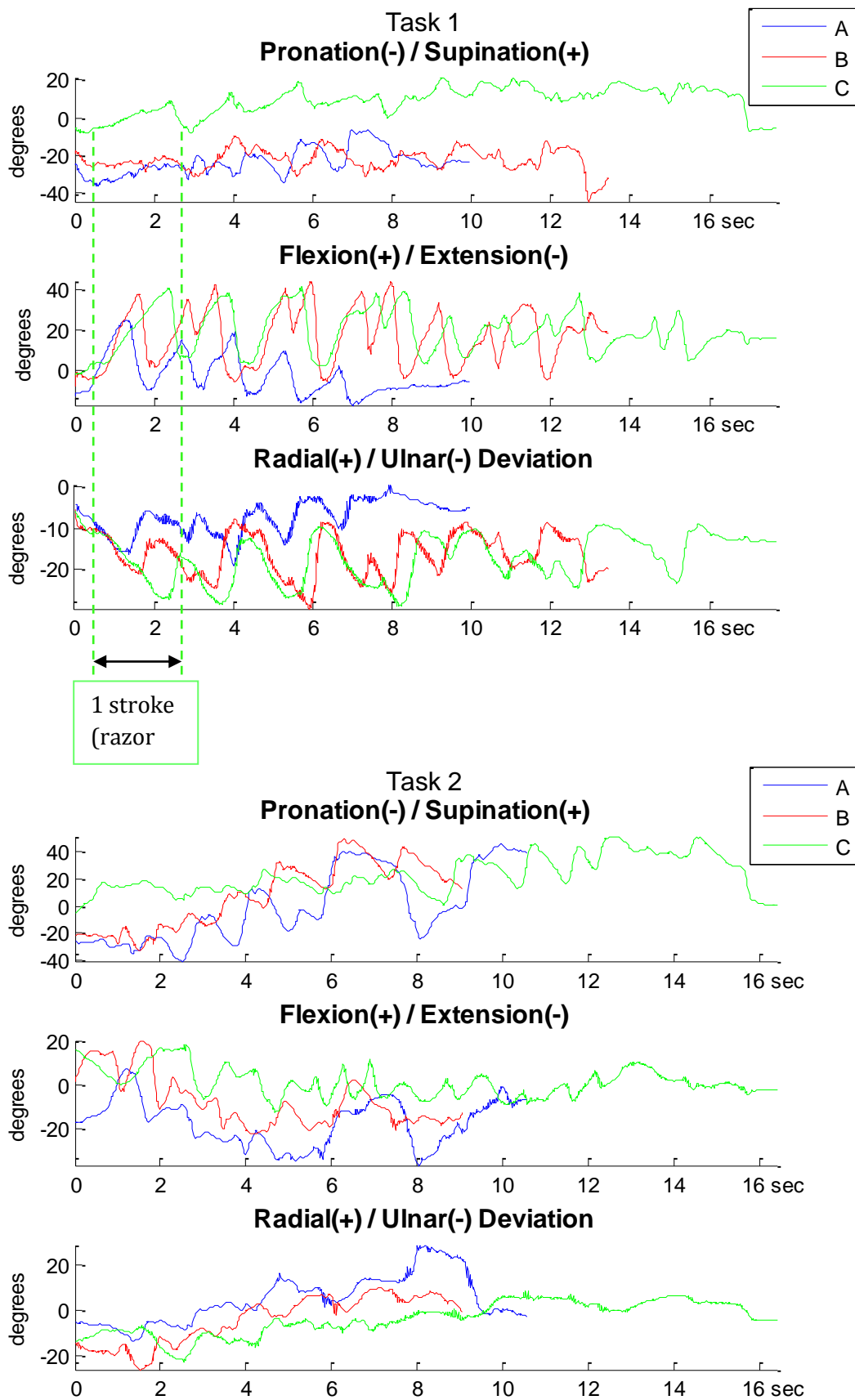
Table 20: Mean joint angles (in deg.) and standard deviation, of a representative subject

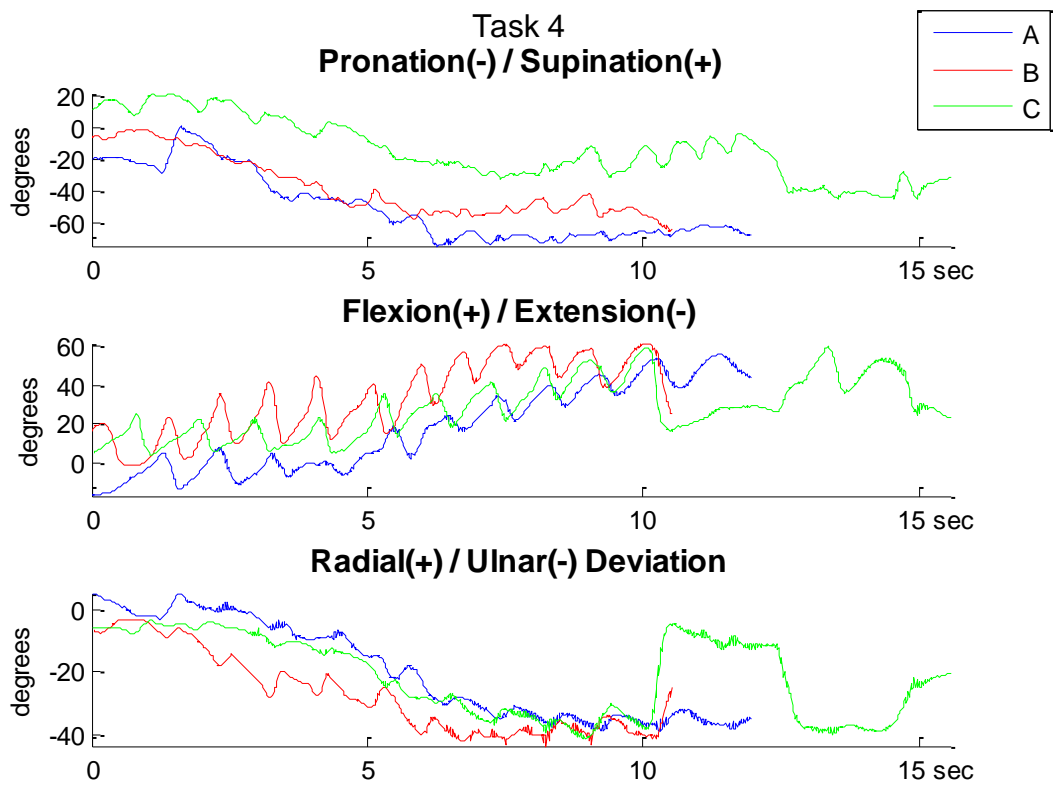
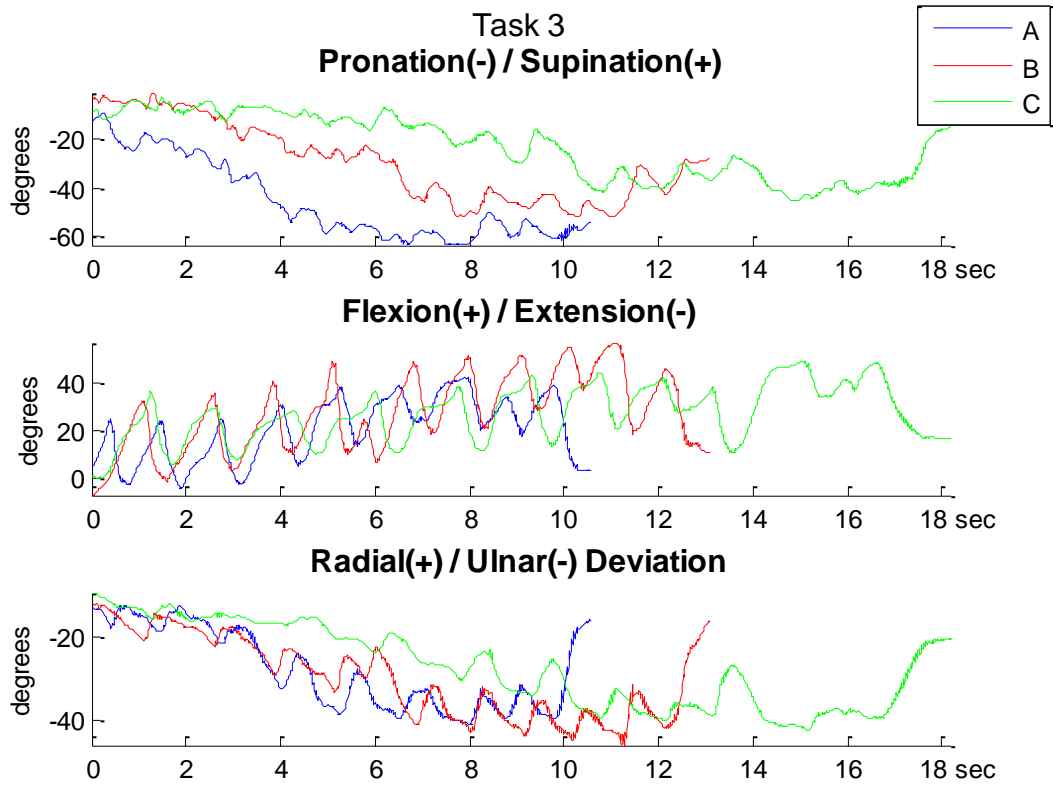
Razor	P/S (s.d.)	F/E (s.d.)	R/U (s.d.)	task1
A	-23.74(7.06)	-2.34(9.79)	-7.30(4.17)	
B	-22.58(5.84)	16.60(13.74)	-16.26(5.23)	
C	8.78(7.67)	19.22(10.58)	-17.22(5.76)	
	P/S	F/E	R/U	task2
A	-0.21(26.28)	-16.80(10.41)	5.09(10.49)	
B	7.90(23.41)	-7.06(11.59)	-3.90(10.33)	
C	22.42(13.44)	1.29(6.45)	-3.40(7.09)	
	P/S	F/E	R/U	task3
A	-45.36(16.16)	20.21(12.73)	-27.68(9.52)	
B	-29.13(15.95)	27.04(15.67)	-29.50(9.63)	
C	-22.82(13.17)	26.77(11.50)	-26.89(9.71)	
	P/S	F/E	R/U	task4
A	-49.36(21.56)	17.00(21.91)	-19.54(15.45)	
B	-36.78(19.05)	33.09(18.96)	-26.99(12.89)	
C	-13.65(19.18)	27.69(14.75)	-21.32(12.89)	
	P/S	F/E	R/U	task5
A	-31.67(8.13)	3.36(16.28)	-11.38(6.69)	
B	-18.77(7.89)	19.48(20.57)	-20.17(8.11)	
C	-2.36(5.98)	17.02(16.64)	-20.52(7.74)	
	P/S	F/E	R/U	task6
A	9.71(21.60)	-15.93(11.16)	6.37(5.18)	
B	12.65(14.55)	-16.53(12.57)	9.18(7.16)	
C	33.40(11.36)	-12.16(4.54)	-0.58(4.08)	
	P/S	F/E	R/U	task7
A	-29.80(20.29)	19.20(12.11)	-23.46(5.81)	
B	-24.28(15.48)	31.99(13.10)	-27.53(6.47)	
C	-18.52(17.95)	35.39(13.69)	-29.63(5.90)	

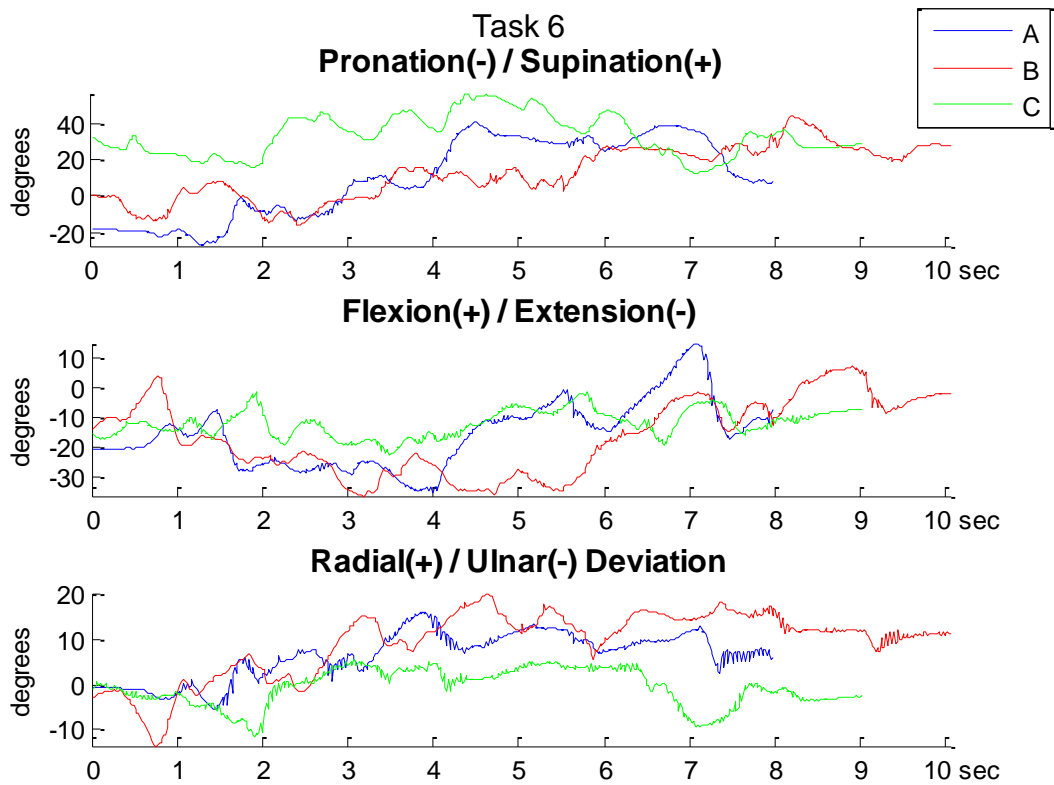
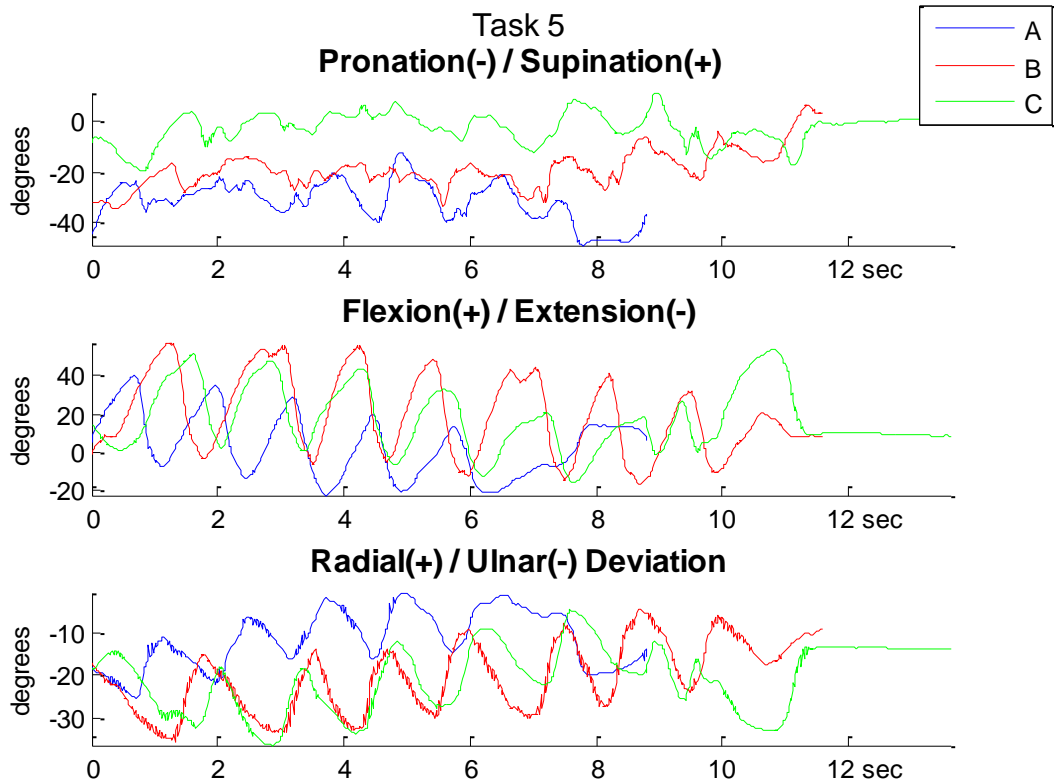
Observations:

- Analogous tendencies to the average, across all subjects.
- Joint angles seem more extreme than those of the average subject (see Table 16) but this could be attributed to individual characteristics (larger joint RoM) and/or variability in sensor setup and reference posture.

The complete data for this specific subject are visualized in graphs (each task separately), in which the angles of the 3 joints (P/S, F/E, R/UD) are plotted versus time. The graphs for the 3 different razors are superimposed, to facilitate comparison:







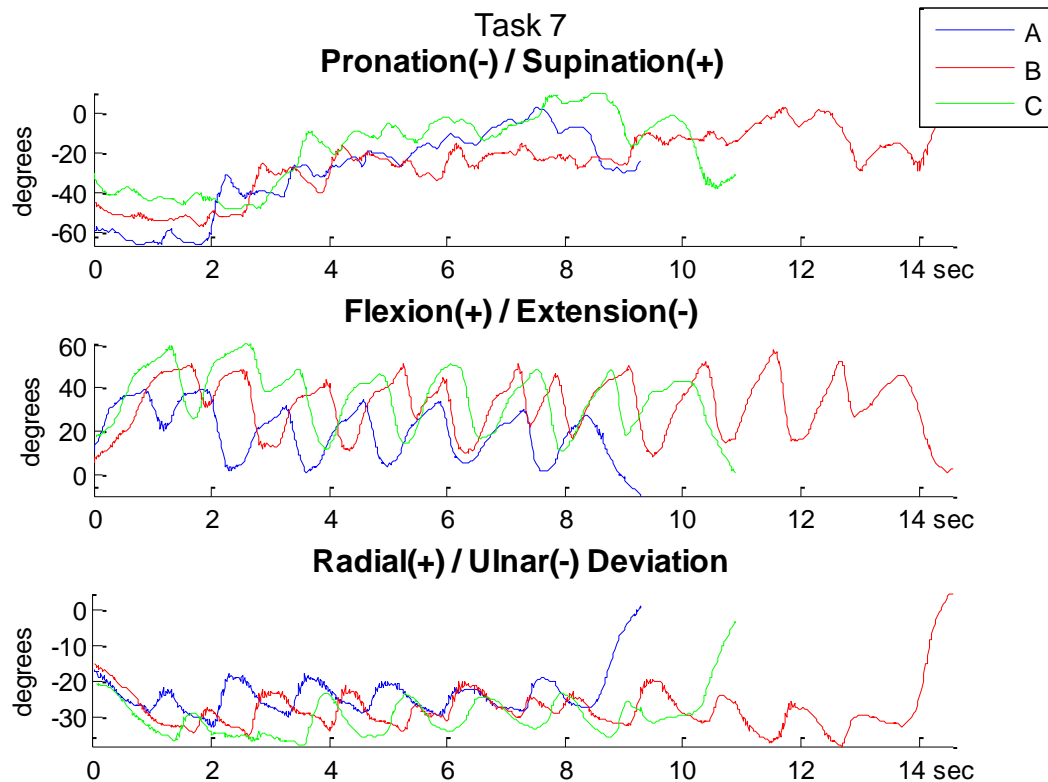


Figure 42: Wrist and forearm motion graphs on all seven tasks, for a single subject

Observations, based on the above graphs (Fig. 42):

- Shaving strokes are distinguishable, in the form of peaks, for some DoFs –most commonly F/E and R/UD which are coupled (see ch. “A.7 Wrist Motion Coupling”).
- Joint motion with all razors follows the same basic patterns, indicating that shaving style is independent of the razor used.

D.2.3 Video Analysis

D.2.3.1 Grip Type

By reviewing the video recordings of the experiment, the grip types (see ch. “B.1 Types of Grip”) used by the subjects can be studied. Interestingly, it was found that the type of grip was mostly associated with the subject’s individual style, rather than the razor or task. However, it should be noted that the grip type of a subject is not unchanging during razors and tasks; rather, it may be slightly adjusted to fit a razor handle or a specific task.

Although grip classification is often arguable, because there are numerous variations, two types of grips were mostly used by the subjects in this study:

-
- *Internal precision grip* variation: Handle is pinched between the 1st and the side of the 3rd digit (thumb and middle finger), and the 2nd digit (index) applies the required vertical pressure, while being parallel to the axis of the handle.
 - *Pinch grip* variation: Handle is pinched between the 1st and 2nd digit (thumb and index).



Figure 43: Grips for razors: Internal precision grip (left), pinch grip (right)

The grip mostly used in this experiment was the internal precision grip, which was the dominant grip for 7 out of 10 subjects, whereas 3 out of 10 preferred the pinch grip. However, occasionally subjects would adapt their grip style to a razor or task. Namely, 3 of the 10 subjects displayed some inconsistency in their grip types, using both the internal precision grip and pinch grip, at times. Furthermore, shaving the upper leg seemed to promote using an internal precision grip, in all 10 subjects.

Gathering of this data was primarily aimed at studying the potential effect the grip type may have on wrist and forearm motion. For that reason, it was more important to relate grip type to the individual, rather than to generally assess shaving styles statistically. This analysis was inconclusive, since the sample size proved relatively small to safely extract such information. However, the results hint that there is no significant correlation between grip type and statistics of joint angles (mean, standard deviation).

D.2.3.2 Shaving Stroke Style

Each subject has a personal shaving style, in terms of the length and speed of each shaving stroke. Information about stroke length was gathered from video analysis, and it was considered during the processing of results.

Length of strokes:

- Large strokes: 4 subjects
- Small strokes: 4 subjects
- Combination of large and small strokes: 2 subjects

As with grip types (see ch. “D.2.3.1 Grip Type”), no specific correlation between shaving stroke style and wrist motion was observed.

D.2.4 Questionnaire

The questionnaire, completed by 10 participants, returned the following results:

Body stance during shaving:

- 9 stand upright, elevating the leg on a supporting surface
- 1 stands, but bends to reach the legs

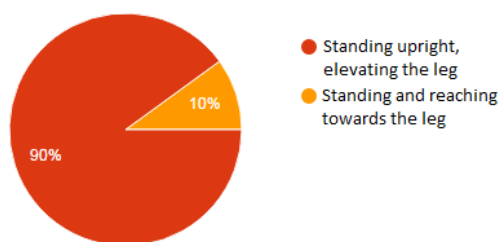
Lubricating fluid:

- Bath foam: 7
- Shaving cream: 2
- Soap: 1

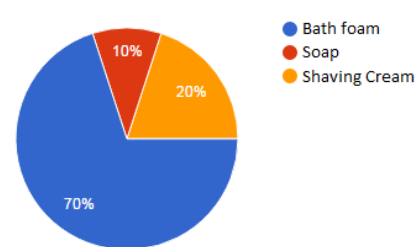
Level of hairiness (on a scale 1-5):

- Level 1: 0
- Level 2: 2
- Level 3: 5
- Level 4: 3
- Level 5: 0

Body stance during shaving



Lubricating fluid



Level of hairiness

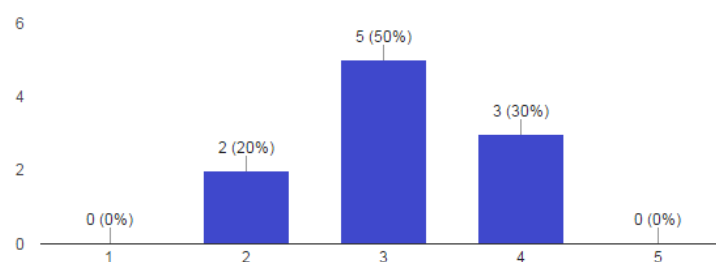


Figure 44: Visualization of questionnaire results

Similarly to previous behavioral factors (see ch. “D.2.3.1 Grip Type” and “D.2.3.2 Shaving Stroke Style”), it is not the general statistics of shaving behavior that concerns this study. Rather, we focus on the effect these factors may have on kinematic behavior of individual subjects. Once again, even though the sample size was small to yield definitive conclusions on the issue, the results suggest there is no link between these factors and kinematic behavior of the subjects (wrist and forearm joint motion).

D.3 Discussion

Combining the information included in the table for joint angles, with observations made from video analysis, we were able to form and confirm the following hypotheses:

- Joint angle results demonstrate an analogy between pairs of tasks: (1-R0 and 5-LI), (2-RR and 6-LR) and (3-RI and 7-LO), which are on the same side of the two legs (e.g. tasks 1 and 5 are on the right side of the right and left leg, respectively, for a right-handed subject). It is natural for this analogy to exist, because the two surfaces of each pair have a similar orientation in space, relatively to the hand used for shaving (subjects only used the dominant hand); therefore, the kinematic behavior was expected to be similar. This fact serves as an argument towards validation of the functionality of the tracking system.
- In the results, there exists a correlation between wrist F/E and R/UD. Namely, wrist flexion promotes ulnar deviation, while wrist extension promotes radial deviation. This is consistent with research on wrist biomechanics (see ch. "A.7 Wrist Motion Coupling").
- Razor handle design has an effect on wrist and forearm joint motion. This was evident by the following tendencies:
 - Forearm pronation decreases (or when the forearm is supinated, supination increases) in the order of razors: A,B,C
 - Wrist flexion increases (or extension decreases) in the order: A,B=C (razors B and C do not produce significant differences)
 - Ulnar deviation increases (or radial deviation decreases) in the order: A,B,C
- Standard deviations in most tasks were not significantly different between razors A, B, C. In other words, the ranges of motion of the wrist and forearm, used by the subjects during shaving, were approximately the same for all razors.
- The task of lower-limb shaving is unlikely to cause either discomfort or risk for musculoskeletal disorder (MSD). The mean joint angles during the task can be considered within the neural limits. The levels of standard deviation indicate that wrist and forearm joints only reach extreme postures during a small fraction of the time. Moreover, the duration of the task is short and the exertion of force required is minimal; there are no other factors to aggravate the risk of discomfort or cumulative trauma (see ch. "A.6 Negative effects of extreme joint angles").

D.3.1 Explanation of Joint Angle Differences

The increase of ulnar deviation (UD) from razor A to B and to C can be attributed to the length of the handle. Larger handle length leads to higher UD (see Fig. 45). In the internal precision grip, a long handle may come into contact with the thenar eminence (muscles at the base of the thumb). When the palm is arched to embrace the handle, the thenar eminence pushes the handle towards a diagonal position across the palm, rather than parallel to the index. Thus, the razor head which holds the blades, changes its angle relative to the surface to be shaved. The subject, having visual contact with the razor head, subconsciously compensates for this change of angle, by rotating the wrist towards ulnar deviation, in order to place the blades vertically to the shaving stroke

direction (from bottom to top of leg). A longer handle is more susceptible to this phenomenon, causing higher ulnar deviation.

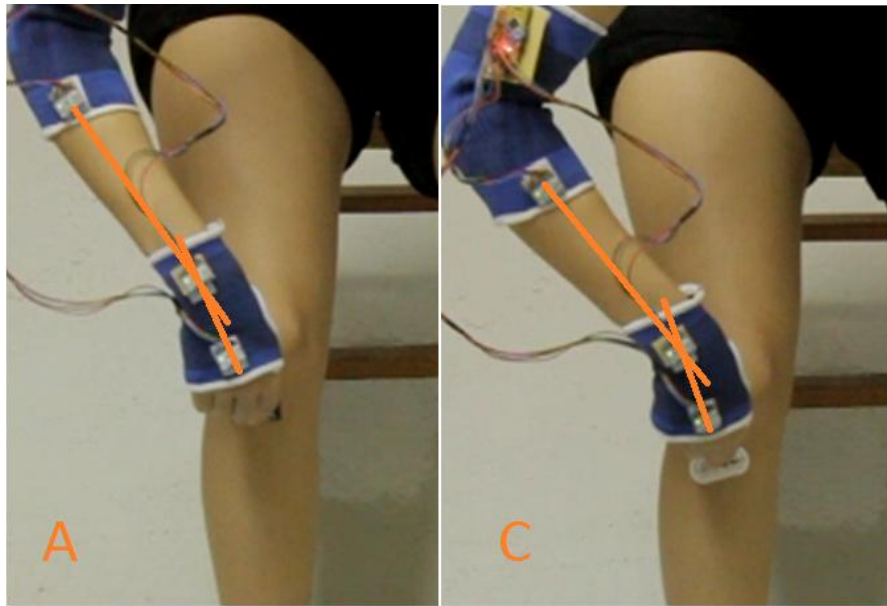


Figure 45: Ulnar deviation with razor A (left) is smaller than with razor C (right)

The suggested length of handle heavily depends on biometrics (hand geometry) of the population aimed to use the razor. In our study, we mainly addressed the female population, and tested 3 different lengths: 10.5 cm, 12.6 cm and 13.5 cm. We noticed an increase in UD associated with an increase in handle length. This increase was slighter from 10.5 cm to 12.6 and larger from 12.6 cm to 13.5 cm. This indicates that, for the participants of this study, a handle length of 12.6 cm or smaller was suitable, in order to decrease the need for ulnar deviation.

Decreased pronation when using razor C could be explained due to the shaving head's rotation around the handle's axes, a feature which is absent in razors A and B. Forearm pronation/supination (P/S) occurs approximately around the same axis as this rotation of the shaving head in razor C. The shaving head is compliant and rotates to adjust to the body contours, requiring less forearm rotation from the subject. However, the difference in P/S between razors A and B is not as apparent, since neither of them has a rotating head around the handle's axis.

Similarly, the reasons for the increase in wrist flexion from razor A to razors B and C (B and C demonstrate no significant differences F/E) are not evident. A possible explanation lies in the pivoting head of razors B and C, since this is their common feature. It is assumed that the pivoting head promotes a more flexed wrist posture: The pivoting head adjusts to the skin surface and may subconsciously encourage the subjects to utilize wrist mobility in F/E, instead of moving their whole arm, which requires larger effort. In contrast, when using razor A which has a fixed shaving plane (angle of shaving head relative to handle), using wrist mobility is not an option, since the angle of the razor relative to the skin needs to be constant. Therefore, when using razor A, subjects move their wrist more "rigidly" to avoid altering the shaving angle; the motion mainly comes from the elbow and shoulder. This explanation however, is not supported by the

figures of standard deviation. Standard deviation would have to be higher in razors B and C, to account for the larger amplitude of motion. Conversely, no significant differences were found on average, between standard deviations when using the 3 razors.

D.3.2 Comparison of Razors

The original purpose of this study was the comparison of 3 alternative design solutions: razors A, B and C, from the scope of ergonomics. As previously discussed (see ch. “B.2.3 Ergonomic Principles for Hand Tool Design”), ergonomic design strives to avoid wrist deviation from neutral posture. Our preliminary hypothesis was that razors with more DoFs ($A < B < C$) would allow the wrist and forearm to maintain a neutral posture, more than razors without mobility. This was true in the case of the forearm (P/S). However, it was disproven in the case of the wrist (F/E and R/UD): more “sophisticated” razors, with higher DoFs, actually promoted a more deviated wrist. The order of design solutions, from best to worst, based on overall wrist and forearm deviation, was found to be: $A > B > C$

To determine the above order of razors, based on which promotes a more deviated wrist and forearm, we normalized mean joint angles based on angle limits (see ch. “D.2.1.1 Comparison of joint angles”). We calculated the Euclidean norm of the normalized angles for each razor, which presents a measure of the magnitude of total deviation in all DoFs.

The assumptions made, for this approach, were the following:

- There is a linear relation between joint angle magnitude and discomfort/risk of MSD (so that the comparison of posture deviation is meaningful).
- Deviations in all joint DoFs (P/S, F/E and R/UD) contribute equally to discomfort/risk of MSD (since their contribution to the calculation of the norm is equivalent).
- Similarly, the “importance” (i.e. time duration, exertion of force) of all tasks is equal.

These assumptions are not entirely accurate: Studies showed that the relationship of wrist posture to carpal tunnel pressure (CTP) (Keir, Bach, Hudes, & Rempel, 2007) and discomfort (Carey & Gallwey, 2002) are not exactly linear. Another study (Werner, Armstrong, Bir, & Aylard, 1997) found that the greatest increase in CTP (see ch. “A.6 Negative effects of extreme joint angles”) is caused primarily by F/E, then P/S, and lastly R/UD, but their contributions were not clearly quantified. However, CTP is not the only factor affecting discomfort and risk of MSD. The above assumptions can be considered an adequate approximation.

D.3.3 Challenging the Results

The above results should be treated with consideration: As stated above, it was found that joint postures during shaving, for all razors, were generally not extreme; hence, they are highly unlikely to cause discomfort or risk of cumulative MSDs on the subjects. This argument is further supported by the low exertion of force and short duration of wrist deviation from neutral posture, during the task of shaving –both of which are

factors that could otherwise contribute to discomfort or risk of musculoskeletal disorders (see ch. “A.6 Negative Effects of Extreme Joint Angles”). Consequently, the negative effects of joint posture during shaving are minimal, for any of the 3 razors.

Taking the previous into account, it may be considered that the importance of wrist and forearm posture is limited for the ergonomic evaluation of razors. Other factors (e.g. handle fit and stability, pressure distribution, performance) would also need to be assessed, in order to evaluate the design of razors in depth. This claim is also supported by the opinions of subjects, which were asked to subjectively rank the 3 razors on handle comfort, during informal conversation, after the experiment. The results were almost unanimous: C>B>A in order of preference –which was not indicated from joint motion.

D.4 Conclusions

This study aimed to examine the correlation between handle design and wrist and forearm joint motion, in 3 alternative design solutions of an everyday product –the razor. The results indicated that such a correlation exists; handle design in razors affects wrist and forearm posture.

Using wrist and forearm deviation from neutral posture as the only criterion, it was found that the order of razors which allowed less deviation is: A (no DoFs, short length), B (1 DoF, medium length), C (2 DoFs, long length). However, this study proved that mean joint posture was within safe limits of joint angles, using all razors. Thereby, the importance of wrist and forearm posture for the task of shaving, in relation to discomfort and risk of cumulative MSD should be considered limited. Consequently, the examination of additional aspects, both subjective and objective, is needed to effectively compare different razors in depth, from the viewpoint of ergonomics/human factors.

A specific design guideline which can be extracted from this experiment is related to the length of razor handles: long handles cause ulnar deviation, therefore it is better to design handles of moderate length. The suggested length depends on the biometrics of the target population, as well as handle shape, but the participants of this specific study performed better, in terms of ulnar deviation, with a length of 12.6 cm or smaller.

Overall, we established a methodology which can be implemented in the comparison of various hand-operated tools, from the perspective of ergonomics/human factors, through studying wrist and forearm joint posture.

D.5 Limitations

D.5.1 Motion Tracking System

In designing the motion tracking system, we deliberately balanced accuracy with inexpensiveness. Our selection of hardware (sensors, microcontroller) was low-cost, and it is possible that using higher quality hardware would yield more accurate results.

Specifically, the “uniformity” (the difference in output for the same input, between two sensors) of the sensors was an issue. In other words, in order to extract the relative

angles between two IMUs, their behavior needs to be identical, for the same input. Otherwise, a false reading (artifact) is created by the difference in the output, leading to error. Even though it is systematic, this error is difficult to compensate for, since it varies for each possible rotation of the sensors.

More expensive sensors may (or may not) have higher production standards, meaning that their uniformity could be superior to those used in this project. Other specifications such as the accuracy and precision of a single sensor would also be better, while the issue of drift might have been further mitigated, even though drift of the sensors used was acceptable.

Furthermore, the clothing (fingerless glove and elbow patch) used to mount the sensors on the subjects is stretchable for larger hands and arms, but not adjustable for smaller hands. As a consequence, minor slipping of the clothing over the skin could have occurred, especially in subjects with smaller hands and arms, causing an artifact similar to soft tissue artifact (see ch. "C.1.1.1 IMU").

D.5.2 Experiment

The most significant limitation of the experiment was the realism of the simulation of the task of shaving. The razor blades were removed or covered with tape, and subjects would merely simulate the act of shaving over the skin (or over tight clothing in 2 cases), without actually performing it. This way, haptic feedback was impeded and kinematic behavior may have not been natural, due to a lack of actual purpose for the subjects.

Another limitation of this study was the inconsistency of the experimental procedure, in setting the neutral posture of each subject. As previously presented (see ch. "D.1.5 Procedure"), the subjects were instructed to hand their arm at their side, without exerting any force, in order to register this posture as their neutral. However, this action needed to be repeated frequently throughout the experiment, to compensate for any accumulated errors, but the subjects' ability to exactly repeat their previous neutral posture was questionable. To eliminate this inconsistency, a clearly defined scheme for setting the neutral posture could have been used; for instance instructing the subjects to press their palm against the side of the leg, or building a platform with a steady handle which the subjects would have to grasp every time.

Finally, the definition of body segments was unclear to the subjects: they would forget the boundaries during completion of the tasks and shave part of a different segment. Instead of verbally explaining the boundaries of each segment, it would be better to mark their boundaries directly on the skin (or clothing), for example with thin, easily removable, adhesive tape, or a pencil suitable for skin.

D.5.3 Analysis

The analysis of results in this thesis did not make use of formal statistical tools – Analysis of Variance (ANOVA). Statistical tests could be used to supply greater credibility to our claims regarding differences in joint angles between the three razors. However, the focus of this thesis is rather to establish a methodology for hand tool comparison, than actually compare these three razors. Spielholz et al. (2001) acted similarly in their study which compared three orbital sander configurations.

D.6 Recommendations for Future Research

From this study, new research questions are raised, which could build on this thesis:

D.6.1 Fit in hand

In this study, we did not examine the issue of handle fit in the hand and its importance in user comfort/discomfort. This mostly depends on handle shape, width and material (friction, softness), while it can be quantified by *pressure distribution* in fingers and palm (Aldien, Welcome, Rakheja, Dong, & Boileau, 2005; Björing, Johansson, & Hägg, 2002), *finger posture* (Werner, Armstrong, Bir, & Aylard, 1997; Carey & Gallwey, 2002), and *subjective evaluations* by users. Similarly to wrist and forearm posture, awkward finger posture and repetitive finger motions can cause prolonged discomfort; thereby it is worthy of examination in delicate tasks.

D.6.2 Natural Behavior

To achieve a controlled environment, all experiments in this study were conducted in a laboratory. The task was merely simulated with blade-less razors and the subjects were restricted to a seated stance with wires attached to them, connecting to a computer. While such experiments are a necessary starting point, it is possible that the results are not a perfect reflection of natural wrist and forearm behavior, due to these restrictions. Experiments held in a more natural setting (upright stance, realistic hair shaving), would provide a more reliable assessment of the kinematics of wrist and forearm motion. Moreover, the hardware could be further developed to become wireless and less intrusive to the subject.

D.6.3 Correlation between Discomfort and Risk of MSD

In this thesis, we have treated perceived discomfort and the risk of musculoskeletal disorder (MSD) as two discrete concepts. However, as previously discussed (see ch. “A.6 Negative effects of extreme joint angles”), studies have found that they share a few common causes, such as prolonged extreme wrist deviation, and high exertions of force. It would be interesting to investigate the relation between the two notions. Does discomfort necessarily imply that the specific task increases the risk for MSD? If a hand tool user feels comfortable, is he always safe from risking MSDs? Ultimately, do the body’s inner signals protect us from developing a musculoskeletal syndrome in the wrist/hand?

Appendix

A. Code

```
// Arduino sketch for 3 MPU6050s using DMP, using I2C device class (I2Cdev)
// 16/09/2016 by Michael Karakikes <mkarakikes@gmail.com>
//
// based on the work of Jeff Rowberg and the libraries found in:
// https://github.com/eadf/MPU6050\_DMP6\_Multiple

// I2Cdev and MPU6050 must be installed as libraries, or else the .cpp/.h
// files for both classes must be in the include path of your project
#include "I2Cdev.h"
#include "MPU6050_Wrapper.h"
#include "TogglePin.h"
#include "DeathTimer.h"
#include "MatrixMath.h"

// Arduino Wire library is required if I2Cdev I2CDEV_ARDUINO_WIRE
// implementation is used in I2Cdev.h
#if I2CDEV_IMPLEMENTATION == I2CDEV_ARDUINO_WIRE
#include "Wire.h"
#endif

/* =====
NOTE: This code was tested on Arduino Nano v3.0
Connections between the 3 MPU-6050s and the Arduino Nano:
    VCCs (all)    -> 5V
    GNDs (all)   -> GND
    SCLs (all)   -> A5
    SDAs (all)   -> A4
    XDAs (all)   -> unused
    XCLs (all)   -> unused
    AD0 (IMU#1)  -> D4
    AD0 (IMU#2)  -> D5
    AD0 (IMU#3)  -> D6
    INTs (all)   -> unused
=====
*/

// IMU outputs quaternion components in a [w, x, y, z] format
#define OUTPUT_READABLE_QUATERNION

const bool useThreeMpus = true;
MPU6050_Array mpus(useThreeMpus ? 3 : 1);

#define AD0_PIN_0 4 // Connect this pin to the AD0 pin on MPU#1
#define AD0_PIN_1 5 // Connect this pin to the AD0 pin on MPU#2
#define AD0_PIN_2 6 // Connect this pin to the AD0 pin on MPU#3

#define LED_PIN 13 // (Arduino led pin is 13)

#define OUTPUT_SERIAL Serial

uint8_t fifoBuffer[64]; // FIFO storage buffer

// orientation variables
Quaternion q; // [w, x, y, z] quaternion container
VectorFloat gravity; // [x, y, z] gravity vector
```

```

float R1[3][3], R2[3][3], R3[3][3]; // Rotation matrices of the 3 IMUs
float R1_offset[3][3] = { // Rotation mat for resetting ref. frame IMU#1
  {1., 0., 0.}, {0., 1., 0.}, {0., 0., 1.}
};
float R2_offset[3][3] = { // Rotation mat for resetting ref. frame IMU#2
  {1., 0., 0.}, {0., 1., 0.}, {0., 0., 1.}
};
float R3_offset[3][3] = { // Rotation mat for resetting ref. frame IMU#3
  {1., 0., 0.}, {0., 1., 0.}, {0., 0., 1.}
};

float offset[3] = {0, 0, 0}; // variable for neutral hand position offsets

const int buttonPin = 7; // the number of the pushbutton pin

int task = 1; // counter for tasks (for annotation in serial output)
int task_temp = 0; // an auxiliary task counter
int prod = 1; // counter for product tested

TogglePin activityLed(LED_PIN, 100);
DeathTimer deathTimer(5000L);

// =====
// === INITIAL SETUP ===
// =====

void setup() {
  // join I2C bus (I2Cdev library doesn't do this automatically)
  #if I2CDEV_IMPLEMENTATION == I2CDEV_ARDUINO_WIRE
    Wire.begin();
    Wire.setClock(400000); // 400kHz I2C clock. Comment out if having
  // compilation difficulties
  #elif I2CDEV_IMPLEMENTATION == I2CDEV_BUILTIN_FASTWIRE
    Fastwire::setup(400, true);
  #endif

  // initialize serial communication
  // (38400 rate is chosen because it is regarded as stable, but it's
  // really up to you depending on your project)
  Serial.begin(38400);

  while (!Serial)
    ;

  // initialize devices
  Serial.println(F("Initializing I2C devices..."));
  mpus.add(AD0_PIN_0);
  mpus.add(AD0_PIN_1);
  mpus.add(AD0_PIN_2);

  mpus.initialize();

  // configure LED for output
  pinMode(LED_PIN, OUTPUT);

  // verify connection
  Serial.println(F("Testing device connections..."));
  if (mpus.testConnection()) {
    Serial.println(F("MPU6050 connection successful"));
  } else {
    mpus.halt(F("MPU6050 connection failed, halting"));
  }

  // wait for ready
  Serial.println(F("\nSend any character to begin DMP programming and demo:
"));
  while (Serial.available() && Serial.read())

```

```

; // empty buffer
while (!Serial.available())
  activityLed.update(); // flash led while waiting for data
while (Serial.available() && Serial.read())
; // empty buffer again
activityLed.setPeriod(500); // slow down led to 2Hz

// load and configure the DMP
Serial.println(F("Initializing DMP..."));
mpus.dmpInitialize();

// Supply your own offsets here:
MPU6050_Wrapper* currentMPU = mpus.select(0); // offsets for IMU#1
currentMPU->_mpu.setXGyroOffset(209);
currentMPU->_mpu.setYGyroOffset(-49);
currentMPU->_mpu.setZGyroOffset(0);
currentMPU->_mpu.setXAccelOffset(-2690);
currentMPU->_mpu.setYAccelOffset(-2041);
currentMPU->_mpu.setZAccelOffset(1805);

if (useThreeMpus) {
  currentMPU = mpus.select(1); // offsets for IMU#2
  currentMPU->_mpu.setXGyroOffset(8);
  currentMPU->_mpu.setYGyroOffset(-9);
  currentMPU->_mpu.setZGyroOffset(4);
  currentMPU->_mpu.setXAccelOffset(-4456);
  currentMPU->_mpu.setYAccelOffset(-1046);
  currentMPU->_mpu.setZAccelOffset(1344);

  currentMPU = mpus.select(2); // offsets for IMU#3
  currentMPU->_mpu.setXGyroOffset(28);
  currentMPU->_mpu.setYGyroOffset(-3);
  currentMPU->_mpu.setZGyroOffset(28);
  currentMPU->_mpu.setXAccelOffset(793);
  currentMPU->_mpu.setYAccelOffset(-1252);
  currentMPU->_mpu.setZAccelOffset(1553);
}

mpus.programDmp(0);
if (useThreeMpus)
  mpus.programDmp(1);
mpus.programDmp(2);

// initialize the pushbutton pin as an input:
pinMode(buttonPin, INPUT);
}

// =====
// ===          handleMPUevent function          ===
// =====

void handleMPUevent(uint8_t mpu) {

  MPU6050_Wrapper* currentMPU = mpus.select(mpu);
  // reset interrupt flag and get INT_STATUS byte
  currentMPU->getIntStatus();

  // check for overflow (this should never happen unless our code is too
  // inefficient)
  if ((currentMPU->_mpuIntStatus & _BV(MPU6050_INTERRUPT_FIFO_OFLOW_BIT))
      || currentMPU->_fifoCount >= 1024) {
    // reset so we can continue cleanly
    currentMPU->resetFIFO();
    Serial.println(F("FIFO overflow!"));
    return;
  }
  // otherwise, check for DMP data ready interrupt (this should happen

```

```

// frequently)
if (currentMPU->_mpuIntStatus & _BV(MPU6050_INTERRUPT_DMP_INT_BIT)) {

    // read and dump a packet if the queue contains more than one
    while (currentMPU->_fifoCount >= 2 * currentMPU->_packetSize) {
        // read and dump one sample
        currentMPU->getFIFOBytes(fifoBuffer);
    }

    // read a packet from FIFO
    currentMPU->getFIFOBytes(fifoBuffer);

#ifdef OUTPUT_READABLE_QUATERNION
    // get quaternion values in easy matrix form: w x y z
    currentMPU->_mpu.dmpGetQuaternion(&q, fifoBuffer);

    // Elements to use in rotation matrix
    float xx = q.x * q.x;
    float xy = q.x * q.y;
    float xz = q.x * q.z;
    float xw = q.x * q.w;
    float yy = q.y * q.y;
    float yz = q.y * q.z;
    float yw = q.y * q.w;
    float zz = q.z * q.z;
    float zw = q.z * q.w;

    // Create Rotation matrix derived from quaternions
    float R[3][3] = { { 1.0 - 2.0 * ( yy + zz ), 2.0 * ( xy - zw ), 2.0 *
( xz + yw ) },
        { 2.0 * ( xy + zw ), 1.0 - 2.0 * ( xx + zz ), 2.0 * ( yz - xw ) },
        { 2.0 * ( xz - yw ), 2.0 * ( yz + xw ), 1.0 - 2.0 * ( xx + yy ) }
    };

    if (mpu == 0) { // For IMU#1
        for (int i = 0; i < 3; i++) {
            for (int j = 0; j < 3; j++) {
                R1[i][j] = R[i][j];
            }
        }
    }
    else if (mpu == 1) { // for IMU#2
        for (int i = 0; i < 3; i++) {
            for (int j = 0; j < 3; j++) {
                R2[i][j] = R[i][j];
            }
        }
    }
    else if (mpu == 2) { // for IMU#3
        for (int i = 0; i < 3; i++) {
            for (int j = 0; j < 3; j++) {
                R3[i][j] = R[i][j];
            }
        }
    }
}
#endif

}
}

// =====
// === MAIN PROGRAM LOOP ===
// =====

void loop() {

    // Variables declaration
    float R1_tr[3][3], R2_tr[3][3], R12[3][3], R23[3][3]; // Transpose and

```

```

// Relative matrices
float R1_reset[3][3], R2_reset[3][3], R3_reset[3][3]; // Reseted R

static uint8_t mpu = 0;
static MPU6050_Wrapper* currentMPU = NULL;

for (int i = 0; i < 3; i++) {
    mpu = ( mpu + 1 ) % 3;
    currentMPU = mpus.select(mpu);

    if (currentMPU->isDue()) {
        handleMPUevent(mpu);
    }
}

// ===== RESETTING COORDINATE SYSTEM =====

// read the state of the pushbutton value:
int buttonState = digitalRead(buttonPin);
int incomingByte = 0; // Incoming from serial

// If incoming data is available in the serial
if (Serial.available() > 0) {
    incomingByte = Serial.read(); // read the incoming byte
}

// Send "r" OR press pushbutton if you want to reset
if ( incomingByte == 114 || buttonState == HIGH ) {
    // Reset reference axes (make current orientation the reference frame)
    // Create a matrix R_offset that resets the reference frame to the
    // current (when multiplied)
    Matrix.Transpose( (float*)R1, 3, 3, (float*)R1_offset );
    Matrix.Transpose( (float*)R2, 3, 3, (float*)R2_offset );
    Matrix.Transpose( (float*)R3, 3, 3, (float*)R3_offset );
    // Angle offsets for neutral position
    for (int i = 0; i < 3; i++) {
        offset[i] = 0;
    }
    Serial.println("/*----- RESET -----
-----*/");
}

else if (incomingByte == 49) {
    // Send "1" to insert a "start" annotation line in the serial output (to
    // separate tasks)
    Serial.print("/*===== BEGIN TASK ");
    Serial.print(task); Serial.print(" Prod."); Serial.print(prod);
    Serial.println(" =====*/");
    task_temp = task; // get the task identifier
}

else if (incomingByte == 50) {
    // Send "2" to insert a "stop" annotation line in the serial output (to
    // separate tasks)
    Serial.print("/*===== END TASK ");
    Serial.print(task); Serial.print(" Prod."); Serial.print(prod);
    Serial.println(" =====*/");
    task++; // counter for task number
    task_temp = 0; // zero value when not in a task (helps with data
    // handling)
}

else if (incomingByte == 51) {
    // Send "3" to annotate change of product
    prod++; // counter for product
    Serial.print("/*////////// PRODUCT ");

```

```

Serial.print(prod); Serial.println("
////////////////////////////////////*/");
task = 1; // reset the task counter
task_temp = 0; // reset the auxiliary counter (not necessary but in
// case I forget to "end task")
}

// ===== ROTATION MATRIX HANDLING =====

// Multiply with R_offset, to find R in the new reference frame
Matrix.Multiply( (float*)R1_offset, (float*)R1, 3, 3, 3, (float*)R1_reset
);
Matrix.Multiply( (float*)R2_offset, (float*)R2, 3, 3, 3, (float*)R2_reset
);
Matrix.Multiply( (float*)R3_offset, (float*)R3, 3, 3, 3, (float*)R3_reset
);

// Find R:1->0 from R:0->1 (= R1) : Inverse of R1 = transpose of R1
// (properties of rotation matrix)
Matrix.Transpose( (float*)R1_reset, 3, 3, (float*)R1_tr );

// Relative rotation matrix between IMUs 1-2 (elbow): R_12 = R_10 * R_02 =
// R_01trans * R_02
Matrix.Multiply((float*)R1_tr, (float*)R2_reset, 3, 3, 3, (float*)R12);

// Find R:2->0 from R:0->2 (= R2) : Inverse of R2 = transpose of R2
// (properties of rotation matrix)
Matrix.Transpose( (float*)R2_reset, 3, 3, (float*)R2_tr );

// Relative rotation matrix between IMUs 2-3 (wrist): R_23 = R_20 * R_03 =
// R_02trans * R_03
Matrix.Multiply((float*)R2_tr, (float*)R3_reset, 3, 3, 3, (float*)R23);

// Check for validity of incoming data.
// Simply check a few cosines from R23
if ( R23[0][0] > 1.01 || R23[2][0] > 1.01 || R23[0][2] > 1.01 ) {
Serial.println("ATTENTION!!! Data going crazy! Press RESET button");
} else { // Otherwise execute angle calculations

// ===== Elbow only (pronation/supination) =====
float pron = atan2( R12[2][1], R12[2][2] ) * 180.0 / M_PI;

// ===== Wrist only (flex/ext & uln/rad) =====
float flex = atan2( R23[0][2], R23[2][2] ) * 180.0 / M_PI;

float uln = atan2( R23[1][0], R23[1][1] ) * 180.0 / M_PI;

// Send "o" for neutral position
if ( incomingByte == 111 ) {
offset[0] = pron;
offset[1] = flex;
offset[2] = uln;
Serial.println("/*----- NEUTRAL POSITION -----
-----*/");
}

// ===== Print on Serial Monitor =====
Serial.print(" p/s:\t"); Serial.print( pron - offset[0] );
Serial.print("\t\tf/e:\t"); Serial.print( flex - offset[1] );
Serial.print("\t\ttr/u:\t"); Serial.print( uln - offset[2] );
Serial.print("\t\tsec: "); Serial.print(millis() / 1000.0, 3); // add a
// time stamp to each output
Serial.print(" pr"); Serial.print(prod); Serial.print(" t");
Serial.println(task_temp); // identifier for each data set

```

```
} // end of calculation and printing of angles

activityLed.update();
// deathTimer.update(); // running time print-out
}
```

Bibliography

Aldien, Y., Welcome, D., Rakheja, S., Dong, R., & Boileau, P.-E. (2005). Contact pressure distribution at hand–handle interface: role of hand forces and handle size . *International Journal of Industrial Ergonomics* , 35, 267-286.

An, K. N. (1984). Kinematic analysis of human movement. *Annals of Biomedical Engineering* , 12, 585-597.

Ascension. (n.d.). Retrieved from Electromagnetic tracking manufacturer:
<http://www.ascension-tech.com/products/>

Biometrics Ltd. (n.d.). Retrieved from Goniometers manufacturer:
<http://www.biometricsltd.com/gonio.htm>

Bisht, D. S., & Khan, M. R. (2013). Ergonomic assessment methods for the evaluation of hand held industrial products: a review. *Proceedings of the World Congress on Engineering, I*.

Björing, G., & Hägg, G. M. (2000). Musculoskeletal exposure of manual spray painting in the woodworking industry – an ergonomic study on painters. *International Journal of Industrial Ergonomics* , 26, pp. 603-614.

Björing, G., Johansson, L., & Hägg, G. M. (2002). Surface pressure in the hand when holding a drilling machine under different drilling conditions . *International Journal of Industrial Ergonomics* , 29, 255-261.

Buchholz, B., & Wellman, H. (1997). Practical Operation of a Biaxial Goniometer at the Wrist Joint. *Human Factors* , 39, 119-129.

Cacha, C. A. (1999). *Ergonomics and safety in hand tool design*. CRC Press.

Carey, E. J., & Gallwey, T. J. (2002). Effects of wrist posture, pace and exertion on discomfort. *International Journal of Industrial Ergonomics* , 29, 85-94.

Charles, S. K. (2008). *It's all in the wrist: a quantitative characterization of human wrist control*. Ph.D. dissertation, Massachusetts Institute of Technology.

Chen, K.-Y., Patel, S. N., & Keller, S. (2016). Finexus: Tracking Precise Motions of Multiple Fingertips Using Magnetic Sensing. *Proceedings of the 2016 CHI Conference on Human Factors in Computing Systems* (pp. 1504-1514). New York, NY, USA: ACM.

Chen, X. (2013). *Human motion analysis with wearable inertial sensors*. Ph.D. dissertation, University of Tennessee.

Cook, J. R., Baker, N. A., Cham, R., Hale, E., & Redfern, M. S. (2007). Measurements of Wrist and Finger Postures: A Comparison of Goniometric and Motion Capture Techniques. *Journal of Applied Biomechanics* , 23, 70-78.

Crisco, J. J., Heard, W. M., Rich, R. R., Paller, D. J., & Wolfe, S. W. (2011). The mechanical axes of the wrist are oriented obliquely to the anatomical axes. *J Bone Joint Surg Am* , 93, 169-177.

CyberGlove. (n.d.). Retrieved from Datagloves manufacturer:
<http://www.cyberglovesystems.com/>

Dempsey, P. G., McGorry, R. W., Leamon, T. B., & O'Brien, N. (2002). Bending the Tool and the Effect on Human Performance: Further Investigation of a Simulated Wire-Twisting Task. *AIHA Journal* , 63, 586-593.

El-Gohary, M., & McNames, J. (2012). Shoulder and Elbow Joint Angle Tracking With Inertial Sensors. *IEEE Transactions on Biomedical Engineering* , 59, 2635-2641.

Freivalds, A. (2011). *Biomechanics of the upper limbs: mechanics, modeling and musculoskeletal injuries*. CRC press.

Garg, R., Kraszewski, A. P., Stoecklein, H. H., Syrkin, G., Hillstrom, H. J., Backus, S., et al. (2014). Wrist Kinematic Coupling and Performance During Functional Tasks: Effects of Constrained Motion. *The Journal of Hand Surgery* , 39, 634 - 642.e1.

Hale, R., Dorman, D., & Gonzalez, R. V. (2011). Individual muscle force parameters and fiber operating ranges for elbow flexion-extension and forearm pronation-supination. *Journal of Biomechanics* , 44, 650-656.

Hedge, A. (1998). Design of hand-operated devices. Taylor & Francis.

InvenSense. (n.d.). Retrieved from <https://www.invensense.com/products/motion-tracking/6-axis/mpu-6050/>

Kadefors, R., Areskoug, A., Dahlman, S., Kilbom, Å., Sperling, L., Wikström, L., et al. (1993). An approach to ergonomics evaluation of hand tools. *Applied Ergonomics* , 24, 203-211.

Keir, P. J., Bach, J. M., Hudes, M., & Rempel, D. M. (2007). Guidelines for Wrist Posture Based on Carpal Tunnel Pressure Thresholds. *Human Factors* , 49, 88-99.

Kortier, H. G., Sluiter, V. I., Roetenberg, D., & Veltink, P. H. (2014). Assessment of hand kinematics using inertial and magnetic sensors. *Journal of NeuroEngineering and Rehabilitation* , 11, 70.

Kuijt-Evers, L. F. (2007). *Comfort in using hand tools: theory, design and evaluation*. Ph.D. dissertation, TU Delft, Delft University of Technology.

Leardini, A., Chiari, L., Croce, U. D., & Cappozzo, A. (2005). Human movement analysis using stereophotogrammetry: Part 3. Soft tissue artifact assessment and compensation. *Gait & Posture* , 21, 212-225.

Lee, C.-C., Nelson, J. E., Davis, K. G., & Marras, W. S. (1997). An ergonomic comparison of industrial spray paint guns. *International Journal of Industrial Ergonomics* , 19, 425-435.

-
- Lee, K.-S., & Jung, M.-C. (2014). Flexion and Extension Angles of Resting Fingers and Wrist. *International Journal of Occupational Safety and Ergonomics* , 20, 91-101.
- Leonard, L., Sirkett, D., Mullineux, G., Giddins, G. E., & Miles, A. W. (2005). Development of an in-vivo method of wrist joint motion analysis . *Clinical Biomechanics* , 20, 166-171.
- Li, Z.-M., Kuxhaus, L., Fisk, J. A., & Christophel, T. H. (2005). Coupling between wrist flexion–extension and radial–ulnar deviation. *Clinical Biomechanics* , 20, 177-183.
- Lintula, M., & Nevala, N. (2006). Ergonomics and the usability of mechanical single-channel liquid dosage pipettes. *International Journal of Industrial Ergonomics* , 36, 257-263.
- Lopez-Nava, I. H., Marquez-Aquino, F., Munoz-Melendez, A., Carrillo-Lopez, D., & Vargas-Martinez, H. S. (2015). Automatic measurement of pronation/supination flexion/extension and abduction/adduction motion of human limbs using wearable inertial and magnetic sensors. *Proc. 4th Int. Conf. Global Health Challenges (IARIA)*, (pp. 55-60).
- Luinge, H. J., Veltink, P. H., & Baten, C. T. (2007). Ambulatory measurement of arm orientation . *Journal of Biomechanics* , 40, 78-85.
- Madgwick, S. O., Harrison, A. J., & Vaidyanathan, R. (2011). Estimation of IMU and MARG orientation using a gradient descent algorithm. *2011 IEEE International Conference on Rehabilitation Robotics*, (pp. 1-7).
- Marras, W. S., & Schoenmarklin, R. W. (1993). Wrist motions in industry. *Ergonomics* , 36, 341-351.
- McGinnis, R. S., Cain, S. M., Tao, S., Whiteside, D., Goulet, G. C., Gardner, E. C., et al. (2015). Accuracy of Femur Angles Estimated by IMUs During Clinical Procedures Used to Diagnose Femoroacetabular Impingement. *IEEE Transactions on Biomedical Engineering* , 62, 1503-1513.
- Mital, A., & Kilbom, A. (1992). Design, selection and use of hand tools to alleviate trauma of the upper extremities: Part II — The scientific basis (knowledge base) for the guide. *International Journal of Industrial Ergonomics* , 10, 7-21.
- Mitobe, K., Kaiga, T., Yukawa, T., Miura, T., Tamamoto, H., Rodgers, A., et al. (2006). Development of a Motion Capture System for a Hand Using a Magnetic Three Dimensional Position Sensor. *ACM SIGGRAPH 2006 Research Posters*. New York, NY, USA: ACM.
- Moeslund, T. B., Hilton, A., & Krüger, V. (2006). A survey of advances in vision-based human motion capture and analysis . *Computer Vision and Image Understanding* , 104, 90-126.
- Neu, C. P., Crisco, J. J., & Wolfe, S. W. (2001). In vivo kinematic behavior of the radio-capitate joint during wrist flexion–extension and radio-ulnar deviation . *Journal of Biomechanics* , 34, 1429-1438.

-
- Nevala, N., Sormunen, E., Remes, J., & Suomalainen, K. (2013). Evaluation of ergonomics and efficacy of instruments in dentistry. *The Ergonomics Open Journal* , 6.
- Oberländer, K. D. (2015). Inertial Measurement Unit (IMU) Technology. *Inverse Kinematics: Joint Considerations and the Maths for Deriving Anatomical Angles* .
- Paschoarelli, L. C., de Oliveira, A. B., & Coury, H. J. (2008). Assessment of the ergonomic design of diagnostic ultrasound transducers through wrist movements and subjective evaluation. *International Journal of Industrial Ergonomics* , 38, 999-1006.
- Polhemus. (n.d.). Retrieved from Electromagnetic tracking manufacturer: <http://polhemus.com/motion-tracking/overview/>
- Putz-Anderson, V., Bernard, B. P., Burt, S. E., Cole, L. L., Fairfield-Estill, C., Fine, L. J., et al. (1997). Musculoskeletal disorders and workplace factors. *National Institute for Occupational Safety and Health (NIOSH)* , 104.
- Radwin, R. G., & Haney, J. T. (1996). *An ergonomics guide to hand tools*. AIHA.
- Rowe, J. B., Friedman, N., Bachman, M., & Reinkensmeyer, D. J. (2013). The Manumeter: A non-obtrusive wearable device for monitoring spontaneous use of the wrist and fingers. *2013 IEEE 13th International Conference on Rehabilitation Robotics (ICORR)*, (pp. 1-6).
- Sabatini, A. M. (2011). Estimating three-dimensional orientation of human body parts by inertial/magnetic sensing. *Sensors* , 11, 1489-1525.
- Schall, M. C. (2014). *Application of inertial measurement units for directly measuring occupational exposure to non-neutral postures of the low back and shoulder*. University of Iowa. University of Iowa.
- Schoenmarklin, R. W., & Marras, W. S. (1993). Dynamic capabilities of the wrist joint in industrial workers. *International Journal of Industrial Ergonomics* , 11, 207-224.
- Shimomura, Y., Minowa, K., Kawahira, H., & Katsuura, T. (2016). Ergonomic design and evaluation of the handle for an endoscopic dissector. *Ergonomics* , 59, 729-734.
- Simone, L. K., & Kamper, D. G. (2005). Design considerations for a wearable monitor to measure finger posture. *Journal of NeuroEngineering and Rehabilitation* , 2, 5.
- Smeragliuolo, A. H., Hill, N. J., Disla, L., & Putrino, D. (2016). Validation of the Leap Motion Controller using markered motion capture technology . *Journal of Biomechanics* , 49, 1742-1750.
- Sperling, L., Dahlman, S., Wikström, L., Kilbom, Å., & Kadefors, R. (1993). A cube model for the classification of work with hand tools and the formulation of functional requirements. *Applied Ergonomics* , 24, 212-220.
- Spielholz, P., Bao, S., & Howard, N. (2001). A Practical Method for Ergonomic and Usability Evaluation of Hand Tools: A Comparison of Three Random Orbital Sander Configurations. *Applied Occupational and Environmental Hygiene* , 16, 1043-1048.

-
- Tolani, D., & Badler, N. I. (1996). Real-time inverse kinematics of the human arm. *Presence: Teleoperators & Virtual Environments*, 5, 393-401.
- Vanegas, M., & Stirling, L. (2015). Characterization of inertial measurement unit placement on the human body upon repeated donnings. *2015 IEEE 12th International Conference on Wearable and Implantable Body Sensor Networks (BSN)*, (pp. 1-6).
- Vicon. (n.d.). Retrieved from Optical Motion Capture systems manufacturer: <https://www.vicon.com/motion-capture/life-sciences>
- Wang, P. T., King, C. E., Do, A. H., & Nenadic, Z. (2011). A durable, low-cost electrogoniometer for dynamic measurement of joint trajectories. *Medical Engineering & Physics*, 33, 546-552.
- Werner, R., Armstrong, T. J., Bir, C., & Aylard, M. K. (1997). Intracarpal canal pressures: the role of finger, hand, wrist and forearm position. *Clinical Biomechanics*, 12, 44-51.
- Wise, S., Gardner, W., Sabelman, E., Valainis, E., Wong, Y., Glass, K., et al. (1990). Evaluation of a fiber optic glove for semi-automated goniometric measurements. *Journal of Rehabilitation Research and Development*, 27, 411.
- Wu, G., van der Helm, F. C., Veeger, H. E., Makhsous, M., Roy, P. V., Anglin, C., et al. (2005). ISB recommendation on definitions of joint coordinate systems of various joints for the reporting of human joint motion—Part II: shoulder, elbow, wrist and hand. *Journal of Biomechanics*, 38, 981-992.
- Yu, D., Lowndes, B., Morrow, M., Kaufman, K., Bingener, J., & Hallbeck, S. (2016). Impact of novel shift handle laparoscopic tool on wrist ergonomics and task performance. *Surgical Endoscopy*, 30, 3480-3490.